



<https://theses.gla.ac.uk/>

Theses digitisation:

<https://www.gla.ac.uk/myglasgow/research/enlighten/theses/digitisation/>

This is a digitised version of the original print thesis.

Copyright and moral rights for this work are retained by the author

A copy can be downloaded for personal non-commercial research or study, without prior permission or charge

This work cannot be reproduced or quoted extensively from without first obtaining permission in writing from the author

The content must not be changed in any way or sold commercially in any format or medium without the formal permission of the author

When referring to this work, full bibliographic details including the author, title, awarding institution and date of the thesis must be given

Enlighten: Theses

<https://theses.gla.ac.uk/>  
[research-enlighten@glasgow.ac.uk](mailto:research-enlighten@glasgow.ac.uk)

# **REGULATION OF GUARD CELL ION CHANNELS**

**ROBERT ADAM GAY**

Thesis submitted for the degree of Doctor of Philosophy

Division of Biochemistry and Molecular Biology,  
Institute of Biomedical and Life Sciences,  
University of Glasgow.

May 2004.

ProQuest Number: 10390540

All rights reserved

INFORMATION TO ALL USERS

The quality of this reproduction is dependent upon the quality of the copy submitted.

In the unlikely event that the author did not send a complete manuscript and there are missing pages, these will be noted. Also, if material had to be removed, a note will indicate the deletion.



ProQuest 10390540

Published by ProQuest LLC (2017). Copyright of the Dissertation is held by the Author.

All rights reserved.

This work is protected against unauthorized copying under Title 17, United States Code  
Microform Edition © ProQuest LLC.

ProQuest LLC.  
789 East Eisenhower Parkway  
P.O. Box 1346  
Ann Arbor, MI 48106 – 1346

GLASGOW  
UNIVERSITY  
LIBRARY:

## Abstract

Stomatal guard cells regulate the stomatal aperture to allow gas exchange whilst minimising water loss from the plant. Stomatal movements are driven by changes in the ion transport across the various membrane systems through ion channels and pumps. Complex signalling events are involved in the regulation of ion channels during stomatal movements. Whilst considerable progress has been made in the understanding of ion transport processes, some questions still remain. Regulation of guard cell ion channels by the gaseous free radical nitric oxide, (NO), was investigated using electrophysiological and  $\text{Ca}^{2+}$  imaging techniques. Treatment of intact guard cells with NO donor and scavenger compounds revealed that NO modulates the  $\text{Ca}^{2+}$ -sensitive inward rectifier  $\text{K}^+$  channel ( $\text{I}_{\text{K, in}}$ ) and anion channel ( $\text{I}_{\text{Cl}}$ ) by enhancing  $\text{Ca}^{2+}$  release from internal stores. The NO-enhanced  $\text{Ca}^{2+}$  release is via a cGMP / cADPR pathway, thus showing similarities with animal NO signalling. Furthermore, abscisic acid (ABA) regulation of  $\text{I}_{\text{K, in}}$  and  $\text{I}_{\text{Cl}}$  is abolished by the nitric oxide scavenger compounds, placing NO as a key component of ABA-mediated ion channel regulation. NO regulation of  $\text{I}_{\text{K, in}}$  and  $\text{I}_{\text{Cl}}$  was abolished by the broad range protein kinase inhibitor staurosporine, which blocked the NO enhancement of  $\text{Ca}^{2+}$  release from internal stores. Stomatal movements also involve changes in volume and surface area, which must be accommodated by delivery and retrieval of membrane material. Fusion and fission of membrane material requires protein machinery called SNARE proteins, which include syntaxins. The discovery of a syntaxin, NtSyr1, which is involved in hormonal control of ion channel gating, along with patch clamp measurements of cell surface area, raised the possibility of interaction between membrane traffic and ion channel regulation. To explore this possibility further, experiments were carried out using pharmacological tools and transgenic plants expressing the cytosolic portion (SP2) of NtSyr1 under the control of a dexamethasone inducible promoter (dexSP2-14 plants). Experiments with the membrane traffic inhibitor brefeldin A (BFA) and the actin antagonist latrunculin B (LATB), showed coupling of  $\text{I}_{\text{K, in}}$  channel activity with membrane traffic and both  $\text{I}_{\text{K, in}}$  and the outward rectifier  $\text{K}^+$  channel ( $\text{I}_{\text{K, out}}$ ) with actin filaments. Furthermore, analysis of voltage evoked  $\text{Ca}^{2+}$  signals in dexSP2-14 plants showed that voltage evoked  $\text{Ca}^{2+}$  signals were altered by SP2 protein expression. These data, along with stomatal aperture measurements, suggest a coupling of membrane trafficking and cell volume regulation processes with ion channel control.

## Acknowledgements

To my parents, *gyda diolch a chariad mawr*

Thanks to...

Mike, for help and advice for so many (many!) years, often above and beyond the call of duty.

Members of the lab both in Wye and Glasgow, especially Carlos, Sergei, Adrian, Ingela, all the 'lunch club', Bron, Colleen and Ufo.

Those outside the lab, especially Marco and Alex, the Tyrrell family, the 'Guinness supper crew', Fr Joe Keenan, the Glasgow O.P.s, fr. John O'Connor O.P, fr. Mike Demkovich O.P.

Prof. Sid Thomas for permission to use the I.G.E.R. library.

## Declaration

All the work presented in this thesis is my own, with the following exceptions:  $K^+$  channel measurements in chapters 3 and 4 were collected jointly with Dr. Carlos García-Mata and Dr. Sergei Sokolovski respectively. In both cases my contribution and that of the researcher was equal. Patch clamp experiments for Figure 3.9 were carried out and analysed by Dr. Sergei Sokolovski. All analyses and interpretations contained in this thesis are my own.

Robert Gay.

## Abbreviations

|                          |   |
|--------------------------|---|
| 7TMS                     | seven transmembrane spanning domain receptor                  |
| AAPK                     | ABA activated protein kinase                                  |
| ABA                      | abscisic acid   |
| AM                       | acetoxymethyl ester   |
| BAPTA                    | 1,2-bis(2-aminophenoxy)ethane-N,N,N',N'-tetraacetate          |
| BFA                      | brefeldin A   |
| $[Ca^{2+}]_{\text{cyt}}$ | cytosolic free $Ca^{2+}$ concentration                        |
| cADPR                    | cyclic ADP ribose   |
| CAR                      | extracellular $Ca^{2+}$ receptor ( <i>Arabidopsis</i> )       |
| CaR                      | extracellular $Ca^{2+}$ receptor (mammals)                    |
| cGMP                     | cyclic GMP  |
| CICR                     | $Ca^{2+}$ induced $Ca^{2+}$ release                           |
| $C_m$                    | membrane capacitance  |
| cPTIO                    | 2-carboxyphenyl-4,4,5,5-tetramethylimidazoline-1-oxyl-3-oxide |
| DAF-2DA                  | diaminofluorescein-2 diacetate                                |
| DIC                      | differential interference contrast                            |
| EGTA                     | ethylenediamine tetraacetic acid                              |
| ER                       | endoplasmic reticulum   |
| $E_{\text{rev}}$         | reversal potential  |
| EtOH                     | ethanol   |
| $E_X$                    | Equilibrium potential (for a given ion, X)                    |
| FV                       | fast vacuolar ion channel                                     |
| GDP                      | guanosine-5'-O-diphosphate                                    |
| GDP- $\beta$ -S          | GDP analogue  |
| GFP                      | green fluorescent protein                                     |
| GTP                      | guanosine-5'-triphosphate                                     |
| GTP- $\gamma$ -S         | non-hydrolysable GTP analogue                                 |
| $H^+$ -ATPase            | proton translocating ATPase                                   |
| HEPES                    | N-[2-hydroxyethyl]piperazine-N'-[2-ethanesulfonic acid]       |
| $I_{\text{Cl}}$          | chloride channel current                                      |
| $I_{K,\text{in}}$        | inward rectifying $K^+$ current                               |
| $I_{K,\text{out}}$       | outward rectifying $K^+$ current                              |



|           |   |
|-----------|---|
| $I_m$     | membrane current  |
| $IP_3$    | inositol 1,4,5 trisphosphate  |
| $IP_6$    | inositol hexakisphosphate   |
| $K_{ATP}$ | ATP-gated $K^+$ channels  |
| $K_d$     | dissociation constant   |
| $K_i$     | half-maximal inhibition   |
| LATB      | latrunculin B   |
| MES       | 2-(N-morpholino)ethanesulfonic acid   |
| NO        | nitric oxide  |
| NOS       | nitric oxide synthase   |
| NR        | nitrate reductase   |
| ODQ       | 1-H-(1,2,4)-oxadiazole-[4,3-a]quinoxalin-1-one  |
| PLC       | phospholipase C   |
| PLD       | phospholipase D   |
| PTFE      | polytetrafluoroethane   |
| SNAP      | S-nitroso-N-acetyl-penicillamine  |
| SNP       | sodium nitroprusside  |
| SOC       | store operated channel  |
| SP2       | cytosolic fragment of NtSyr1  |
| dexSP2-14 | transgenic <i>N. tabacum</i> expressing the SP2 protein under control of a dexamethasone inducible promoter |
| SV        | slow vacuolar ion channel   |
| $TEA^+$   | tetraethylammonium ion  |
| $t_{1/2}$ | activation halftime   |
| $\tau$    | time constant   |
| V-ATPase  | vacuolar ATPase   |
| VK        | vacuolar $K^+$ channel  |
| V-PPase   | vacuolar pyrophosphatase  |

# TABLE OF CONTENTS

|   |           |
|---|-----------|
| Title page  | 1         |
| Abstract  | 2         |
| Acknowledgements  | 3         |
| Declaration   | 4         |
| Abbreviations   | 5         |
| Table of contents   | 7         |
| List of figures   | 10        |
| <b>Chapter 1: Introduction</b>  | <b>11</b> |
| 1.1 Guard cells in plants   | 12        |
| 1.2 Guard cells as a model system   | 13        |
| 1.3 Guard cell $K^+$ channels   | 13        |
| 1.3.1 $I_{K,in}$ and $I_{K,out}$ : Plasma membrane $K^+$ channels           | 13        |
| 1.3.2 $K^+$ channel regulation by phytohormones                             | 14        |
| 1.3.3 $K^+$ channel regulation by phosphorylation                           | 15        |
| 1.3.4 Cytosolic pH  | 16        |
| 1.3.5 Actin Filaments   | 17        |
| 1.3.6 Heterotrimeric G-proteins   | 17        |
| 1.4 Ion channels on the tonoplast   | 19        |
| 1.5 $Ca^{2+}$ signalling in animals   | 20        |
| 1.5.1 $Ca^{2+}$ sensing and influx pathways                                 | 20        |
| 1.5.2 $Ca^{2+}$ release from internal stores                                | 21        |
| 1.6 Guard cell $Ca^{2+}$ signalling   | 22        |
| 1.6.1 Early studies – $Ca^{2+}$ release from internal stores                | 22        |
| 1.6.2 $Ca^{2+}$ entry into the cell and its regulation                      | 23        |
| 1.6.3 Oscillations and encoding specificity in guard cell $Ca^{2+}$ signals | 24        |
| 1.7 Guard cell anion channels   | 26        |
| 1.7.1 S- and R-type anion channels  | 26        |
| 1.7.2 Regulation of anion channels  | 27        |
| 1.8 Membrane trafficking in guard cells                                     | 28        |
| 1.8.1 Measuring changes in membrane surface area                            | 28        |
| 1.8.2 SNARE proteins and ABA signalling in guard cells                      | 29        |
| 1.9 Membrane fusion: an overview from animals                               | 30        |
| 1.9.1 Membrane fusion proteins – components of the SNARE complex            | 31        |
| 1.9.2 SNARE complex structure   | 32        |
| 1.9.3 Regulation of SNARE complex assembly                                  | 34        |
| 1.9.4 Direct interactions between SNARE proteins and ion channels           | 36        |
| 1.10 SNARE proteins in plants   | 37        |
| 1.11 Aims and objectives of the research                                    | 38        |
| <br>Chapter 2: Materials and Methods  | <br>40    |
| 2.1 Techniques for studying ion channels                                    | 41        |
| 2.2 Electronic setup and voltage clamping                                   | 43        |
| 2.3 Noise and vibration isolation   | 45        |
| 2.4 Electrodes  | 46        |
| 2.5 Halfcells   | 47        |
| 2.6 Chamber and housing design  | 47        |
| 2.7 Experimental procedure  | 52        |

|  |                |
|--|----------------|
| <b>2.8 Separation and analysis of ionic currents</b>   | <b>53</b>      |
| <b>2.9 <math>\text{Ca}^{2+}</math> imaging</b>   | <b>56</b>      |
| <br><b>Chapter 3: NO regulates ion channels in guard cells</b>   | <br><b>62</b>  |
| <b>3.1 Introduction</b>  | <b>63</b>      |
| <b>3.2 Materials and Methods</b>   | <b>67</b>      |
| <b>3.3 Results</b>   | <b>69</b>      |
| 3.3.1. NO targets $I_{K,in}$ and $I_{Cl}$  | 69             |
| 3.3.2. $I_{K,in}$ inactivation and $I_{Cl}$ activation require elevations in $[\text{Ca}^{2+}]_{cyt}$  | 73             |
| 3.3.3. NO elevates resting and voltage-evoked $[\text{Ca}^{2+}]_{cyt}$ increases   | 77             |
| 3.3.4. NO does not promote $\text{Ca}^{2+}$ channel gating at the plasma membrane  | 80             |
| 3.3.5. $[\text{Ca}^{2+}]_{cyt}$ rise and $I_{K,in}$ inactivation by NO are sensitive to antagonists of guanylate cyclase and cADPR mediated $\text{Ca}^{2+}$ release | 84             |
| <b>3.4 Discussion</b>  | <b>89</b>      |
| 3.4.1. Introduction  | 89             |
| 3.4.2. NO: component of ABA signalling in guard cells  | 89             |
| 3.4.3. NO signalling in guard cells: a central role for $\text{Ca}^{2+}$   | 91             |
| 3.4.4. NO signalling in guard cells: common themes with animal cells?  | 92             |
| 3.4.5. Summary   | 93             |
| <br><b>Chapter 4: Protein kinases and nitric oxide signal transduction in guard cells</b>  | <br><b>94</b>  |
| <b>4.1 Introduction</b>  | <b>95</b>      |
| <b>4.2 Materials and Methods</b>   | <b>98</b>      |
| <b>4.3 Results</b>   | <b>99</b>      |
| 4.3.1 Staurosporine blocks the effect of NO on $I_{K,in}$ and $I_{Cl}$   | 99             |
| 4.3.2 Protein kinase(s) are essential to the NO-induced enhancement of $\text{Ca}^{2+}$ release from internal stores   | 103            |
| 4.3.3 The protein tyrosine phosphatase inhibitor PAO promotes release of $\text{Ca}^{2+}$ from internal stores   | 105            |
| 4.3.4 The protein tyrosine kinase inhibitor genistein does not block the inhibition of $I_{K,in}$ by NO  | 107            |
| 4.3.5 Genistein does not inhibit the effect of NO on the voltage evoked increase in $[\text{Ca}^{2+}]_{cyt}$   | 112            |
| <b>4.1 Discussion</b>  | <b>115</b>     |
| 4.4.1. Introduction  | 115            |
| 4.4.2. Protein kinases and guard cell signalling   | 116            |
| 4.4.3. What is the identity of the protein kinase involved in NO signal transmission?  | 117            |
| 4.4.4. Summary   | 118            |
| <br><b>Chapter 5: Integration of membrane traffic and cell volume with ion channels and <math>\text{Ca}^{2+}</math> signalling</b>                                   | <br><b>119</b> |
| <b>5.1 Introduction</b>  | <b>120</b>     |
| <b>5.2 Materials and Methods</b>   | <b>124</b>     |
| <b>5.3 Results I: Pharmacology</b>   | <b>126</b>     |
| 5.3.1 Brefeldin A inhibits $I_{K,in}$ but not $I_{K,out}$  | 126            |
| 5.3.2 Brefeldin A inhibition of $I_{K,in}$ is dose-dependent   | 130            |
| 5.3.3 Latrunculin B inhibits both $I_{K,in}$ and $I_{K,out}$   | 130            |

|  |     |
|--|-----|
| 5.3.4 LATB inhibition of $I_{K,in}$ and $I_{K,out}$ is dose-dependent                                    | 132 |
| 5.3.5 BFA and LATB impair normal stomatal movements  | 135 |
| <b>5.4 Results II: Analysis of SP2 transgenic plants</b>   | 138 |
| 5.4.1 Expression of the SP2 protein causes a shift in the CICR threshold                                 | 138 |
| 5.4.2 Expression of the SP2 protein inhibits ABA-induced stomatal closure                                | 140 |
| 5.4.3 Expression of the SP2 protein leads to solute accumulation   | 142 |
| 5.4.4 Expression of the SP2 protein inhibits NO mediated stomatal closure                                | 144 |
| <b>5.5 Discussion</b>  | 146 |
| 5.5.1 Introduction   | 146 |
| 5.5.2. The mechanism of BFA action   | 147 |
| 5.5.3. LATB and control of cell volume via actin   | 149 |
| 5.5.4. Probing the link between ion channel regulation and membrane trafficking: experimental approaches | 151 |
| 5.5.5. Syntaxins, $Ca^{2+}$ signalling and stomatal closure  | 152 |
| 5.5.6. Summary   | 154 |
| <br>Chapter 6: General Discussion  | 155 |
| <b>6.1 Introduction</b>  | 156 |
| <b>6.2 NO and its place in guard cell signalling</b>   | 160 |
| 6.2.1 ABA signalling - NO is not the whole story   | 160 |
| 6.2.2. NO enhancement of $Ca^{2+}$ release from internal stores  | 161 |
| 6.2.3. Protein kinase activity and NO enhanced $Ca^{2+}$ release   | 163 |
| <b>6.3. Coordinating membrane traffic and ion channel control</b>  | 163 |
| 6.3.1. SNARE protein function – more than membrane fusion?   | 163 |
| 6.3.2. Evidence for coupling of membrane traffic and ion channel control in plants.                      | 165 |
| 6.3.3. Coupling guard cell membrane traffic and ion channel control – future prospects                   | 166 |
| <br>References   | 167 |

Appendix: Carlos Garcia-Mata, Robert Gay, Sergei Sokolovski, Adrian Hills, Lorenzo Lamattina and Michael R. Blatt (2003). Nitric oxide regulates  $K^+$  and  $Cl^-$  channels in guard cells through a subset of abscisic acid-evoked signalling pathways. *Proc. Natl. Acad. Sci. USA* **100**: 11116-11121

## LIST OF FIGURES AND TABLES

|                     |  |     |
|---------------------|--|-----|
| <b>Figure 2.1.</b>  | A simplified voltage clamp circuit   | 44  |
| <b>Figure 2.2.</b>  | Representation of a half-cell  | 48  |
| <b>Figure 2.3.</b>  | Detail of chamber design   | 40  |
| <b>Figure 2.4.</b>  | Housing with chamber and reference electrode assembled   | 51  |
| <b>Figure 2.5.</b>  | Details of current trajectory analysis   | 55  |
| <b>Figure 2.6.</b>  | The structure of Fura-2  | 61  |
| <b>Figure 3.1.</b>  | NO inhibits $I_{K,in}$ but not $I_{K,out}$ .   | 70  |
| <b>Figure 3.2.</b>  | Summary of NO effects on $I_{K,in}$ , $I_{K,out}$ and $I_{Cl}$ .   | 72  |
| <b>Figure 3.3.</b>  | NO scavenger cPTIO blocks inactivation of $I_{K,in}$ and activation of $I_{Cl}$ by ABA and NO but not ABA-mediated activation of $I_{K,out}$ . | 74  |
| <b>Figure 3.4.</b>  | Buffering $[Ca^{2+}]_{cyt}$ abolishes the effect of NO on $I_{K,in}$ .   | 76  |
| <b>Figure 3.5.</b>  | Summary of the effect of $Ca^{2+}$ buffering on $I_{K,out}$ , $I_{K,in}$ and $I_{Cl}$ .  | 78  |
| <b>Figure 3.6.</b>  | NO promotes evoked $[Ca^{2+}]_{cyt}$ increases without affecting $[Ca^{2+}]_{cyt}$ recovery.   | 81  |
| <b>Figure 3.7.</b>  | Summary of the effect of NO on $Ca^{2+}$ signalling.   | 82  |
| <b>Figure 3.8.</b>  | NO increases rate of $Ca^{2+}$ release.  | 83  |
| <b>Figure 3.9.</b>  | Patch clamp analysis of $Ca^{2+}$ -channel activity at the plasma membrane.  | 85  |
| <b>Figure 3.10.</b> | NO enhances evoked $[Ca^{2+}]_{cyt}$ increases without promoting $Ca^{2+}$ -channel activity at the plasma membrane.                           | 86  |
| <b>Table 3.11.</b>  | Summary of the effects of cGMP / cADPR pathway antagonists on $I_{K,in}$ and $Ca^{2+}$ signalling.   | 88  |
| <b>Figure 4.1.</b>  | The effect of NO on $I_{K,in}$ is inhibited by staurosporine.  | 100 |
| <b>Figure 4.2.</b>  | Summary of staurosporine on the action of NO on $I_{K,in}$ , $I_{K,out}$ and $I_{Cl}$ .  | 102 |
| <b>Figure 4.3.</b>  | Staurosporine blocks the normal effect of NO on promotes evoked $[Ca^{2+}]_{cyt}$ .  | 104 |
| <b>Figure 4.4.</b>  | Summary of the effect staurosporine on the NO enhanced $Ca^{2+}$ signal.   | 106 |
| <b>Figure 4.5.</b>  | PAO enhances $Ca^{2+}$ release from internal stores.   | 108 |
| <b>Figure 4.6.</b>  | Genistein does not affect the NO induced inhibition of $I_{K,in}$ .  | 110 |
| <b>Figure 4.7.</b>  | Summary of genistein on the action of NO on $I_{K,in}$ .   | 111 |
| <b>Figure 4.8.</b>  | Summary of the effect of genistein on the NO enhanced $Ca^{2+}$ signal.  | 113 |
| <b>Figure 5.1.</b>  | BFA inhibits $I_{K,in}$ but not $I_{K,out}$ .  | 127 |
| <b>Figure 5.2.</b>  | BFA inhibition of $I_{K,in}$ is dose-dependent.  | 128 |
| <b>Figure 5.3.</b>  | Time-course of $I_{K,in}$ inhibition by BFA.   | 129 |
| <b>Figure 5.4.</b>  | LATB inhibits $I_{K,in}$ and $I_{K,out}$ .   | 131 |
| <b>Figure 5.5.</b>  | LATB inhibition of $I_{K,in}$ is dose-dependent.   | 133 |
| <b>Figure 5.6.</b>  | LATB inhibition of $I_{K,out}$ is dose-dependent.  | 134 |
| <b>Figure 5.7.</b>  | BFA inhibits stomatal opening.   | 136 |
| <b>Figure 5.8.</b>  | LATB induces stomatal closure.   | 137 |
| <b>Figure 5.9.</b>  | Expression of the SP2 fragment of NtSyr-1 induces a negative shift in the threshold for voltage evoked increases in $[Ca^{2+}]_{cyt}$          | 139 |
| <b>Figure 5.10.</b> | Expression of the SP2 fragment of NtSyr-1 inhibits ABA-induced stomatal closure.   | 141 |
| <b>Figure 5.11.</b> | Expression of the SP2 protein increases the osmotic content of dexSP2-14 plants.   | 143 |
| <b>Figure 5.12.</b> | Expression of the SP2 fragment of NtSyr-1 inhibits NO-induced stomatal closure.  | 145 |
| <b>Table 6.1</b>    | Summary of factors affecting $I_{K,in}$ , $I_{K,out}$ , $I_{Cl}$ , $I_{Ca}$ and $[Ca^{2+}]_{cyt}$  | 157 |

# **CHAPTER 1:**

## **INTRODUCTION**

## 1.0. Introduction

### 1.1. Guard cells in plants

Guard cells are situated at the end of the transpiration stream in the epidermal layer of the leaf. They perform an essential role for the plant, since they allow uptake of  $\text{CO}_2$ , which is fixed during the photosynthetic process. Uptake of  $\text{CO}_2$  is not without its problems, since the open stomatal pore provides a perfect pathway for water loss into the atmosphere. Thus the stomatal guard cells must be responsive to their environment so that  $\text{CO}_2$  uptake and water loss are balanced as best as possible. Indeed, guard cells are able to translate a whole host of signals into changes in aperture. Signals known to induce stomatal movements include abscisic acid (ABA), high  $\text{CO}_2$ , nitric oxide (NO), ozone,  $\text{H}_2\text{O}_2$ , and temperature (Assmann, 1993; Garcia-Mata and Lamattina, 2001; Garcia-Mata and Lamattina, 2003; Roelfsema and Hedrich, 2002; Schroeder *et al.*, 2001; Willmer and Fricker, 1996). Clearly a system which is able to integrate such a wide variety of signals must be complex, though the net result of the complex signalling is a simple opening or closing of the stomatal pore. The cellular basis of this opening and closing of the stomatal pore is a large change in turgor pressure and a change in cell surface area. In fact, the cell surface area may double during the opening process (Willmer and Fricker, 1996; Raschke, 1975; Raschke, 1979). The increases and decreases in turgor are driven by changes in the flux of solutes, especially of  $\text{K}^+$  and  $\text{Cl}^-$ . Changes in these ions alone may be as much as 2-4 pmol per cell, an effective change in osmoticum of 200-300 mOsm (Blatt, 2000).

## 1.2. Guard cells as a model system.

Guard cells provide an attractive model system for the study of cell signalling and membrane transport. The fact that they lack plasmodesmata makes them ideal for electrophysiological characterisation by impalement (Willmer and Sexton, 1979; Blatt, 1987). Epidermal tissue can be easily isolated facilitating the production of protoplasts for microscopy and for patch-clamp analysis. Guard cell protoplasts may be visually distinguished from epidermal protoplasts on the basis of size and the presence of chloroplasts. Methods for larger scale guard cell protoplast preparation for biochemical and molecular approaches are also available (Kruse *et al.*, 1989; Pandey *et al.*, 2002). Cells may also be studied in the intact plant. Choice of system should normally be made so as to balance the need to control the experimental system with the need to retain cells in a 'physiological' setting.

## 1.3. Guard cell $K^+$ channels

### 1.3.1. $I_{K,in}$ and $I_{K,out}$ : Plasma membrane $K^+$ channels

The guard cell plasma membrane has long been known to be  $K^+$  permeable, clear evidence of the existence of  $K^+$  transport systems. There are two distinct ion channel pathways for the uptake and efflux of  $K^+$  across the plasma membrane in guard cells. Both inward and outward currents were described, and the channels mediating these currents were shown to be highly selective for  $K^+$  (Schroeder *et al.*, 1987). The properties of the inward and outward currents differ, suggesting separate channels for inward and outward  $K^+$  movement. The outward channel ( $I_{K,out}$ ) was characterised in both single channel and whole cell studies (Blatt, 1987; Blatt, 1988b; Hosoi *et al.*, 1988).  $I_{K,out}$  was shown to be a depolarisation activated, TEA<sup>+</sup> sensitive current, whose gating properties respond to external  $K^+$  (Blatt, 1988a). A kinetic approach



determined that external  $K^+$  sensing was by 2 distinct binding sites on the extracellular face of the channel, located away from the channel pore (Blatt and Gradmann, 1997). In contrast,  $I_{K,in}$  was shown to be hyperpolarisation activated, yet unlike  $I_{K,out}$  its gating is unresponsive to changes in external  $K^+$  (Blatt, 1992).

### 1.3.2. $K^+$ channel regulation by phytohormones

Both  $I_{K,in}$  and  $I_{K,out}$  are regulated by phytohormones including abscisic acid (ABA), auxin, and jasmonic acid (Blatt and Thiel, 1994; Evans, 2003; Thiel *et al.*, 1993). ABA rapidly alters the amplitude of both channel currents, shifting the plasma membrane to a state of net  $K^+$  loss (Blatt, 1990). Increasing cytosolic free  $Ca^{2+}$  ( $[Ca^{2+}]_{cyt}$ ) significantly inhibited  $I_{K,in}$  activity (Schroeder and Hagiwara, 1989). Changes in  $[Ca^{2+}]_{cyt}$  were placed in the context of ABA induced  $K^+$  channel regulation when rises in cytoplasmic free  $Ca^{2+}$  were demonstrated in response to application of exogenous ABA to guard cells (McAinsh *et al.*, 1990). Thus it was thought that ABA regulation of  $I_{K,in}$  and  $I_{K,out}$  might proceed via  $Ca^{2+}$ .

Exploration of the origin of this  $Ca^{2+}$  rise has uncovered several possible pathways that might contribute. The  $Ca^{2+}$  might originate from internal stores such as the vacuole or endoplasmic reticulum, and release from these stores may be under the control of inositol trisphosphate ( $IP_3$ ) receptors, cyclic ADP ribose (cADPR) receptors, or voltage gated channels (Allen *et al.*, 1995; Blatt *et al.*, 1990; Gilroy *et al.*, 1990; Muir and Sanders, 1996). There are also pathways for  $Ca^{2+}$  influx in to the cell across the plasma membrane (Grabov and Blatt, 1998b; Hamilton *et al.*, 2000; Pei *et al.*, 2000). These issues will be discussed in detail in later sections.

### 1.3.3. $I_{K,in}$ and $I_{K,out}$ : Regulation by phosphorylation

A body of evidence points towards regulation of guard cell  $K^+$  channels by phosphorylation and dephosphorylation events. A pharmacological approach using an inhibitor of the  $Ca^{2+}$ /calmodulin dependent protein kinase calcineurin was adopted by Luan *et al.* (1993). Treatment with the inhibitor removed the  $Ca^{2+}$  mediated inactivation of  $I_{K,in}$ , with the opposite effect seen in cells having the active form of calcineurin. Since, coexpression of CDPK and KAT1, a guard cell expressed channel has been shown to reduce current carried by KAT1 (Kamasani *et al.*, 1997). The target of CDPK phosphorylation *in vivo* is still unknown, although KAT1 can be directly phosphorylated *in vitro* in a  $Ca^{2+}$  dependent manner (Li *et al.*, 1998).

Protein phosphatases of both type 1 and type 2A (PP1 and PP2A) seem to be involved in regulating guard cell ion channels (Li *et al.*, 1994; Thiel and Blatt, 1994). Phosphatase activity can also be placed as part of the ABA mediated regulation from experiments with ABA insensitive mutants, defective in type 2C protein phosphatases (Leung *et al.*, 1994; Leung *et al.*, 1997). Expression of the mutant form of the *Arabidopsis* abil phosphatase 2C in *Nicotiana tabacum* suppressed the normal wild-type response of both  $I_{K,in}$  and  $I_{K,out}$  to ABA (Armstrong *et al.*, 1995).

### 1.3.4. Cytosolic pH.

Both internal and external pH can modulate  $K^+$  channel activity in guard cells.  $I_{K,out}$  is largely unaffected by external pH above 4.5, in contrast to  $I_{K,in}$ , which is activated by external acidification. Subsequent experiments confirmed the initial observations, suggesting that  $H^+$  can increase the number of activatable channels in the plasma

membrane (Blatt, 1992a; Ilan *et al.*, 1996). Cloned inward  $K^+$  channels known to be expressed in guard cells have allowed exploration of the molecular basis of external pH sensitivity. Both KAT1 and KST1, guard cell expressed  $K^+$  channels show pH sensitivity seen for the whole cell current in guard cells (Hoth *et al.*, 1997). Two histidine residues in KST1, one in the S3-S4 linker segment and one in the pore loop are responsible for conferring the acidification mediated activation. In fact, changing the pore histidine to an arginine residue inverts the pH sensitivity. The role of the pore in external pH sensing was also shown by pore domain swapping experiments, where the pH sensitivity characteristics of chimeric channels were identical to those of the channel whose pore was used (Hoth *et al.*, 2001).

Cytosolic pH is also of importance in regulating  $I_{K,in}$  and  $I_{K,out}$ , but the action appears to be by a different mechanism to that of the external pH effect, suggesting that the  $H^+$ -ATPase alone is not the dominant pathway for cytosolic pH regulation. Treatment with ABA does cause an alkalinisation of the cytosol in guard cells of between 0.03 and 0.4 (Blatt and Armstrong, 1993; Irving *et al.*, 1992). Alkalinisation of the cytosol by ABA activates  $I_{K,out}$ , an effect not seen when the cytosolic pH was buffered (Blatt and Armstrong, 1993).  $I_{K,in}$  showed opposite behaviour, and was activated by acidification and inhibited by alkalinisation (Blatt and Armstrong, 1993). In effect, the cytosolic pH response of both  $I_{K,in}$  and  $I_{K,out}$  was consistent with the response of these channels to ABA. Evidence from excised patches suggests that protons in the cytosol may interact with membrane bound components, possibly even the channels themselves (Miedema and Assmann, 1996). More detailed analysis of the pH signal has pointed towards an interaction with  $Ca^{2+}$  signalling, possibly in modulating elements of the  $Ca^{2+}$  signalling pathway (Grabov and Blatt, 1997).

### 1.3.5. Actin Filaments

Experiments using the actin antagonist cytochalasin D and the actin stabiliser phalloidin have implicated actin in stomatal function. Initial results showed that actin filaments were organised in a radial pattern in open stomata, and that treatment with cytochalasin D abolished this pattern (Kim *et al.*, 1995). Phalloidin treated guard cells failed to perform normal stomatal closure in response to ABA. Modulation of  $I_{K,in}$  was shown in response to cytochalasin D, with treated cells exhibiting whole cell currents of a higher amplitude (Hwang *et al.*, 1997). Interestingly *abil-1* plants do not show normal actin dynamics in response to ABA, neither do wild type plants when treated with kinase and phosphatase inhibitors (Eun *et al.*, 2001; Hwang and Lee, 2001). A role for  $Ca^{2+}$  has also been implied in guard cell actin dynamics (Hwang and Lee, 2001). Liu and Luan (1998) demonstrated that filament organisation was altered by osmotic shock, and suggested this may be a factor in the  $I_{K,in}$  inhibition they observed in response to hyperosmotic shock. Whether or not actin filaments are directly linked to  $I_{K,in}$  in guard cells as a turgor sensing mechanism is unclear. However, summation of the evidence thus far may indicate a role for actin as a signalling target relatively downstream of other known participants.

### 1.3.6. Heterotrimeric G-proteins

G-proteins have long been known to be involved in ion channel regulation. Heterotrimeric G-proteins function by binding GTP, which leads to dissociation of the component  $\alpha$  subunit from the  $\beta\gamma$  subunits, which may go on to regulate downstream signalling components (Brown and Birnbaumer, 1990; Wickman and Clapham, 1995). Evidence for G-protein regulation of guard cell ion channels is now mounting. The

existence and functioning of G-proteins as ion channel regulators in guard cells was implied by use of the non-hydrolysable GTP analogue GTP- $\gamma$ -S and its GDP equivalent GDP- $\beta$ -S (Fairley and Assmann, 1991). GTP- $\gamma$ -S was shown to decrease  $I_{K,in}$ , suggesting that GTP hydrolysis was required for normal  $I_{K,in}$  functioning. Interestingly, chelation of cytosolic  $Ca^{2+}$  removed the GTP- $\gamma$ -S inhibition of  $I_{K,in}$ , suggesting a role for  $Ca^{2+}$  in G-protein mediated control. The treatment of cells with pertussis toxin and cholera toxin, respectively G-protein agonist and antagonist, also decreased  $I_{K,in}$ . Studies with isolated patches showed that G-protein regulation could modulate  $I_{K,in}$  via membrane localised signalling cascades, and that modulation of channel activity was probably via changes in the open probability (Wu and Assmann, 1994). The role of a 7TMS receptor, a G-protein signalling component has also been implicated in regulating  $I_{K,in}$  (Armstrong and Blatt, 1995). The study used a 7TMS receptor mimetic, which inactivated  $I_{K,in}$ , an effect which was blocked by loading with GDP- $\beta$ -S. Kelly *et al.* (1995) produced evidence that conflicted with other studies, indicating opposite effects of GDP- $\beta$ -S, probably due to use of a different experimental approach. All these experiments were useful evidence of G-protein activity in guard cells, though direct evidence showing whether G-proteins are expressed in guard cells was lacking until recently. RT-PCR experiments with mRNA from guard cell protoplasts showed high expression levels of the  $G_\alpha$  subunit encoded by GPA1 (Wang *et al.*, 2001). T-DNA knockout mutants, *gpa1* showed a lack of stomatal opening inhibition in response to ABA, which could be attributed at the transport level to ABA insensitivity of  $I_{K,in}$ . ABA insensitivity was also observed in the anion currents, which showed decreased activation upon ABA stimulation. However, ABA induced stomatal closure was identical in wild type and *gpa1* plants,

suggesting signalling mechanisms controlling stomatal closure and inhibition by ABA may differ.

#### 1.4. Ion channels on the tonoplast

In most plant cells the vacuole forms a large part of the total cell volume. Indeed, the vacuole forms an important store of solutes of importance in stomatal movement, including  $K^+$ , anions and  $Ca^{2+}$ . The guard cell tonoplast is energised by a  $H^+$ -translocating inorganic pyrophosphatase (V-PPase) and a  $H^+$ -translocating phosphatase (V-ATPase) (Darley *et al.*, 1998). It is still unclear whether or not the V-PPase has the ability to transport  $K^+$  into the vacuole against its electrochemical gradient, and arguments have been presented both for and against (Davies *et al.*, 1992; Ros *et al.*, 1995; Sato *et al.*, 1994). However, it seems more plausible that the V-PPase indirectly energises the uptake of a  $H^+/K^+$  antiporter by setting the  $H^+$  gradient. Three classes of ion channels dominate the tonoplast. These are termed the fast vacuolar (FV), vacuolar  $K^+$  (VK) and slow vacuolar (SV) channels. Both the FV and VK channels are highly selective for  $K^+$  (Allen and Sanders, 1996). The SV channel was originally identified as being  $Cl^-$  permeable (Hedrich *et al.*, 1988). Subsequent investigations have rejected  $Cl^-$  permeability, and have shown permeability to  $K^+$ ,  $Mg^{2+}$  and  $Ca^{2+}$  (Ward and Schroeder, 1994; Allen and Sanders, 1996). However, in all cases the ionic conditions used in the experiments have a large effect on the permeability observed. The  $Ca^{2+}$  permeability provides a possible candidate pathway for  $Ca^{2+}$  induced  $Ca^{2+}$  release (CICR). FV, VK and SV all differ in their  $Ca^{2+}$  sensitivities. FV seems to be active only at  $[Ca^{2+}]_{\text{cyt}}$  below 100nM, whereas VK is active at  $[Ca^{2+}]_{\text{cyt}}$  above 100nM. The SV channel activates only at high  $[Ca^{2+}]_{\text{cyt}}$  (above 600nM). The fact that SV only responds to higher  $[Ca^{2+}]_{\text{cyt}}$  might rule out a

role during the early stages of CICR, though does not discount a role in sustaining elevated releases of  $[Ca^{2+}]_{cyt}$ .

## **1.5. $Ca^{2+}$ signalling in animals**

### **1.5.1. $Ca^{2+}$ sensing and influx pathways**

As already mentioned,  $Ca^{2+}$  is an important in the regulation of ion channels in guard cells. However, understanding of  $Ca^{2+}$  signalling in plants is far from advanced. Much of the work carried out in plants thus far has drawn heavily on exploring themes drawn from studies in animals. For this reason, a brief survey of some aspects of animal  $Ca^{2+}$  signalling is presented here. The first  $Ca^{2+}$  wave to be described was seen in fertilised oocytes (Berridge and Dupont, 1994). These wave events could be seen to propagate both spatially and temporally. Later, repetitive  $Ca^{2+}$  spikes were also described (Clapham, 1995). A variety of  $Ca^{2+}$  events have now been described, and significant progress has been made in elucidating the mechanisms and proteins involved. In animal cells,  $Ca^{2+}$  signals are short events, starting with a small 'elemental' signal that leads to  $Ca^{2+}$ -induced  $Ca^{2+}$  release (CICR). The source of the initial  $Ca^{2+}$  signal may be either release from internal stores caused by an effector, or influx across the plasma membrane (Berridge *et al.*, 2003). Uptake of  $Ca^{2+}$  from outside the cell may occur in response to a variety of signals ranging from depletion of internal stores through to depolarisation of the plasma membrane (Berridge *et al.*, 2003; Carafoli, 2003). A wide range of ion channels can mediate calcium entry into the cell. These channels include a large number of voltage-gated channels, receptor operated channels, and second messenger operated channels. Voltage-gated channels have been extensively studied, and form an important pathway for rapid  $Ca^{2+}$  entry during action potentials in neurons (Catterall, 1998). Uptake of  $Ca^{2+}$  in response to store depletion is mediated by store operated channels (SOCs). It is likely that SOC

are members of the TRP channel superfamily (Montell *et al.*, 2002). Cells are also able to sense and adapt to depleted extracellular  $\text{Ca}^{2+}$  by means of the extracellular  $\text{Ca}^{2+}$  receptor (CaR) (Hofer and Brown, 2003)

### 1.5.2. $\text{Ca}^{2+}$ release from internal stores

Triggers for release of  $\text{Ca}^{2+}$  from internal stores include  $\text{Ca}^{2+}$ ,  $\text{IP}_3$ , cADPR and NAADP (Berridge, 1998; Berridge *et al.*, 2003). The  $\text{IP}_3$  pathway is triggered by the synthesis of  $\text{IP}_3$  by phospholipase C (PLC), which then gates  $\text{IP}_3$  receptors which allow  $\text{Ca}^{2+}$  efflux from internal stores (Irvine, 2003). The characteristics of the  $\text{IP}_3$  mediated response depend on the hormone receptor activated (van der Wal *et al.*, 2001). The differences in  $\text{Ca}^{2+}$  signal generated may be the result of activation of different isoforms of PLC (Kim *et al.*, 1997). Protein-protein interactions are known to couple  $\text{IP}_3$  receptors both physically and functionally to  $\text{Ca}^{2+}$  entry pathways and hormone receptors at the plasma membrane. Specificity may also be governed by phosphorylation events (Carafoli *et al.*, 2001).

Both cyclic ADP ribose (cADPR) and NAADP are nucleotide signals, and are both produced by the same pathway, even the same enzyme in mammals. The product of the enzyme is dependent on the substrate used, which can be either NAD or NADP which give rise to cADPR and NAADP respectively (Lee, 1997). The role of NAADP is less well understood, but it is known that NAADP pathways of  $\text{Ca}^{2+}$  release cannot support CICR, and that NAADP receptors reside on the lysosomal membrane (Churchill *et al.*, 2002; Patel *et al.*, 2001). In contrast, cADPR is known to support CICR. Interestingly, cADPR does not bind directly to the ryanodine receptor, and requires an effector protein (Noguchi *et al.*, 1997). Like  $\text{IP}_3$  receptors, ryanodine



receptors form complexes with other proteins, including those that govern phosphorylation, and sensitivity to levels of  $\text{Ca}^{2+}$  in the lumen (Valdivia *et al.*, 1995).

The strength of the  $\text{Ca}^{2+}$  signal is related both to the type and the strength of the stimulus. Localised photolysis of caged  $\text{Ca}^{2+}$  has revealed that it is possible to trigger CICR from a single ryanodine or  $\text{IP}_3$  receptor, known respectively as quarks and blips, depending on the type of receptor involved (Bootman *et al.*, 1997; Lipp and Niggli, 1998). More commonly, groups of ryanodine and  $\text{IP}_3$  receptors work together as functional units to give rise to sparks and puffs (Cheng *et al.*, 1993; Yao *et al.*, 1995). Both sparks and puffs may be considered the events which are key to triggering spatial propagation of the  $\text{Ca}^{2+}$  signal, forming a  $\text{Ca}^{2+}$  wave.

## **1.6. Guard cell $\text{Ca}^{2+}$ signalling**

### **1.6.1. Early studies – $\text{Ca}^{2+}$ release from internal stores**

The first  $\text{Ca}^{2+}$  signalling event in guard cells was observed as a 3-5 minute elevation in  $[\text{Ca}^{2+}]_{\text{cyt}}$  in response to ABA (McAinsh *et al.*, 1990; McAinsh *et al.*, 1992). The ABA response of guard cells was sensitive in part to  $\text{Ca}^{2+}$  channel blockers, which hinted at a possible role of both  $\text{Ca}^{2+}$  influx and a release of  $\text{Ca}^{2+}$  from internal stores in generating the  $\text{Ca}^{2+}$  signal (McAinsh *et al.*, 1991). Subsequently,  $\text{Ca}^{2+}$  signals were shown in response to a wide range of external stimuli including external  $\text{Ca}^{2+}$ , ozone,  $\text{H}_2\text{O}_2$  and  $\text{CO}_2$  (Clayton *et al.*, 1999; McAinsh *et al.*, 1995; McAinsh *et al.*, 1996; Webb *et al.*, 1996). Progress has been made in identifying the components of the  $\text{Ca}^{2+}$  signalling systems, particularly in the context of ABA-induced stomatal closure.

$\text{Ca}^{2+}$  signalling in guard cells shares common themes with animal  $\text{Ca}^{2+}$  signalling. Guard cells are able to synthesise a range of phosphoinositides (Parmar and Brearley, 1993; Parmar and Brearley, 1995). There is evidence for  $\text{IP}_3$  mediated  $\text{Ca}^{2+}$  signalling in guard cells. Turnover of  $\text{IP}_3$  and its precursor phospholipids has been demonstrated in response to ABA in guard cells (Lee *et al.*, 1996). Furthermore, activation of phospholipase C activity is essential in the initiation of ABA induced  $\text{Ca}^{2+}$  oscillations and stomatal closure, something which has been demonstrated using both pharmacological and transgenic approaches (Hunt *et al.*, 2003; Staxen *et al.*, 1999).

Another inositol metabolite that has an important role is  $\text{IP}_6$ . ABA stimulates the production of  $\text{IP}_6$  in guard cells (Lemtiri-Chlieh *et al.*, 2000). Furthermore,  $\text{IP}_6$  inactivates  $\text{I}_{\text{K,in}}$  in guard cells in a  $\text{Ca}^{2+}$  dependent manner. It has recently been shown that  $\text{IP}_6$  can promote increases in  $[\text{Ca}^{2+}]_{\text{cyt}}$  by enhancing release from intracellular stores. Both SV and FV channels on the tonoplast were demonstrated to be targets for  $\text{IP}_6$ , and could be pathways of  $\text{Ca}^{2+}$  entry into the cytosol in response to  $\text{IP}_6$  (Lemtiri-Chlieh *et al.*, 2003).

### 1.6.2. $\text{Ca}^{2+}$ entry into the cell and its regulation

Evidence for  $\text{Ca}^{2+}$  entry through plasma membrane  $\text{Ca}^{2+}$  channels in guard cells was initially provided by Grabov and Blatt (1998). Cytosolic  $\text{Ca}^{2+}$  increases were observed in response to hyperpolarisation of the plasma membrane, and these increases were capable of facilitating inactivation of  $\text{I}_{\text{K,in}}$  (Grabov and Blatt, 1999). Imaging the  $\text{Ca}^{2+}$  increases gave sufficient spatial and temporal resolution to show that the  $\text{Ca}^{2+}$  increase was initiated in the proximity of the plasma membrane, then spreading to more central regions, suggesting  $\text{Ca}^{2+}$  induced  $\text{Ca}^{2+}$  release initiated by influx across

the plasma membrane (Grabov and Blatt, 1998). The pathway for  $\text{Ca}^{2+}$  influx via the plasma membrane has now been identified in both *Vicia faba* and *Arabidopsis* (Hamilton *et al.*, 2000; Pei *et al.*, 2000). Interestingly the properties of these channels differ significantly. The *Arabidopsis* channel shows little voltage dependent activity unless  $\text{H}_2\text{O}_2$  is present (Pei *et al.*, 2000). In contrast, the *Vicia* channel strongly rectifies at negative voltages and is sensitive to external  $\text{Ca}^{2+}$  (Hamilton *et al.*, 2000; Hamilton *et al.*, 2001). Although the channel shows much increased activity in response to ABA and  $\text{H}_2\text{O}_2$ , neither of these factors is a requirement for measuring channel activity (Hamilton *et al.*, 2000; Kohler and Blatt, 2002). Phosphorylation can also directly regulate the hyperpolarisation activated  $\text{Ca}^{2+}$  channels. Koehler and Blatt (2002) observed 'rundown' of the channel in the absence of ATP, and went on to show that phosphorylation of the channel or another membrane component is required for ABA activation of the channel.

### 1.6.3. Oscillations and encoding specificity in guard cell $\text{Ca}^{2+}$ signals

Since  $\text{Ca}^{2+}$  signalling responses are seen in response to a plethora of stimuli in guard cells and in other plant cell types, an important question that arises is how is specificity encoded in these signals. One candidate that might lead to specificity is the oscillation frequency, already shown to mediate levels of gene expression (Li *et al.*, 1998), control transcription factor activity (Dolmetsch *et al.*, 1998) and alter certain signalling cascade proteins (DeKoninck and Schulman, 1998). Allen *et al.* (2001) measured frequency and amplitude of guard cell  $\text{Ca}^{2+}$  oscillations. They found that both parameters could vary when induced by different external  $\text{Ca}^{2+}$  concentrations, having a larger amplitude and lower frequency at higher external  $\text{Ca}^{2+}$ . Plants defective in V-ATPase expression (*det3*), which is thought to be important for

energising endomembrane transport, were also studied. These plants failed to produce  $\text{Ca}^{2+}$  oscillations, though they were still able to increase cytosolic  $\text{Ca}^{2+}$ . In contrast *det3* and wild type plants showed similar oscillatory behaviour in response to ABA, though in both the oscillations differed to those seen in response to external  $\text{Ca}^{2+}$  (Allen *et al.*, 2000). Of particular significance were the results on hyperpolarisation induced  $\text{Ca}^{2+}$  oscillations, which extended previous observations by Grabov and Blatt (1998). Calcium oscillations were seen in response to hyperpolarising conditions where external  $\text{Ca}^{2+}$  was present, the frequency of which was dependent on the length of time spent in the hyperpolarisation buffer. The farnesyltransferase mutant *eral-2* has also been shown to have altered  $\text{Ca}^{2+}$  oscillations. In response to ABA *eral-2* guard cells show greater increases in  $[\text{Ca}^{2+}]_{\text{cyt}}$ , which can be attributed to enhanced activity of the plasma membrane  $\text{Ca}^{2+}$  channel (Allen *et al.*, 2002).

The plasma membrane  $\text{Ca}^{2+}$  channel in *Arabidopsis* is ABA insensitive in the *abi1-1* and *abi2-1* mutants. This has been shown to be due to the inability of *abi1-1* plants to synthesise reactive oxygen species and the inability of *abi2-1* plants to respond to synthesised or exogenously applied  $\text{H}_2\text{O}_2$  (Murata *et al.*, 2001). The authors also show that NADPH may be the substrate for  $\text{H}_2\text{O}_2$  production. Confirmation of the importance of NADPH in ABA induced control of  $\text{Ca}^{2+}$  signalling came from studies of *AtrbohD* and *AtrbohF* single and double mutants, which have severely reduced  $\text{H}_2\text{O}_2$  production in response to ABA. These plants fail to show ABA induced stomatal closure, and are unable to initiate ABA induced oscillations in  $[\text{Ca}^{2+}]_{\text{cyt}}$  (Kwak *et al.*, 2003). The defective oscillations were shown to be caused by ABA insensitivity of the plasma membrane  $\text{Ca}^{2+}$  channel, whose, ABA sensitivity required ROS production.

#### **1.6.4. Sensing external $\text{Ca}^{2+}$**

The fact that  $\text{Ca}^{2+}$  signalling in guard cells is responsive to external  $\text{Ca}^{2+}$  has been demonstrated (Grabov and Blatt, 1998; Grabov and Blatt, 1999). One candidate external  $\text{Ca}^{2+}$  sensor is the voltage gated  $\text{Ca}^{2+}$  channel, which responds to external  $\text{Ca}^{2+}$  (Hamilton *et al.*, 2001). However the mechanism of  $\text{Ca}^{2+}$  sensing is not clear. One possible mechanism might be through the  $\text{Ca}^{2+}$  sensing receptor (CAR) recently isolated (Han *et al.*, 2003). The CAR is a single membrane spanning domain protein with no homology to the animal CaR discussed earlier. The CAR has the ability to bind up to 12  $\text{Ca}^{2+}$  at the N terminus of the receptor, with a  $K_d$  for  $\text{Ca}^{2+}$  of about 1.2mM. The study demonstrated that the CaR is essential for  $\text{Ca}^{2+}$  induced stomatal closure and CICR, but seems not to be essential for ABA induced stomatal closure. No indication is available as yet as to how the CAR might relay the external  $\text{Ca}^{2+}$  signal to the cell. It is possible that the CAR might form an important part of a  $\text{Ca}^{2+}$  'signalosome' with other proteins, possibly including  $\text{Ca}^{2+}$  channels, an avenue which is now likely to be explored.

#### **1.7. Guard cell anion channels.**

##### **1.7.1. S- and R-type anion channels**

Anion channels are of crucial importance in guard cells, since they may facilitate depolarisation of the membrane and promoting stomatal closure. They also have a role in charge balance when  $I_{K,out}$  is active. Initial characterisation lead to the idea that there were two different types of anion current in guard cells, referred to as S- and R-type currents. S-type currents are slowly activating, and were shown to increase in response to increasing cytosolic  $\text{Ca}^{2+}$  (Schroeder *et al.*, 1990; Allen *et al.*, 1999). In contrast, R-type currents, which activate and subsequently deactivate rapidly, were

shown to respond to external  $\text{Ca}^{2+}$  (Hedrich *et al.*, 1990). The physiological role of the R-type current is as yet unknown, since the whole cell current seems to be dominated by the S-type current (Grabov *et al.*, 1997). One suggestion is that both the S and R-type currents are carried by the same channel, which switches between different gating modes (Dietrich and Hedrich, 1998; Raschke, 2003). The molecular identity of guard cell anion channels remains unknown. Pharmacological studies have shown that ATP binding cassette (ABC) transporter antagonists inhibit S-type anion currents, which provides some evidence that the channels could belong to the ABC transporter family, in common with other anion channels (Leonhardt *et al.*, 1999).

#### **1.7.2. Regulation of anion channels**

As for guard cell  $\text{K}^+$  currents, phosphorylation is likely to be important in anion channel regulation. Studies using the protein kinase inhibitor K252a showed that inhibition of protein kinase activity strongly inhibited S-type anion channel activity (Schmidt *et al.*, 1995), though similar inhibition was not seen by use of broad range protein kinase inhibitors in impaled guard cells (Grabov *et al.*, 1997). Candidate protein kinases have been identified in guard cells which are both  $\text{Ca}^{2+}$  dependent and independent (Li and Assmann, 1997; Mori and Muto, 1997; Lee and Assmann, 1998). Molecular identification of a  $\text{Ca}^{2+}$  dependent ABA activated protein kinase (AAPK) has been achieved (Li *et al.*, 2000). Expression of a mutant form of AAPK abolished ABA induced activation of S-type anion currents.

Protein phosphatases were shown to be important in studies using both the inhibitors and by studies with *abil* plants (Schmidt *et al.*, 1995; Grabov *et al.*, 1997; Pei *et al.*, 1997). Results were conflicting, with Pei *et al.* (1997) showing loss of ABA activation

in *abi1-1* and *abi2-1* whilst Grabov *et al.* (1997) showed no change of whole cell anion currents in response to ABA in *abi1-1* transformed *N. benthamiana* plants. Differences in approach are likely to account for the conflicting results.

## **1.8. Membrane trafficking in guard cells.**

### **1.8.1. Measuring changes in membrane surface area**

The large volume changes guard cells undergo in transition between opening and closing the stomatal aperture require retrieval and insertion of plasma membrane material, since the plasma membrane can only stretch by some 2% without breakage (Wolfe and Steponkus, 1981; Wolfe and Steponkus, 1983). In recent years, changes in membrane surface area in guard cells have been measured using capacitance techniques. Since membrane capacitance is proportional to surface area, measurement of capacitance allows real time analysis of exo- and endocytosis at high resolution using a variant of the patch clamp technique (Homann and Tester, 1998). Initial studies with guard cell protoplasts showed that varying osmotic conditions stimulated changes in the surface area of the protoplasts (Homann, 1998). Hypo-osmotic conditions lead to an increase of up to 60% in the surface area of the protoplasts, with a decrease of similar magnitude seen in response to hyperosmotic conditions. The results were consistent with the changes in guard cell volume that are seen in response to favourable and unfavourable osmotic conditions *in planta*. The amplitude of the capacitance response of the protoplast was proportional to the osmotic gradient imposed, and the process was shown to be  $\text{Ca}^{2+}$  independent (Homann, 1998). The response to hyperosmotic shock was explored further by combining styryl dye labelling of the plasma membrane with capacitance measurements, and internalisation of membrane was observed (Kubitscheck *et al.*, 2000). Internalisation resulted in a

pool of membrane material close to the plasma membrane. The proximity of this membrane to the plasma membrane itself suggests it is an ideal source of membrane for rapid reincorporation to increase cell surface area, though as yet there is no evidence that this is the case. More recently, it has been found that hydrostatic pressure can stimulate exocytosis in guard cell protoplasts (Bick *et al.*, 2001). The stimulation however had a maximum threshold, above which no further exocytosis is seen. This may be the guard cell's mechanism for controlling the maximum size and is likely to be mediated in part by actin, since treatment with the actin inhibitor cytochalasin D could allow exocytosis above the normal maximum threshold (Bick *et al.*, 2001). Such results again may suggest a link between signalling controlling guard cell volume and signalling controlling ion channels, since actin filaments have been shown to regulate guard cell  $K^+$  channel activity as previously discussed (Hwang *et al.*, 1997); Liu and Luan, 1998).

### **1.8.2. SNARE proteins and ABA signalling in guard cells**

The cloning of a SNARE protein involved in ABA perception in guard cells further strengthens the case for a link between exocytotic/cell volume control of ion channel channels in guard cells. The proteins NtSyr1 from tobacco and AtSyr1 from Arabidopsis (redesignated Syp121 by Sanderfoot *et al.*, 2001) were isolated by Leyman *et al.*, (1999) through a heterologous screen to isolate an ABA receptor. The assay was based on the fact that ABA can induce increases in cytosolic free  $Ca^{2+}$ , and exploited endogenous  $Ca^{2+}$  activated  $Cl^-$  currents in *Xenopus* oocytes as a marker for ABA induced  $Ca^{2+}$  increases. A response was seen when *N. tabacum* mRNA was injected into oocytes, and following sub-fractionation a single clone was identified. The clone had homology to the syntaxin family, and shared common features with



mammalian syntaxins such as the H3 domain and the H<sub>a-c</sub> domains. A function of the syntaxin in guard cell ion channel regulation was shown by loading with the Bot N/C toxin, which specifically cleaves syntaxins. Treatment with Bot N/C removed the ABA sensitivity of  $I_{K,in}$  and  $I_{Cl}$  in impaled guard cells. Loading of a truncated NtSyr1 lacking the transmembrane domain removed the wild-type response of both  $K^+$  channels and  $I_{Cl}$ , suggesting that the cytosolic domain had competitive inhibitor activity (Leyman *et al.*, 1999).

### 1.8.3. Membrane fusion: an overview

Eukaryotic cells are delimited and compartmentalised by membranes. Some of these membrane bound structures form a transport network for the movement of material within the cell, and to and from the cell's external environment. Membrane fusion events are essential for exchange between compartments, and must be tightly regulated to ensure that compartments retain both their integrity and identity. The process of membrane fusion itself is complex. In the aqueous environment, considerable repulsive forces exist which make it impossible for two phospholipid bilayers to fuse spontaneously. A number of proteins have now been identified that are essential for both driving and regulating the fusion process (Chen and Scheller, 2001; Jahn and Sudhof, 1999; Lin and Scheller, 2000). It is also essential that the fusing compartments remain intact during the fusion process, so that there is no loss of compartment contents or integrity. This is achieved by the formation of a fusion pore between the distal membranes, which then enlarges and allows fusion of the proximal membranes (Jahn and Sudhof, 1999). The composition of the fusion pore is still open to debate. There are two opposing views; one that there is formation of a fusion pore whose content is mainly proteinaceous (Lindau and Almers, 1995) and the

other opinion that the fusion pore is mainly lipid (Monck *et al.*, 1995). The most extensively described membrane fusion process is that of exocytosis, the model system for which has been the process of neurotransmitter release (Jahn and Sudhof, 1999). It is becoming increasingly clear, however, that certain common features are shared in all eukaryotic cells.

#### **1.8.4. Membrane fusion proteins – components of the SNARE complex**

The first insights into the molecular basis of membrane fusion and vesicle trafficking came from study of the *N*-ethylmaleimide (NEM) block of golgi vesicle trafficking, which lead to the purification of a protein involved in the trafficking process. The protein was named NEM-sensitive fusion protein (NSF) (Block *et al.*, 1988). NSF was shown to be a soluble ATPase of 100 kDa, thought initially to exist in trimeric form (Whiteheart *et al.*, 1994) though a later study suggested that a hexameric form was more likely (Fleming *et al.*, 1998). NSF action was shown to require the action of another soluble protein, named soluble NSF attachment protein (SNAP) which was a 37 kDa protein purified from both bovine brain and yeast cells. SNAPs exist in multiple isoforms, though the  $\alpha$ -SNAP isoform is expressed in most tissues (Clary *et al.*, 1990).

$\alpha$ -SNAP and NSF were also found as a 20S complex with other proteins in neuronal cells (Sollner *et al.*, 1993). This complex contained three previously cloned proteins: VAMP, Syntaxin and SNAP-25. Vesicle associated membrane protein 1 (VAMP 1 – also known as synaptobrevin) was cloned by screening an expression library with antibodies raised against purified synaptic vesicles (Trimble *et al.*, 1988). VAMP-1 was found to be a 120 amino acid protein possessing a C terminal transmembrane

domain, and is classified as v-SNARE because of its location on the vesicle membrane. Syntaxin 1 was also cloned using an expression cloning strategy (Bennett *et al.*, 1992). As for VAMP-1 it has a C terminal membrane anchor. Immunofluorescence microscopy localised syntaxin 1 to the presynaptic membrane, thus it is a designated target SNARE (t-SNARE). SNAP-25 is a 25kDa protein that was cloned from neuronal cells, and shown to be membrane associated (Oyler *et al.*, 1989). In contrast to the other complex proteins, SNAP-25 lacks an obvious transmembrane anchor domain. Although it was suggested that the amphipathic nature of the N terminus might facilitate alignment with membranes, subsequent analysis revealed that the cysteine rich region is probably palmitoylated, with the palmitic acid residues acting to anchor the protein to the membrane (Arai *et al.*, 1990). SNAP-25 is also classed as a t-SNARE. VAMP, syntaxin and SNAP-25 alone are sufficient to allow membrane fusion *in vitro* (Weber *et al.*, 1998) and the complex is commonly known as the SNAP receptor (SNARE) complex.

#### 1.8.5. SNARE complex structure

The SNARE complex is thought to be held together by hydrophobic interactions which occur via so-called 'coiled-coil' domains (Chapman *et al.*, 1994; Spring *et al.*, 1993) which consist of heptad repeats of amino acids. The site of interaction between syntaxin 1A and both VAMP 1 and 2 was placed between amino acids 194 and 267, proximal to the transmembrane domain (Calakos *et al.*, 1994). This domain is commonly referred to as the H3 domain. Three other syntaxin domains which are important in complex formation, Ha, Hb and Hc. These are located N-terminally and 3D structural analysis indicates that these Ha,b,c domains fold autonomously (Fernandez *et al.*, 1998) and regulate the availability of the H3 domain for complex

formation with SNAP-25 and VAMP (Calakos *et al.*, 1994; Chapman *et al.*, 1995). VAMP proteins have a coiled coil domain which spans the major part of the cytosolic portion of the protein, being around 60 amino acids in size (Trimble *et al.*, 1988). SNAP-25 has 2 coiled-coil domains, interrupted by the cysteine rich palmitoylation domain (Veit *et al.*, 1996).

The first crystal structure of a SNARE complex was published in 1998 (Sutton *et al.*, 1998). Experiments used the cytosolic domain of synaptobrevin II, the H3 domain of syntaxin 1A and both the N and C termini of SNAP-25B. The topology of the complex was found to be cylindrical, and the four component helices arranged in a bundle. As expected, the coiled-coil domains of each protein formed the centre of the cylinder. At the very centre of these coiled-coil domains there were four key residues, three glutamines and an arginine, one residue from each of the four helices that comprise the complex. The surface charge profile also showed specific charge domains of possible significance in the interaction with regulatory proteins .

Syntaxin is able to interact with the protein nSec1 (commonly referred to as Munc-18, Munc-18-1 and also rbSec1). In neurons this interaction can only take place when the syntaxin is not in a complex, and binding of nSec1 induces a conformational change in the syntaxin, which forms a closed conformation (Dulubova *et al.*, 1999; Misura *et al.*, 2000). Crystallographic analysis indicates that nSec1 structure is the same whether it is bound to syntaxin or not (Bracher *et al.*, 2000; Misura *et al.*, 2000) . It is likely that the role of nSec1 is to stabilise the closed conformation and regulate whether or not the SNARE complex forms or not, though the fact that nSec1 can bind

the SNARE complex in yeast (Carr *et al.*, 1999) suggests that it may either have multiple roles or that it has different roles in different organisms and cell types.

In neuronal cells,  $\text{Ca}^{2+}$  is an important regulator of vesicle fusion at the pre-synaptic membrane. A calmodulin binding protein was isolated and cloned from synaptic vesicles (Perin *et al.*, 1990) and later named synaptotagmin. Generation of mice carrying a mutation in synaptotagmin 1 showed a role for the protein in  $\text{Ca}^{2+}$  triggered exocytosis, possibly forming part of the  $\text{Ca}^{2+}$  sensing apparatus (Brunger, 2001; Geppert *et al.*, 1994). Schiavo *et al.* (1997) showed that synaptotagmin can directly interact with SNAP-25 in a  $\text{Ca}^{2+}$  independent manner. However, binding with two other SNAREs, Syntaxin and VAMP was only possible in the absence of  $\text{Ca}^{2+}$ . Indeed,  $\text{Ca}^{2+}$  binding results in conformational changes in synaptotagmin which lead to oligomerisation of the protein, which has been suggested to cue the assemble of the membrane fusion machinery to allow the fusion event to take place (Desai *et al.*, 2000).

#### **1.8.6 Regulation of SNARE complex assembly**

Small GTPases are involved in the assembly of SNARE complexes. Of particular interest in the case of synaptic SNARE complexes is the Rab GTPase Rab3a, a synaptic vesicle protein (Sudhof, 1997). The Rab GTPase family has many members that are know to function in vesicle trafficking, and are generally 25 to 30kDa monomeric proteins, anchored into the membrane by isoprene units (Rutherford and Moore, 2002). In common with all GTPases, Rab proteins have the ability to function as molecular switches by changing between GTP and GDP bound states. An important regulatory feature is that GTP and GDP exchange can only happen at the

site of action in the cell (Zerial and McBride, 2001). Another important feature of Rabs is that they have a requirement for effector proteins.

The membrane tethering process is primarily dependent on Rabs and their effectors. Tethering may involve both symmetrical or asymmetrical recruitment of Rabs to the target and donor membranes (Cao *et al.*, 1998). The yeast Rab Sec4p facilitates the tethering of Golgi vesicles to the plasma membrane. The localisation of the protein to the bud formation zone of the plasma membrane ensures that cell polarity is maintained (Finger *et al.*, 1998). This tethering role is also important in clathrin coated vesicle formation (Bucci *et al.*, 1992). Rab proteins are also a component of the vesicle budding machinery. Whether or not Rab1 facilitates budding has been controversial, and the answer seems dependent on the experimental system used (Allan *et al.*, 2000; Nuoffer and Balch, 1994). A role in vesicle movement along the cytoskeleton has also been shown: Rab5 and Rab6 seem to be important for microtubule dependent movement (Hill *et al.*, 2000), whereas Sec4p and Rab27a seem to act on actin-myosin based vesicle movement, possibly via direct interaction with myosin itself (Menasche *et al.*, 2000; Schott *et al.*, 1999).

In neurons Rab3 functions in the assembly of the SNARE complex and also seems to regulate the vesicle targeting process, since *rab-3* knockout *C. elegans* show accumulated vesicles throughout the length of the axon that seem to be unable to reach the fusion zone and are compromised in their ability to fuse (Nonet *et al.*, 1997; Sogaard *et al.*, 1994). Kinetic and quantal analysis of vesicle docking in *rab3A* mouse hippocampal neurons showed a lack of control of the number of fusion events per stimulus as compared with wild type, suggesting yet another role for Rab3 in the

fusion process (Geppert *et al.*, 1997). A clue as to the apparent diversity of function attributed to Rab3A may come from the effector proteins with which it interacts, namely rabphilin-3A and rim, which respectively localise to the vesicle and presynaptic plasma membranes (Stahl *et al.*, 1996; Wang *et al.*, 1997). The mode of action of these effectors is as yet largely unknown, although the Rab3A/rabphilin-3A complex has been crystallised (Ostermeier and Bronger, 1999).

#### **1.8.7. Direct interactions between SNARE proteins and ion channels.**

Local increases in cytosolic free  $\text{Ca}^{2+}$  have long been associated with synaptic vesicle release. These increases occur as  $\text{Ca}^{2+}$  microdomains close to the presynaptic membrane, and are in the order of 200-300  $\mu\text{M}$  (Llinas *et al.*, 1992). Because of spatial and temporal restrictions, it is not surprising that the  $\text{Ca}^{2+}$  channels responsible for the  $\text{Ca}^{2+}$  increase and the secretory machinery are closely linked. A link between  $\text{Ca}^{2+}$  channels and syntaxins has been long established. The first cloned syntaxin (1A) was isolated as a co-immunoprecipitation partner to an N-type  $\text{Ca}^{2+}$  channel (Bennett *et al.*, 1992a). Subsequent co-expression experiments with syntaxin 1A and N and L-type channel pore subunits showed that syntaxin was able to modulate the behaviour of these channels (Wiser *et al.*, 1996). In both channel types, current amplitudes were reduced by up to 70%, with kinetic alterations in activation and deactivation also evident. Truncated syntaxin 1A lacking the transmembrane anchor domain did not show altered channel parameters, suggesting that this domain was important for the interaction and effect of syntaxin 1A on the gating of N and L-type  $\text{Ca}^{2+}$  channels (Wiser *et al.*, 1996). Biochemical data supports this idea, showing that syntaxin residues 181 to 288 are essential for this interaction *in vitro* (Sheng *et al.*, 1994). The

site of interaction on the  $\text{Ca}^{2+}$  channels appears to be an 88 amino acid sequence in the loop between the second and third transmembrane domain, known as the synprint site (Sheng *et al.*, 1994). Both synaptotagmin and SNAP-25 can also bind to N and L-type  $\text{Ca}^{2+}$  channels (Leveque *et al.*, 1994). Association of SNARE proteins with the synprint site is  $\text{Ca}^{2+}$  dependent, with maximal binding *in vitro* observed at  $20\mu\text{M}$   $\text{Ca}^{2+}$ , which corresponds well with the threshold for  $\text{Ca}^{2+}$  induced fusion *in vivo* (Sheng *et al.*, 1996). Beyond this concentration,  $\text{Ca}^{2+}$  channels will dissociate from the SNARE complex. This is probably a key step, which actually allows fusion of synaptic vesicles to take place.

The cystic fibrosis transmembrane regulator (CFTR) is a chloride channel also regulated by SNARE proteins. Co-expression of CFTR with syntaxin 1A lead to decreased chloride current amplitude (Naren *et al.*, 1997). In contrast to the findings with  $\text{Ca}^{2+}$  channels, the cytosolic domain of syntaxin 1A was the binding site of the channel. Specific binding analysis shows that the N terminal cytoplasmic domain of CFTR interacts with the H3 domain of syntaxin 1A (Naren *et al.*, 1998).

### **1.9. SNARE proteins in plants.**

Although Nt-Syr1 was the first plant syntaxin to be isolated in the context of ion channel control, other syntaxins had previously been cloned. KNOLLE is a protein from the syntaxin family that was isolated by positional cloning of an embryo development mutant in *Arabidopsis* (Lukowitz *et al.*, 1996). The *knolle* mutation is in fact thought to be involved in the formation of the cell plate during cell division (Lauber *et al.*, 1997). Another cytokinesis mutant, *keule*, displays a similar phenotype, and was postulated to be potentially related to KNOLLE in some way. The recent



positional cloning of KEULE has proven that to be the case, since the gene encodes a Sec1 homologue (Assaad *et al.*, 2001). The authors were also able to demonstrate that KEULE and KNOLLE interact *in vitro*. The role of both proteins in cytokinesis was supported by *keule knolle* plants that were completely unable to undergo cytokinesis.

All the SNARE proteins in *Arabidopsis thaliana* are now known, though most of the information published to date comes from *in silico* analysis. The *Arabidopsis* genome contains 24 syntaxins (*Arabidopsis* genome initiative, 2000) which have been phylogenetically analysed and renamed according to group (SYP1-8) and subgroup (Sanderfoot *et al.*, 2000). Other SNARE sequences include 3 genes encoding SNAP25 homologues, two membrin orthologues, 14 VAMPs (Sanderfoot *et al.*, 2000). There are sequences for proteins which interact with SNAREs including a single NSF, and two  $\alpha$ -SNAPs (Sanderfoot *et al.*, 2000). From experimental work published it is clear that genetic dissection of the function of SNARE proteins in plants is far from straightforward, and there is a need to find alternative means of analysis. Insertional mutagenesis of SYP2 and SYP4 family members leads to unviable pollen, thus showing that both families lack redundancy (Sanderfoot *et al.*, 2001a).

#### **1.10. Focus of the research.**

Guard cells have been a model system for the study of ion transport and signalling in plants for the last 20 years. Whilst significant progress has been made in identifying the main pathways for ion transport in guard cells, much work has yet to be done to unravel the signalling components and regulatory networks that coordinate ion transport. Two new avenues for exploration have recently opened: one is the identification of nitric oxide (NO) as an essential component of ABA-induced

stomatal closure (Garcia-Mata and Lamattina, 2002; Neill *et al.*, 2002), and the other the discovery of a possible link between ion channel regulation and membrane traffic (Leyman *et al.*, 1999; Homann and Thiel, 2002; Hurst *et al.*, 2004). The aim of this study is to explore the role of NO as a signalling molecule and possible ion channel regulator, and to examine the interaction of vesicle trafficking and its machinery with guard cell ion channels and  $\text{Ca}^{2+}$  signalling.

## **CHAPTER 2:**

# **MATERIALS AND METHODS**

## 2.1 Techniques for studying ion channels.

A range of techniques are available to study transport of ions across membranes. The technique of choice is dependent on the nature of the biological question being addressed. Choice of technique relies on balancing the need for physiological reality with the need for biophysical definition. Radiotracer flux analysis can be used to measure fluxes of ions in whole cells or tissues (MacRobbie, 1981), thus leaving cells relatively undisturbed. The disadvantage of the system is that there can be no control over membrane voltage. Patch clamping has increasingly become the technique of choice. Patch clamping in plants requires the removal of the cell wall in order to gain access to the plasma membrane so that a high resistance seal may be formed. This can be by laser ablation (Henriksen *et al.*, 1996) or more commonly by enzymatic digestion of the cell wall (Tester, 1990; Ward, 1997). The technique has the advantage that both whole cell and single channel data can be obtained. Voltage clamping is possible, along with a degree of control of the composition of solutes on both sides of the membrane. The technique is applicable to a wide range of cell types. Recent advances in cell marking technology have made it possible to identify the tissue of origin of protoplasts derived from multi tissue digestions (Maathuis *et al.*, 1998). Ion channels may also be incorporated into planar lipid bilayers (White and Tester, 1994). This allows for high-resolution measurements of single channels. It also allows for measurement of ion channels on endomembrane systems, which are not easily accessible for patch clamp measurements.

Another technique traditionally used is to impale cells with microelectrodes. Impalement with a single barrel allows measurement of the membrane potential, and can give an insight into the transport processes occurring across that membrane.

Voltage clamping may be performed in certain cell types, provided these cells are electrically isolated from other cells (Blatt, 1987; Gradmann *et al.*, 1978; Sanders, 1988). Discontinuous single electrode voltage clamping may be carried out, (e.g. Forestier *et al.*, 1998; Raschke *et al.*, 2003), however it is more common to use a second barrel for two electrode voltage clamping. The impalement technique allows the study of cells in a more physiological context than patch clamping or bilayer studies, whilst retaining a reasonable level of resolution.

Voltage clamping is a vital tool for studying the transport of ions across membranes. It is a difficult task to study ionic currents under conditions where the free running membrane potential is constantly changing. Thus voltage clamping provides a constant specified voltage, allowing the components of the current across the membrane to be studied.

It is useful for us to consider ion channels as enzymes that catalyse the thermodynamically 'downhill' movement of ions. In such instances, the electrochemical gradient across the membrane is a 'substrate' for the movement of these ions, such that positive ions will move towards the compartment which is relatively negative, and *vice versa*. The electrochemical gradient between the compartments either side of the membrane is termed the membrane potential. Measurement of the membrane potential gives us an insight as to which ionic species will tend to move in which direction under a given set of conditions. The membrane potential is of added importance in some cases, since certain membrane transporters, for example ion channels, symporters (e.g.  $H^+$ / sucrose symporter), and ion pumps (e.g.  $H^+$ -ATPases) respond directly to voltage.

## 2.1 Electronic Setup and Voltage Clamping.

The total current flowing across the membrane,  $I_m$ , of any given cell has two basic components: The ionic current due to the movement of charged ionic species across the membrane,  $I_{ionic}$ , and the membrane capacitance,  $C_m$ . Thus:

$$I_m = I_{ionic} + C_m \frac{\delta V}{\delta t}$$

Where  $\delta V/\delta t$  is the change of voltage with respect to time. Thus, when the voltage is clamped, ( $\delta V/\delta t = 0$ ) the equation can be simplified:

$$I_m = I_{ionic}$$

Thus the current flowing across the membrane when the voltage change is removed is representative of the ionic currents

The voltage clamp circuit used to clamp the membrane potential to a required value is a negative feedback loop (Figure 2.1). The membrane potential is measured by one barrel of the electrode and recorded by the preamplifier. The preamplifier has a high input resistance to minimise current leakage into the microelectrode and prevent current draw from the microelectrode. Both current leakage and current draw can introduce errors into the measurement of the membrane potential. The measured membrane potential is compared to the computer generated command value by a high gain differential amplifier (Y-Science, Glasgow, UK). The difference between the two

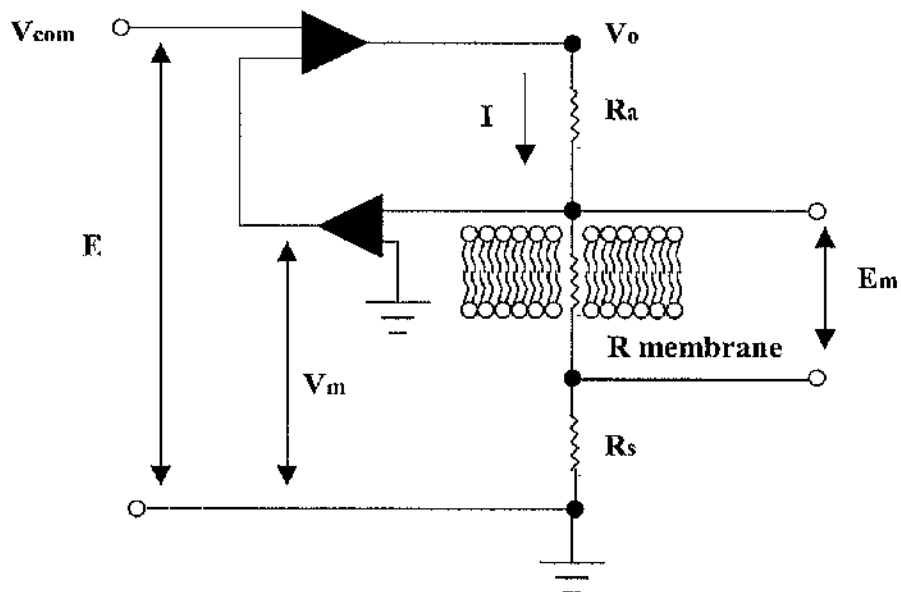


**Figure 2.1. A simplified voltage clamp circuit (Blatt, 1991).** The specified voltage command ( $V_{com}$ ) is generated by a computer and sent to the clamping amplifier. The preamplifier output ( $V_m$ ) is compared to  $V_{com}$  by the clamping amplifier, which then outputs a current into the cell via the microelectrode ( $R_a$ ).

voltages is inverted, amplified then sent back as a current via the second barrel of the microelectrode. The amplitude of the current required to clamp the membrane potential is equal to the inverse of the membrane current. For the work described here the command voltage was generated by a Pentium II<sup>®</sup> 450 computer (Dell, UK) running the Henry EP suite program (generated in-house). Data was digitised to produce binary data for storage onto the hard disk using a WyeScience Digital-Analogue converter (Y-Science, Glasgow, UK). Before storage, data was low pass filtered by a 6-pole Bessel filter at either 0.3 or 1 kHz.

### **2.3 Noise and vibration isolation.**

Measurements at the resolution used are particularly sensitive to electrical interference. There are three common sources of such interference. Cables connecting the half-cells to the amplifier and BNC cables connecting various parts of the setup may pick up radiative electrical noise from outside sources such as lights, computers and other equipment or from the mains supply. In addition, noise may enter the setup via magnetic induction. Such problems were overcome by using shielded cables to connect the half-cells to the amplifier, and also by enclosing the microscope, micromanipulator, chambers and electrodes in a Faraday cage. Vibration is a possible source of problems with the setup since the size of the cells impaled is small, such that even the smallest disturbances could be detrimental to the survival of the impaled cell. This was overcome by keeping the distances between the base of the micromanipulator and the electrode to a minimum by making short half-cells and electrodes. Additionally, apparatus within the Faraday cage was placed on a vibration isolation table (Photon Control, Cambridge, UK).



## 2.4 Electrodes.

Microelectrodes were pulled from capillary borosilicate glass with a triangular cross section, the wall thickness 0.25mm and an internal diameter of 1.25mm (Dial Glassworks, Stourbridge, West Midlands, UK.). The puller used was a modified two stage PD5 horizontal puller (Narashige Scientific Instrument Lab, Tokyo, Japan.). Either two or three barrels were clamped into the puller and then heated for 20 seconds without pulling before twisting through 360°. The barrels were then allowed to cool for 30 seconds before pulling. Heater and magnet settings were adjusted to optimise shape and tip size. Typical pulling times for optimal tip size and shape were around 30-45 seconds for double barrelled electrodes and 80 - 120 seconds for triple barrelled electrodes. In order that the electrodes could be inserted into half-cells and secured, barrels were heated in a small gas flame and shaped using forceps.

Microelectrodes were filled using a 2ml syringe attached to a 200µl Gilson tip that had been pulled to a fine tip in a small gas flame. The triangular cross-section allowed simple filling of the microelectrodes whereby the tip was filled by capillary action, followed by back filling to the top of the barrel. The standard filling solution for all the barrels was 0.2 M potassium acetate (titrated to pH 7.5 with dilute acetic acid). Potassium acetate was chosen to minimise the possibility of salt loading artefacts . Barrels were coated with paraffin wax to reduce capacitance and connected to the headstage amplifier by half-cells. One barrel was sealed into a half-cell using molten dental wax (Type 1 impression compound, Kerr UK Ltd., Peterborough, UK.), whilst the others were manoeuvred into contact with the half-cell solution using the micromanipulator controls.

## **2.5 Half-cells.**

Half-cells were used as the means to connect the microelectrode to the voltage clamp apparatus. Half-cells were home made using methods previously described (Blatt, 1991). Casing for the half-cells was provided by cutting approximately 5cm of a 2ml Sterilin disposable pipette. A silicone rubber bung of an appropriate size was cut using a cork borer and inserted into the end of the pipette section. A piece of silver wire (approximately 5cm in length) was cut and soldered onto a jack. The wire was cleaned to remove the silver oxide layer, then inserted through the silicone bung and then pushed through until the jack was flush with the end of the pipette. A silver chloride layer was applied by filling the half-cells with sodium hyperchlorite solution (12% w/v available chlorine) for at least 2 hours in the dark. The solution was then removed and the inside of the half-cell rinsed and then filled with 1M KCl. Half-cells were stored at 4°C in 1M KCl. During storage, jacks were connected together to ensure electrical equivalence. The method of construction of the reference (bath) half-cell was the same, with the following exceptions. A glass pipette was used in place of plastic, and a plastic sleeve was screwed on to the jack end to allow easy clamping to the chamber housing. Electrical contact between the reference half-cell and the bath was by means of a salt bridge. The bridge was made by filling polythene tubing (Portex, Hythe, Kent, UK) with 2% agar dissolved in 1M KCl. This was cut into appropriate lengths and sealed into the half-cell by use of dental wax. Salt bridges were used for multiple experiments.

## **2.6 Chamber and housing design.**

Experiments were carried out using custom made chambers constructed of stainless steel blocks glued onto a thin glass slide with silicon adhesive (RS components,

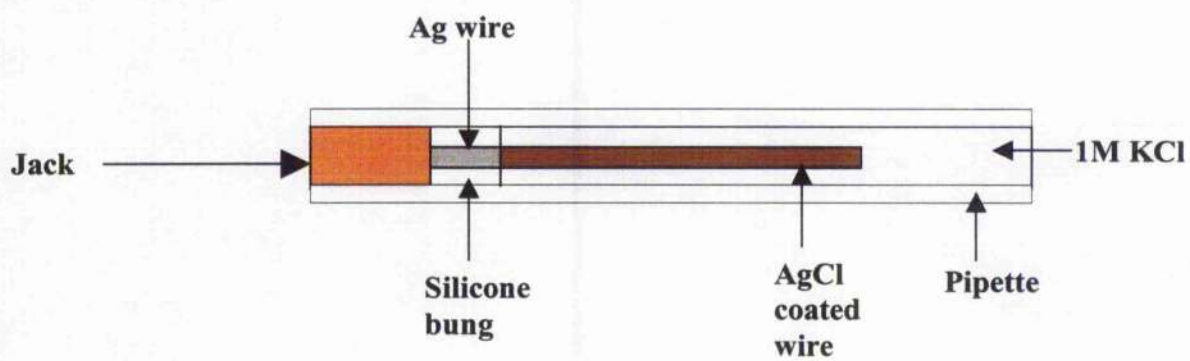


**Figure 2.2 Representation of a half-cell (cross sectional view, not to scale).**

Corby, Northants, UK.) (see Figure 2.3). The larger of the two blocks had a 1.5mm diameter hole drilled into it to allow insertion of the agar salt bridge into the chamber solution. A coverslip was used to form the top of the chamber. The chamber was attached to the microscope stage via a purpose built housing. The housing also provided means of securing the reference half-cell.

Solution perfusion was by means of a gravity fed flow system. Solutions were contained in aspirator flasks, each connected via PTFE tubing to a valve system giving two separate lines allow efficient changing between different solutions. A dual, four-way stopcock was fitted to enable solution flow from both sets of lines simultaneously, one to the chamber and another to a waste flask. Solution flow rate could be adjusted by a luer lock valve attached to the needle, which fed solution into the chamber. Waste solution was removed by means of a Pasteur pipette that had been drawn to a fine tip in a Bunsen flame. This was secured to a micromanipulator to allow adjustment of the position. The waste pipette was connected to a plastic tube leading to a 5L waste flask, which in turn was connected to a 1L flask containing silica gel, then to either a pump or a vacuum line outside the Faraday cage. Use of silica gel was to help remove water from the vacuum line, which can act as an antenna for electrical noise.

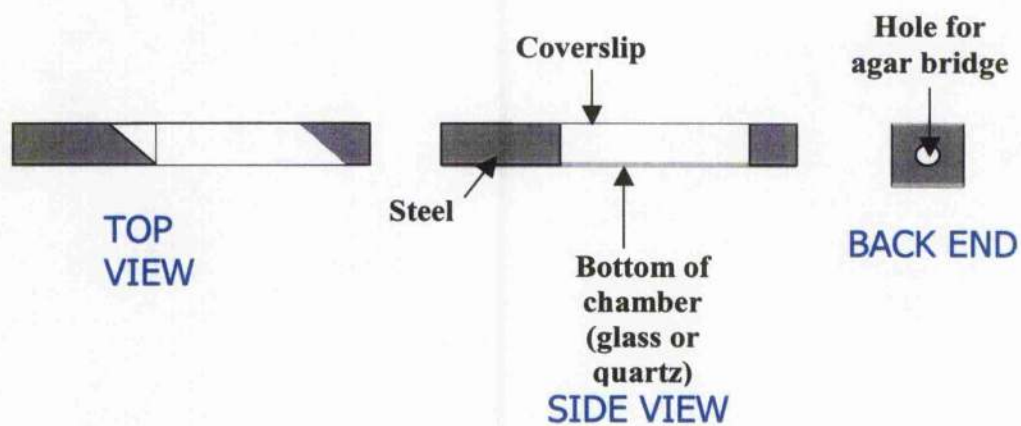


**Figure 2.3. Detail of chamber design.** Steel blocks are attached to the glass/quartz base using silicon adhesive. Coverslips were attached following chamber preparation using pressure sensitive adhesive.

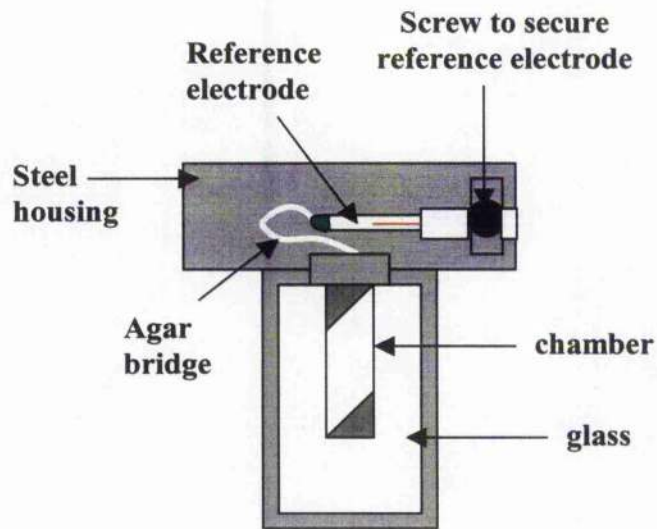


**Figure 2.4. Housing with chamber and reference electrode assembled.** Chamber was fixed in position using a small screw. Agar bridge was inserted through the back of the chamber and the reference electrode secured as shown. The agar bridge was secured in place using dental wax.

## 2.7 Experimental Procedure.

*Nicotiana tabacum* 'Petite Havanna' seeds were sown twice weekly by spreading approximately 30 seeds onto the surface of a 12cm diameter pot containing pre-watered compost. Pots were kept in a glasshouse (16 hours lights, 8 hours darkness) in propagators with the lids on (100% humidity) until shortly after germination. Once plants were 0.5cm, a suitable number of individuals were transferred into individual pots (20cm diameter). Plants used for experiments were typically at the 4 leaf stage, usually around 4 weeks after germination. *Vicia faba* cv Bunyard's Exhibition plants were sown in 15cm diameter pots, three seeds in each pot. Once sown, all *V. faba* plants were kept in a growth chamber (Conviron, Winnipeg, Canada) with 16hours light, 8 hours darkness, 70% humidity. In all cases, epidermal peels were taken from the abaxial side of the leaf using sharp forceps, cut with a razor blade and then mounted in the chamber using pressure sensitive medical adhesive (PSA 50/50, Factor II Inc., Lakeside, Arizona, USA). The adhesive was spread on the chamber in an 'H' shape and allowed to air dry for at least 15 minutes prior to mounting to ensure sufficient solvent evaporation. Epidermal strips were fixed to the adhesive by applying gentle pressure using thumb and forefinger. The strip was immediately bathed in the standard buffer (5mM Ca-MES containing either 0.1 or 10mM KCl). A coverslip was fixed to the top of the chamber using two small spots of adhesive. The chamber was then secured into the housing and the agar bridge of the reference half-cell placed through the blocks into the chamber and fixed in place. The housing was then fixed into position on the microscope stage. The solution delivery needle and suction pipette to remove solution were both manoeuvred into position and perfusion was started immediately. Tissue was examined for suitable cells using either an Axiovert 35 or an Axiovert S100 TV (Carl Zeiss Microscopy, Jena, Germany) fitted

with Nomarski Differential Interference Contrast (DIC) optics. Microelectrodes were moved into position using a Fluxley-type micromanipulator to within 1mm of the tissue by eye, then guided down to rest on the opposing guard cell to the target cell using both low (x100) and high (x400) magnification. The cell dimensions were measured using an ocular micrometer and cell surface area and volume were calculated assuming cylindrical geometry. The microelectrode tip was then advanced against the cell wall of the target cell then gently inserted. Cells chosen were typically small and highly turgid cells from young leaves, since these often were easiest to impale and allowed recording of large currents. Treatments were applied to the cells by additions to the standard buffer as described in each chapter. All chemicals were analytical grade either from Sigma (Sigma-Aldrich Ltd., Poole, Dorset, UK), BDH (Merk Ltd., Poole, Dorset, UK.), or Fluka (Fluka Ltd, Poole, Dorset, UK.).

## **2.8 Separation and analysis of ionic currents**

There are three main ways of dissecting the whole cell currents obtained by voltage clamping. Firstly, it is possible to exclude certain ions from the measurement solutions so that the ions available as charge carriers are controlled. In the case of patch clamping, where a degree of control over the solutions on both sides of the membrane is possible, this approach can be readily used. However, in whole cell impalement experiments the possibility of controlling ionic composition in the cytosol is limited. Secondly, it is possible to use toxins and blocking agents that eliminate the contribution of ion channels that are not of interest. Such agents include toxins derived from venom such as dendrotoxin, or ions such as  $\text{TEA}^+$ , both of which block  $\text{K}^+$  channels (Tester, 1988; Weller *et al.*, 1985). This pharmacological approach can be particularly useful if the ion channel of interest is masked by the activity of other



ion channels that dominate the membrane. An example in guard cells is the use of TEA<sup>+</sup> to eliminate K<sup>+</sup> currents, enabling the study of anion channels (Grabov *et al.*, 1997). However, even when steps have been taken to block or avoid measuring unwanted currents, current traces must be examined for background ion channel activity and the IV profiles corrected accordingly. Both I<sub>K,in</sub> and I<sub>K,out</sub> in guard cells are no exception. The activity of both the H<sup>+</sup>-ATPase and anion channels are evident in the K<sup>+</sup> channel recordings, contributing to the instantaneous current seen at the beginning of the voltage clamp step (Figure 2.4). In guard cells this instantaneous current (I<sub>i</sub>) may be subtracted from the maximal current (I<sub>max</sub>), giving the time-dependent (I<sub>td</sub>) current that represents K<sup>+</sup> channel activity.

Kinetic information may also be gained from analysis of currents recorded by voltage clamp. This information may come from the IV profiles and the activation kinetics of the current. Data plotted as IV curves may be fitted with the Boltzmann function (equation 2.1), which is of the form:

$$I = \left( \frac{g_{\max}(V - E_K)}{1 + e^{\delta z F(V - V_{1/2}) / RT}} \right) \quad \text{Equation 2.1}$$

Where  $g_{\max}$  is the maximum conductance, V the clamp voltage,  $E_K$  the equilibrium potential for K,  $V_{1/2}$  the voltage giving half maximal current activation, z the gating charge, F the Faraday constant,  $\delta$  the gating charge, R the gas constant and T the absolute temperature. In all cases, data presented in this thesis were fitted with  $E_K$  fixed to -75mV, consistent with external K<sup>+</sup> of 10mM and internal K<sup>+</sup> of about 200mM.

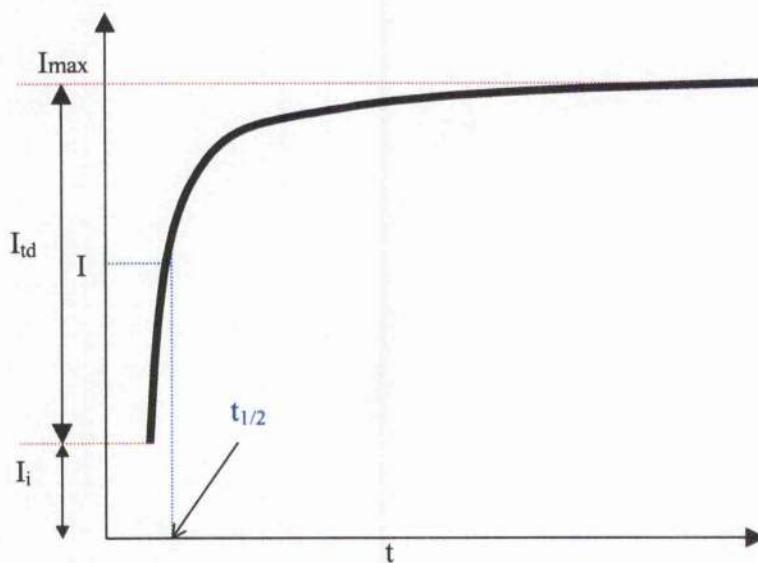


**Figure 2.5. Details of current trajectory analysis.** Components of the total current are shown. The instantaneous current ( $I_i$ ) is subtracted from the maximal current ( $I_{\max}$ ) to obtain the time-dependent current ( $I_{td}$ ). The halftime ( $t_{1/2}$ ) is also shown.

compares favourably with measured values. Any changes seen in the  $V_{1/2}$  and  $\delta$  in response to treatments were interpreted as changes in channel gating (further discussion of this is given in the results where appropriate). Current traces may be analysed to determine the halftime of current activation ( $t_{1/2}$ ), as shown in figure 2.5. The halftime of activation is  $0.693 \times \tau$ , (which is the time constant for current activation), can give information about any changes in channel kinetics that have occurred in response to a given treatment. Whilst  $\tau$  can only be obtained by fitting of exponential curves,  $t_{1/2}$  could be determined empirically using Henry software (Y-Science, Glasgow, UK).

## **2.9 $\text{Ca}^{2+}$ imaging**

### **2.9.1. Choice of probe**

There are a range of fluorescent probes available for the measurement of  $\text{Ca}^{2+}$  *in vivo*, the first of which to be developed was quin-2 (Tsien and Poenie, 1986). There is now a whole range of probes available that can be excited by both ultraviolet (UV) and visible light. One of the most commonly used probes is fura-2, which is UV excitable. The majority of the probes are based on  $\text{Ca}^{2+}$  chelating compounds, particularly EGTA and BAPTA. In the case of fura-2, it contains the 4 carboxylic acid moieties that are responsible for  $\text{Ca}^{2+}$  binding in EGTA along with aromatic and heterocyclic rings that give the fluorescent properties to the molecule (see figure 2.6). Binding of  $\text{Ca}^{2+}$  leads to withdrawal of the N lone pair electrons from the ring, thus causing a shift in the excitation spectrum with no real change in the emission maximum (Tsien and Poenie, 1986). Thus fura-2 can be used as a ratiometric probe, since the ratio between the free dye (measured at 380nm) and the  $\text{Ca}^{2+}$  bound dye (measured at 340nm) can be related to the  $\text{Ca}^{2+}$  concentration. There are distinct advantages and

disadvantages to using fura-2. It may be loaded by a number of means, including iontophoretic and pressure injection, acid loading and passive loading of the esterified form. The fact that fura-2 is a ratiometric dye reduces errors in the results caused by photobleaching. It has a relatively high fluorescence yield, and low  $Mg^{2+}$  sensitivity (McCormack and Cobbold, 1991). A major problem with the use of fura-2 is its high rate of photobleaching. Rapid data acquisition causes rapid photobleaching, and so the timeframe available during high temporal resolution measurements is short, typically no longer than 20 minutes. This problem cannot simply be overcome by loading larger amounts of fura-2, as this will have a detrimental effect on measured  $Ca^{2+}$  concentrations and the  $Ca^{2+}$  buffering effect compromises the ability of cells to respond.

Fura-2 was the  $Ca^{2+}$  probe of choice in this study, due mainly to its ease of use. Other probes are often difficult to use in guard cells. The photoprotein aequorin can be either microinjected or stably transformed. However the spatial resolution with aequorin is poor, since the fluorescence yield is low (Brownlee, 2000). Recent development of GFP variants to image  $Ca^{2+}$  has been very successful (Miyawaki *et al.*, 1997; Miyawaki *et al.*, 1999). These proteins can be imaged with high spatial resolution, but require two-photon confocal imaging apparatus. Plants must also be stably transformed with the constructs.

### **2.9.2. Fura-2 loading methods.**

Fura-2 may be loaded into cells by a variety of methods. The molecule (as presented in figure 2.6) is in itself cell impermeant in most buffers. It can however be acid loaded, or more commonly microinjected or pressure injected into cells. Fura-2 may

also be obtained in acetoxymethyl ester (AM ester) form, which is membrane permeable. Once in the cytosol the fura-2 is released by endogenous esterases. This technique has severe limitations in that it is difficult to ascertain the extent of de-esterification in the cytosol, making calibration difficult. In plant cells use of fura-2-AM is further complicated by the presence of esterase activities in the cell walls, leading to poor uptake (Kuchitsu *et al.*, 2002). Both AM ester loading and acid loading were attempted as means of loading guard cells in this study. AM ester loading of fura-2 as described by was not successful with either *V. faba* or *N. tabacum*.

Acid loading of cells was attempted using solutions described by MacRobbie (1981). Visual checks of confirmed that it was possible to acid load fura-2, however in all cases the loaded cells were unresponsive to hyperpolarisation when impaled with double-barrelled microelectrodes. Experiments were carried out where the incubation time and external fura-2 concentration were manipulated, however the necessary control over the loading process could not be gained.

All  $\text{Ca}^{2+}$  experiments presented here were carried out using iontophoretic loading. Triple barrelled microelectrodes were manufactured as described above. The third barrel was filled with fura-2 and electrodes were mounted on the micromanipulator as described for the double-barrelled microelectrodes. Cells were observed using at 630x magnification with additional magnification from a 2.4x optivar. The target cell was centred in the field of view and three background images were taken before impalement. Image acquisition was carried out using a GenIV intensified Pentamax-512 charge-coupled device camera (Princeton Instruments, Trenton, NJ, USA).

Excitation wavelengths of 340nm and 390nm were specified using a monochromator. Exposure times were 400ms and 500ms at 340nm and 390nm respectively. Between exposures, the monochromator set the wavelength to 590nm. The fluorescence excitation source was a xenon arc lamp (Osram, Munich, Germany). Background fluorescence could be subtracted offline by averaging the three images acquired prior to impalement and subtracting them from the images of loaded cells. Image acquisition was controlled by MetaFluor, and offline analysis was carried out using MetaMorph (Universal Imaging Software, Media, PA, USA). Images in this study are presented using the 'Tsien' colour scale, with the exception of kymographs and their associated images, which are presented in pseudo-colour scale for clarity.

Following impalement, cells were perfused with 5mM Ca-MES (pH6.1), 10mM KCl immediately clamped to -50mV to prevent spontaneous hyperpolarisation (Grabov and Blatt, 1998). Fura-2 was ejected from the electrode by application of a negative going current. The amplitude of the injected current was kept to a minimum, since higher currents increased the likelihood of blocking the injection barrel and dye crystallisation in the tip. Blocked tips could often be cleared by reversing the current polarity for a short time, or by switching in the capacitance control module to a level that caused the system to oscillate (known as 'ringing'). Dye loading continued until the fluorescence intensity at 340nm was between 400 and 750, dependent on the size of the cell. Estimated fura-2 concentrations in loaded cells were  $< 10\mu\text{M}$

### 2.9.3. Calibration

Fluorescence measurements were related to  $[Ca^{2+}]_{\text{cyt}}$  according to equation 2.2:

$$[Ca^{2+}] = K_d \left( \frac{Sf_2}{Sb_2} \right) \left( \frac{R - (\eta R_{\min})}{\eta(R_{\max} - R)} \right) \quad \text{Equation 2.2}$$

Where  $R_{\max}$  and  $R_{\min}$  are the fluorescence ratios in saturating  $Ca^{2+}$  and zero  $Ca^{2+}$  respectively, and  $Sf_2$  and  $Sb_2$  the fluorescence intensity at 380nm in  $Ca^{2+}$  free and  $Ca^{2+}$  bound conditions respectively,  $R$  the ratio,  $K_d$  the dissociation constant (224nM, as described by Grynkiewicz *et al.* (1985), and  $\eta$  the viscosity (which was defined as 1). Calibration was carried out *in vitro* as follows. Solutions were prepared to define the fluorescence in  $Ca^{2+}$  free and saturated  $Ca^{2+}$  concentrations. The  $Ca^{2+}$  free solution contained 5mM HEPES (pH 7.5), 50mM BAPTA, 10mM KCl, 10 $\mu$ M fura-2 and the saturated  $Ca^{2+}$  solution contained 5mM HEPES (pH 7.5), 1mM  $CaCl_2$ , 10mM KCl and 10 $\mu$ M fura-2. Solution droplets were placed on a microscope slide under a coverslip. The depth of the solution droplet was defined by resting the coverslip on other fragments of 100 $\mu$ M coverslip, thus defining a solution depth similar to that of the epidermal layer. Images were taken with both solutions at a gain setting of 50, as used in the imaging experiments. Calibration gave minimum and maximum ratios of 0.5 and 3 respectively, with  $Sf_2$  and  $Sb_2$  of 3 and 1 respectively.

### 2.9.4. Numerical analysis

Where appropriate, data are expressed as mean  $\pm$  standard error (SE) of (n) observations. Significance of any observed differences between treatments was assessed by calculating the 95% confidence interval ( $1.6 \times \Sigma$  SE).

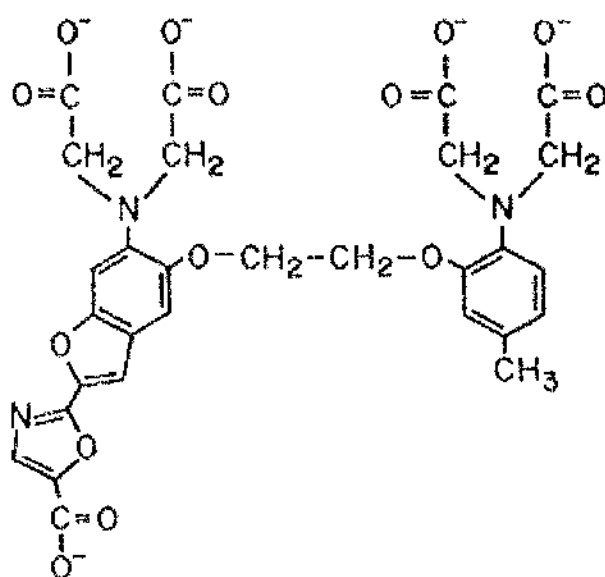


**Figure 2.6.** The structure of fura-2. Taken from McCormack and Cobbold (1991). The  $\text{Ca}^{2+}$  is bound by the tetra carboxylic acid groups of the EGTA moiety.



**CHAPTER 3:**  
**NITRIC OXIDE AND ABA SIGNALLING IN**  
**GUARD CELLS**

### 3.1. Introduction

Nitric oxide (NO) has emerged as an important molecule in both mammalian and plant physiology. The chemical properties of NO make it a good candidate as a signalling molecule. As a reactive free radical gas it has a relatively short half-life, yet is soluble in both lipid and aqueous environments, allowing diffusion from cell to cell and also within cellular compartments (Lamattina *et al.*, 2003; Neill *et al.*, 2003; Stamler *et al.*, 1992; Wojtaszek, 2000). Since the discovery of NO as an endothelial relaxing factor (Ignarro *et al.*, 1987), it is now known that NO is implicated in a myriad of physiological processes in mammals, ranging from regulation of blood pressure and platelet aggregation through to immune responses and neurotransmission (Gibson and Garbers, 2000; Jaffrey and Snyder, 1995; Moncada *et al.*, 1991). Nitric oxide has received much less attention in plants until relatively recently. Initially, studies focussed on the problems associated with the toxic effects of NO. Indeed, emission of NO by herbicide treated plants and the negative effects of pollutant NO on plant growth were demonstrated some time before the discovery of NO in mammals (Anderson and Mansfield, 1979; Klepper, 1979). It is now known that NO can also have a protective role in plants by acting as an antioxidant to mop up other free radicals (Beligni *et al.*, 2002; Beligni and Lamattina, 1999a; Beligni and Lamattina, 1999b; Beligni and Lamattina, 2002).

In mammals, NO is synthesised by the enzyme nitric oxide synthase (NOS). The NOS enzyme is a homodimer, and three isoforms have been identified and characterised. Two of the NOS isoforms show constitutive expression in endothelial (eNOS) and neuronal cells (nNOS), whilst the third is inducible (iNOS) (Furchgott, 1995; Groves and Wang,

2000). NO is synthesised in a two-step reaction from L-arginine, producing NO and L-citrulline (Campos *et al.*, 1995; Korth *et al.*, 1994). In plants, NO synthesis is far from well characterised. A range of studies have been carried out using both pharmacological and immunological approaches which have indicated the presence of animal-type NOS in plants (Barroso *et al.*, 1999; Delledonne *et al.*, 1998; Durner *et al.*, 1998; Ribeiro *et al.*, 1999). However, the *Arabidopsis* genome does not contain a mammalian NOS-like sequence (Garcia-Mata and Lamattina, 2003). Possible candidate enzymes include nitrate reductase (NR) which can produce NO both *in vitro* and *in vivo* (Desikan *et al.*, 2002; Rockel *et al.*, 2002; Yamasaki and Sakihama, 2000). A variant of the glycine decarboxylase P protein has been suggested as a candidate plant iNOS since it displays NOS like activity (Chandok *et al.*, 2003). Another NOS candidate has also been identified, and is required for NO synthesis in *Arabidopsis* guard cells (Gou *et al.*, 2003). Non-enzymic methods of NO production include the conversion of NO<sub>2</sub> to NO by carotenoids (Cooney *et al.*, 1994).

NO seems to be a central part of plant responses to pathogens, particularly in the induction of the hypersensitive response (HR) and systemic-acquired resistance (SAR) (Durner *et al.*, 1998; Delledonne *et al.*, 1998; Neill *et al.*, 2003; Lamattina *et al.*, 2003). Synthesis of NO accompanies the production of other reactive oxygen species (ROS) and lead to changes in gene expression necessary for initiating programmed cell death and restriction of pathogen spread (Beligni *et al.*, 2002). There is also evidence to suggest that NO signalling in plants may share common themes with NO signalling in animals. It has been established that a major route for mammalian NO signalling occurs via cyclic GMP

(cGMP). NO can bind to the soluble form of guanylyl cyclase, which leads to a 400 fold increase in cGMP production (Friebe and Koesling, 2003). In *Arabidopsis* suspension cultures, inhibition of guanylyl cyclase lead to inhibition of pathogen induced cell death that is normally seen upon pathogen infection (Clarke *et al.*, 2000). Treatment of plants with an NO donor has also been shown to lead to elevation of cGMP levels and promote the induction of cyclic ADP ribose, another NO signalling component from animals which is also know to operate in plants (Durner *et al.*, 1998; Allen *et al.*, 1995).

More recently NO has received some attention in the context of guard cell signalling. Application of NO donor compounds to plants can lead to enhanced drought tolerance. The enhanced drought tolerance can be attributed to induction of  $\text{Ca}^{2+}$  dependent stomatal closure by NO (Garcia-Mata and Lamattina, 2001). Using the NO sensitive dye diaminofluorescein-2 diacetate (DAF-2DA) (see Kojima *et al.*, 1998), it was subsequently shown that application of ABA can induce *de novo* synthesis of NO in guard cells in *Vicia faba*, *Pisum sativum* and *Arabidopsis thaliana* (Garcia-Mata and Lamattina, 2002; Neill *et al.*, 2002; Desikan *et al.*, 2002). In all cases the production of NO was essential for ABA mediated stomatal closure. However, there is an apparent divergence in the source of the NO between species. ABA-induced stomatal closure in *Pisum* was abolished by NOS inhibitors (Neill *et al.*, 2002). In *Arabidopsis* double mutant *nia1*, *nia2* plants which have very low levels of NR activity, NO production induced by ABA was strongly inhibited, and the cells showed an ABA insensitive phenotype in stomatal closure assays (Desikan *et al.*, 2002).

Whilst there is evidence for a role for NO in ABA signalling in guard cells, data on the mechanistic basis for its action is lacking. In animal systems there is a body of evidence indicating that NO can regulate membrane transport processes. Certain ion channels show altered gating in response to NO, including  $\text{Ca}^{2+}$ -dependent  $\text{K}^+$  channels,  $\text{Ca}^{2+}$  channels and  $\text{Na}^+$  channels (Bolotina *et al.*, 1994; Clementi and Meldolesi, 1997; Renganathan *et al.*, 2001; Tang *et al.*, 2001). Indeed, Neill *et al.* (2002) demonstrated that cADPR pathways might be important in the NO response in guard cells. It was decided to investigate the effect of NO on known transport and signalling processes involved in ABA signalling in guard cells. Both  $I_{\text{K,in}}$  and  $I_{\text{K,out}}$  were recorded under voltage clamp, and  $\text{Ca}^{2+}$  signalling events followed by use of the patch clamp technique and by imaging  $\text{Ca}^{2+}$  dynamics during voltage clamp. Results show that NO regulates  $I_{\text{K,in}}$  and  $I_{\text{Cl}}$  channels at the plasma membrane via a cGMP/cADPR triggered  $\text{Ca}^{2+}$  release, and that NO mediated ion channel control is an essential part of ABA triggered events leading to stomatal closure.

### 3.2. Materials and methods.

Measurements of  $K^+$  channel activity and  $Ca^{2+}$  imaging were performed as described in chapter 2. The following provides an outline of procedures used for experiments in this chapter. For  $K^+$  channel measurements, guard cells were impaled with double barrelled microelectrodes and currents recorded under voltage clamp using bipolar staircase protocols (detail in section 3.3). For  $Ca^{2+}$  experiments cells were impaled with triple barrelled microelectrodes, with the third barrel was filled with Fura-2. After impalement cells were clamped to  $-50mV$  so as to avoid triggering  $Ca^{2+}$  signals which occur during spontaneous hyperpolarisation of the plasma membrane (Grabov and Blatt, 1998). Cells were loaded with fura-2 by iontophoretic injection. Voltage step and ramp protocols were used to evoke increases in  $[Ca^{2+}]_{cyt}$  (Grabov and Blatt, 1997; Grabov and Blatt, 1999). Intracellular free  $Ca^{2+}$  concentrations were determined by the ratio of the fluorescence intensities as described in section 2.9.

For both  $K^+$  channel measurements and  $Ca^{2+}$  imaging experiments, cells were bathed in the standard buffer (5mM Ca-MES (pH 6.1), 10mM KCl) which was supplemented where necessary with 20 $\mu$ M ABA, 10 $\mu$ M SNAP, 20 $\mu$ M c-PTIO, 1 $\mu$ M ryanodine and 20 $\mu$ M ODQ. All compounds were added to the standard buffer from concentrated stocks. ABA, SNP, SNAP and c-PTIO were prepared as stocks in EtOH (1:1 EtOH water for SNAP). Ryanodine and ODQ were prepared as stocks in DMSO. Since SNAP and SNP spontaneously release NO upon dissolving, fresh stocks were made daily and kept in the freezer to slow NO release. Stock solutions containing SNAP and SNP were discarded after 5 hours and fresh stocks prepared.

Patch clamp experiments in this chapter were carried out as previously described (Hamilton *et al.*, 2000; Hamilton *et al.*, 2001; Kohler and Blatt, 2002).

### 3.3. Results.

#### 3.3.1. NO targets $I_{K,in}$ and $I_{Cl}$

The effect of the NO donor compounds SNP and SNAP on  $I_{K,in}$  and  $I_{K,out}$  currents in intact *Vicia faba* cells was assayed. Epidermal strips were perfused with solutions containing either 10 $\mu$ M SNP ( $n = 22$ ) or SNAP ( $n = 27$ ) and currents recorded by voltage clamp using double-barrelled microelectrodes. Figure 3.1 shows data from one representative cell treated with 10 $\mu$ M SNAP. Both original current traces and steady-state IV curves show that 10 $\mu$ M SNAP induced a significant decrease in  $I_{K,in}$  but not in  $I_{K,out}$ . The effect was complete within 1 minute and could be fully reversed by washout with either 10mM KCl, 5mM Ca-MES (pH 6.1) for 4-6 minutes or 20 $\mu$ M c-PTIO for two minutes. Even after prolonged treatment of cells for up to 10 minutes with 10 $\mu$ M SNAP,  $I_{K,out}$  remained unaltered. Fitting of IV curves to a Boltzmann function showed that the half-maximal activation voltage ( $V_{1/2}$ ) was shifted negative from  $-173 \pm 4$  mV to  $-192 \pm 9$  mV, a displacement of about -18mV, suggesting that NO alters  $I_{K,in}$  channel gating. Figure 3.2A summarises the effects of NO on  $I_{K,in}$  and  $I_{K,out}$ . Mean  $I_{K,in}$  current amplitude at -200mV before treatment was  $-0.52 \pm 0.08$  nA, decreasing significantly to  $-0.15 \pm 0.05$  nA upon application of 10 $\mu$ M SNAP. The change in  $I_{K,in}$  current amplitude was more than a 3-fold decrease. Washout with 20 $\mu$ M c-PTIO allowed recovery of  $I_{K,in}$  to  $-0.44 \pm 0.06$  nA, which is not significantly different from current amplitude before treatment ( $n = 27$ ). Mean  $I_{K,out}$  current before treatment was  $1.3 \pm 0.1$  nA which showed a slight decrease to  $1.2 \pm 0.1$  nA with 10 $\mu$ M SNAP, followed by a slight increase to  $1.5 \pm 0.1$  nA upon washout with 20 $\mu$ M c-PTIO. However these changes were not significant ( $n = 27$ ).



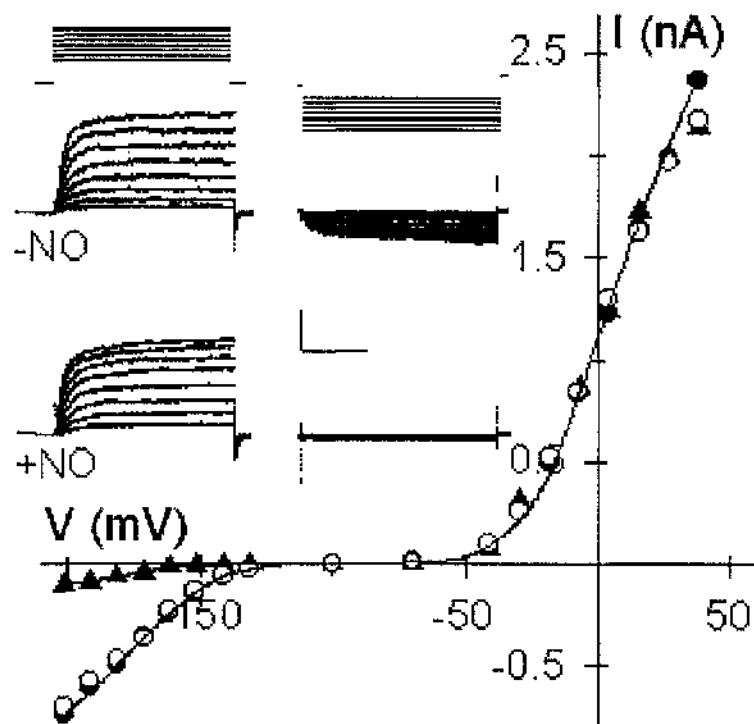


**Figure 3.1 NO inhibits  $I_{K,in}$  but not  $I_{K,out}$ .** Voltage-clamp recordings from an intact *Vicia* guard cell are shown. Steady-state current-voltage curves determined from voltage-clamp steps before (●), after 2 min of exposure to 10  $\mu$ M SNAP (▲), and after 6 min of washing in buffer-SNAP (○).  $K^+$ -channel currents were obtained by subtracting instantaneous current from steady-state current at each voltage. Data for  $I_{K,in}$  and  $I_{K,out}$  are shown with fitted Boltzmann functions. (Inset) Current traces for  $I_{K,out}$  (Left) and  $I_{K,in}$  (Right) before (Middle) and during (Bottom) NO treatment. Zero current is indicated on the left. Voltage protocols (Top) of steps between -200 and +50 mV from holding voltage of -100 mV are shown. (Scale: horizontal, 2 s; vertical, 1 nA.)

The effect of NO on the background currents was also examined. It has been previously demonstrated that the background currents are representative of anion channel activity (Grabov *et al.*, 1997; Pei *et al.*, 1997). Figure 3.2B shows the response of  $I_{Cl}$  to 10 $\mu$ M SNAP. Current was determined as the instantaneous current at -200mV. Current amplitudes were comparable to those seen by in patch clamp experiments. Upon treatment  $I_{Cl}$  increased from -44pA to -108pA ( $n = 22$ ), representing a 2-fold increase in current. This increase was also fully reversible within the same timescale as shown for  $I_{K,in}$ .

The effect of NO on the activation kinetics of  $I_{K,in}$  was examined. Halftimes for current activation were determined before and after treatment with SNAP. The mean halftime for activation of  $I_{K,in}$  at -200mV before treatment was  $314 \pm 35$ ms, similar to values previously reported (Armstrong and Blatt, 1995; Blatt, 1988). Halftimes altered to  $538 \pm 72$ ms ( $n = 8$ ) in SNAP and  $593 \pm 85$ ms ( $n = 6$ ) in SNP, indicating that NO slowed the activation kinetics of  $I_{K,in}$ . The slowing of  $I_{K,in}$  activation kinetics combined with the change in the  $V_{1/2}$  provides evidence that NO alters the channel gating properties. Whilst there is a difference in kinetics between SNAP and SNP treatment, it should be noted that the change is not significant.

It is known that ABA-induced stomatal closure requires synthesis of NO, since treatment with ABA together with cPTIO abolishes the normal closure response. In order to place the effect of NO on  $I_{K,in}$  and  $I_{Cl}$  in the context of ABA signalling cells were treated with

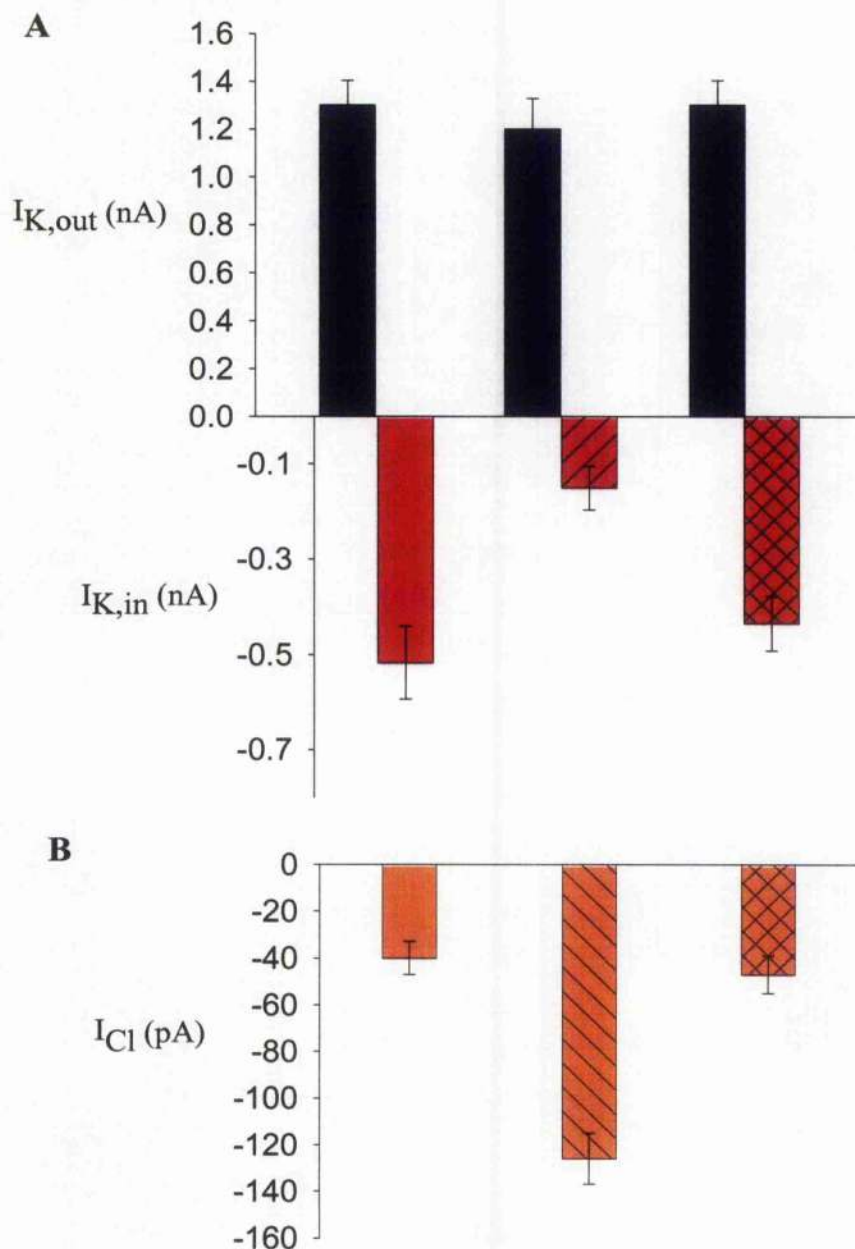


**Figure 3.2 Summary of NO effects on  $I_{K,in}$ ,  $I_{K,out}$  and  $I_{Cl}$ .** Steady-state current determined as described in main text for  $I_{K,out}$  at +30 mV and  $I_{K,in}$  at -200 mV (**A**), and  $I_{Cl}$  at -70 mV (**B**). Figure shows mean  $\pm$  SE for current amplitude for control -NO (plain bars), +NO (bars with lines) and washout with cPTIO (crossed bars) for each current.

10 $\mu$ M ABA both in the presence and absence of 20 $\mu$ M cPTIO (Figure 3.3). In the absence of cPTIO, treatment with ABA for 10-15 minutes showed a characteristic decrease in  $I_{K,in}$  and an increase in  $I_{K,out}$  as previously reported (Blatt, 1990; Blatt and Armstrong, 1993). In contrast cells treated with ABA with cPTIO showed the normal response of  $I_{K,out}$  to ABA, but showed no change in  $I_{K,in}$  (Figure 3.3A).  $I_{K,out}$  current amplitude at +30mV increased from  $1.2 \pm 0.1$  nA before treatment to  $2.3 \pm 0.1$  nA in cells treated with ABA and cPTIO, which was not significantly different from cells treated with ABA alone.  $I_{K,in}$  currents remained close to the control amplitude.  $I_{Cl}$  currents increased in response to ABA as previously reported. However, when treated with ABA and cPTIO,  $I_{Cl}$  amplitude remained close to the control level (Figure 3.3B). These results indicate that the synthesis and availability of NO is a requirement for ABA modulation of  $I_{K,in}$  and  $I_{Cl}$  but not  $I_{K,out}$ .

### 3.3.2. $I_{K,in}$ inactivation and $I_{Cl}$ activation require elevations in cytosolic free $Ca^{2+}$

Changes in cytosolic free  $Ca^{2+}$  ( $[Ca^{2+}]_{cyt}$ ) are an important component of guard cell signalling, and are central to ABA induced ion channel control leading to stomatal closure (Blatt *et al.*, 2002; Schroeder *et al.*, 2001). Increases in  $[Ca^{2+}]_{cyt}$  strongly inhibit  $I_{K,in}$  but not  $I_{K,out}$  (Schroeder and Hagiwara, 1989). It is also clear that regulation of  $I_{K,in}$  by  $[Ca^{2+}]_{cyt}$  is coupled to the plasma membrane voltage. The slowly activating anion channels which dominate the anion current in intact cells are activated by elevated

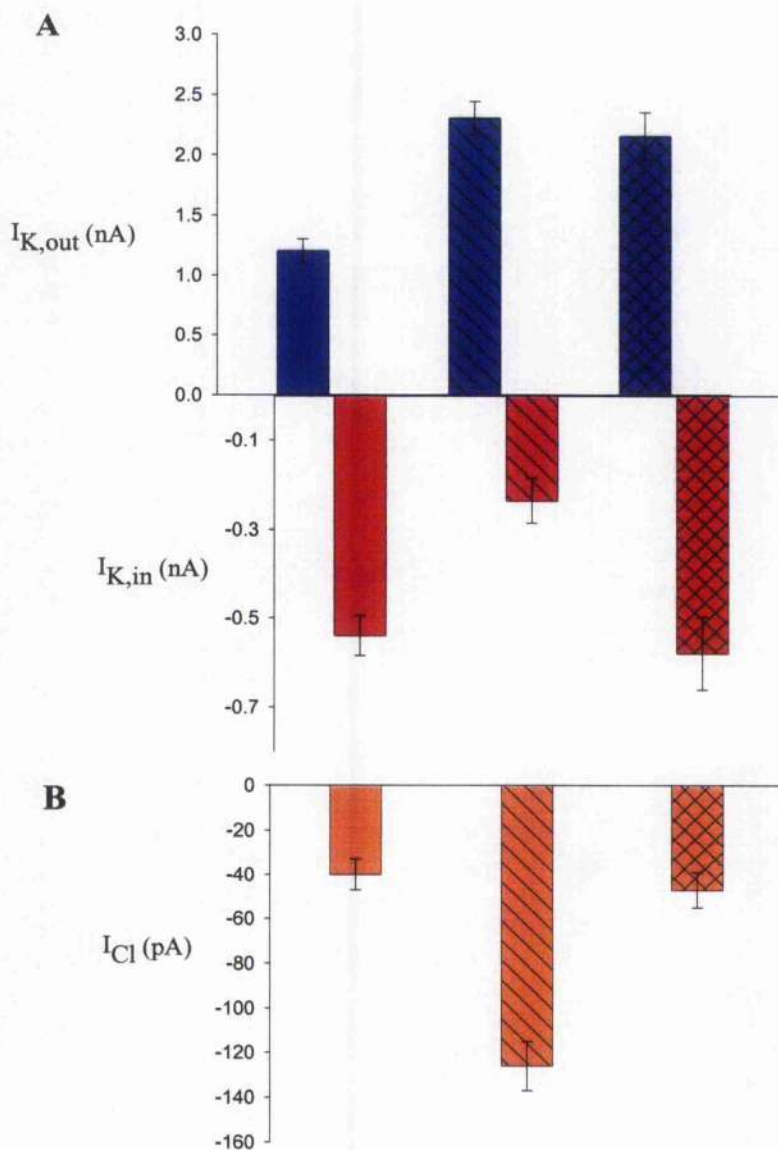


**Figure 3.3. NO scavenger cPTIO blocks inactivation of  $I_{K,in}$  and activation of  $I_{Cl}$  by ABA and NO but not ABA-mediated activation of  $I_{K,out}$ .** Steady-state current determined as described in main text for  $I_{K,out}$  at +30 mV,  $I_{K,in}$  at -200 mV (**A**), and  $I_{Cl}$  at -70 mV (**B**) before (plain bars) and after a 10-min exposure to ABA with (crossed bar) or without (lined bar) 20  $\mu$ M cPTIO.

$[Ca^{2+}]_{cyt}$  (Schroeder and Hagiwara, 1990), yet  $I_{K,out}$  is  $Ca^{2+}$  insensitive (Blatt and Grabov, 1997; Hosoi *et al.*, 1988). Since  $[Ca^{2+}]_{cyt}$  is a common theme in guard cell signalling, it was decided to test whether the effect of NO on  $I_{K,in}$  and  $I_{Cl}$  was  $Ca^{2+}$  sensitive.

To test the hypothesis we filled electrodes with 0.2M K-acetate (pH 7.5) with 50mM BAPTA or 50mM EGTA to chelate cytosolic  $Ca^{2+}$ . Following impalement, cells were left for 10 minutes to allow loading of the chelator into the cytosol by diffusion prior to treatment with SNAP. Figure 3.4 shows current trajectories and IV curves from one representative cell loaded with BAPTA and treated with 10 $\mu$ M SNAP. After two minutes treatment with SNAP,  $I_{K,in}$  and  $I_{K,out}$  currents showed little change. Since 2 minutes is double the time normally taken to complete the  $I_{K,in}$  response to NO, it was concluded that the effect of NO was essentially abolished by the BAPTA. The normal effect of NO on the voltage dependence was also abolished by  $Ca^{2+}$  chelators. Cells loaded with EGTA and BAPTA showed essentially no shift in  $V_{1/2}$  in response to NO, giving a mean  $V_{1/2}$  of  $-181 \pm 4$ mV essentially the same as in the absence of NO. Similar results were obtained in other cells treated with BAPTA ( $n = 8$ ) and EGTA ( $n = 2$ ), suggesting that an increase in  $[Ca^{2+}]_{cyt}$  is essential for the action of NO on  $I_{K,in}$ .

Figure 3.5A summarises the effect of buffering  $[Ca^{2+}]_{cyt}$  on  $I_{K,in}$  and  $I_{K,out}$ . Mean  $I_{K,in}$  current in the presence of 50mM BAPTA or EGTA (results combined,  $n = 10$ ) was  $0.71 \pm 0.13$ nA. Current amplitude in cells loaded with  $Ca^{2+}$  chelators alone was not

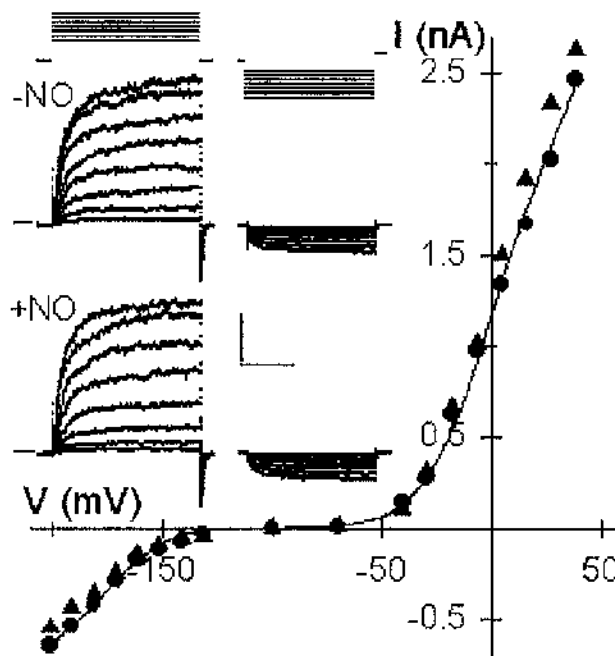


**Figure 3.4 Buffering  $[Ca^{2+}]_{cyt}$  abolishes the effect of NO on  $I_{K, in}$ .** Voltage-clamp recordings from an intact *Vicia* guard cell impaled and buffer-loaded from a microelectrode containing 50mM 1,2-bis(2-aminophenoxy)ethane-*N,N,N',N'*-tetraacetate (BAPTA). Shown are steady-state current-voltage curves determined from voltage-clamp steps before (●) and after 6 min of exposure to 10  $\mu$ M SNAP (▲). Data for  $I_{K, in}$  and  $I_{K, out}$  were fitted to Boltzmann functions. (Inset) Current traces for  $I_{K, out}$  (Left) and  $I_{K, in}$  (Right) before (Middle) and during (Bottom) NO treatment. Zero current is indicated on the left. Voltage protocols (Top) of steps between -200 mV and +50mV from holding voltage of -100 mV. (Scale: horizontal, 2 s; vertical, 1 nA.)

Significantly different from cells impaled with 0.2M K-acetate alone. Upon treatment with 10 $\mu$ M SNAP the mean current amplitude was  $-0.65 \pm 0.1$  nA, essentially the same as the mean control level. The amplitude of  $I_{K,out}$  was not greatly changed by any of the treatments, confirming its insensitivity to 10 $\mu$ M SNAP, and discounting the possibility that elevated  $[Ca^{2+}]_{cyt}$  'protects'  $I_{K,out}$  against any effect of NO. The effect of buffering  $[Ca^{2+}]_{cyt}$  on the NO effect on  $I_{Cl}$  was also examined (Figure 3.5B). Mean  $I_{Cl}$  current amplitude before treatment was  $-44 \pm 6$  pA, which remained essentially unchanged when  $Ca^{2+}$  chelator loaded cells were challenged with NO. These data support an essential role for elevated  $[Ca^{2+}]_{cyt}$  in both the inhibition of  $I_{K,in}$  and the stimulation of  $I_{Cl}$  by NO.

### 3.3.3. NO elevates resting and voltage-evoked $[Ca^{2+}]_{cyt}$ increases

Since the data from use of EGTA and BAPTA support a role for  $Ca^{2+}$  in the NO regulation of  $I_{K,in}$  and  $I_{Cl}$ , this was investigated further by impaling guard cells with triple barrelled microelectrodes and imaging the voltage-induced response of  $[Ca^{2+}]_{cyt}$  to NO. Following impalement the membrane voltage was clamped to  $-50$  mV and the cells loaded with Fura-2. Following stabilisation of the resting  $[Ca^{2+}]_{cyt}$  level, cells were stimulated by a 20s voltage step to  $-200$  mV in the presence and absence of 10 $\mu$ M SNAP. Figure 3.6 shows data from one representative cell. The resting level of  $[Ca^{2+}]_{cyt}$  was about 160 nM, which is similar to values previously reported in both plants and animals (Fricker *et al.*, 1991). Stepping the voltage to  $-200$  mV evoked a rise in  $[Ca^{2+}]_{cyt}$  to about



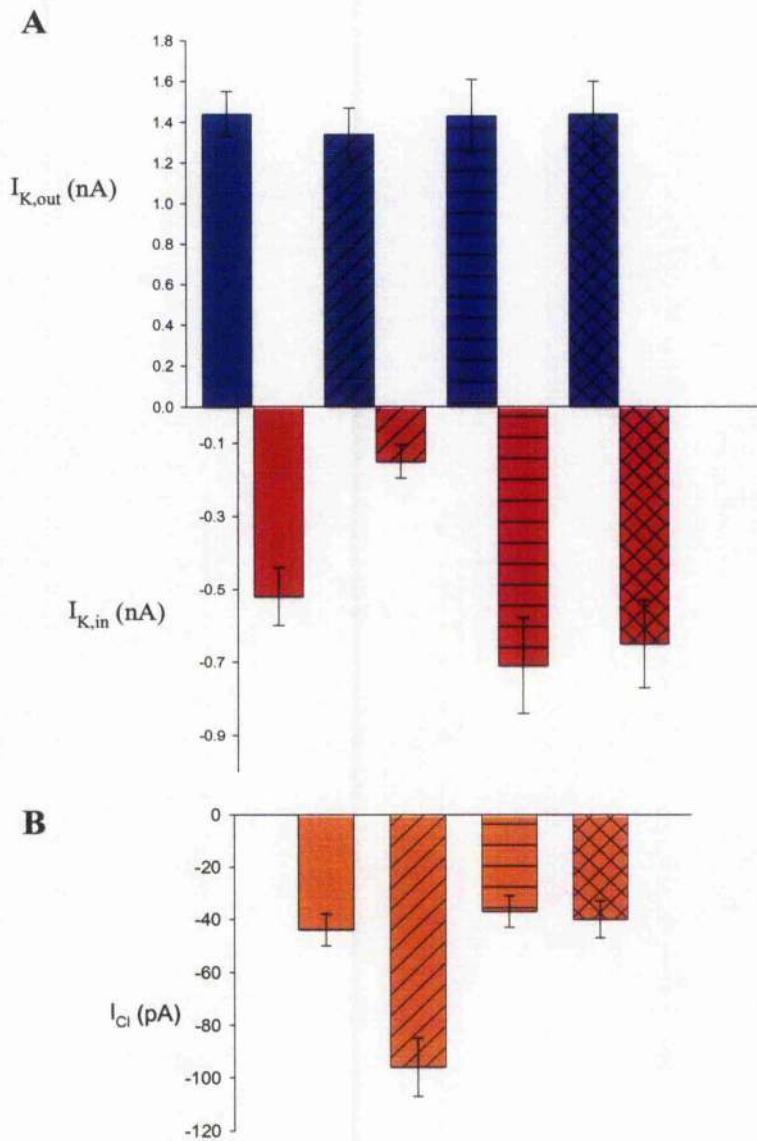


**Figure 3.5. Summary of the effect of  $Ca^{2+}$  buffering on  $I_{K,out}$ ,  $I_{K,in}$ , and  $I_{Cl}$ .** Data for  $I_{K,in}$  and  $I_{K,out}$  (**A**) and  $I_{Cl}$  (**B**) were determined as previously described in Figure 3.3. Graph shows mean current before (plain bars) and after exposure to 10  $\mu M$  SNAP with (crossed bars) ( $n = 10$ ) and without (diagonal lined bars) ( $n = 27$ ) 50 mM EGTA or 50 mM BAPTA loading. Also shown are means for cells loaded with  $Ca^{2+}$  buffer before treatment with NO (horizontal lined bars) ( $n = 10$ ).

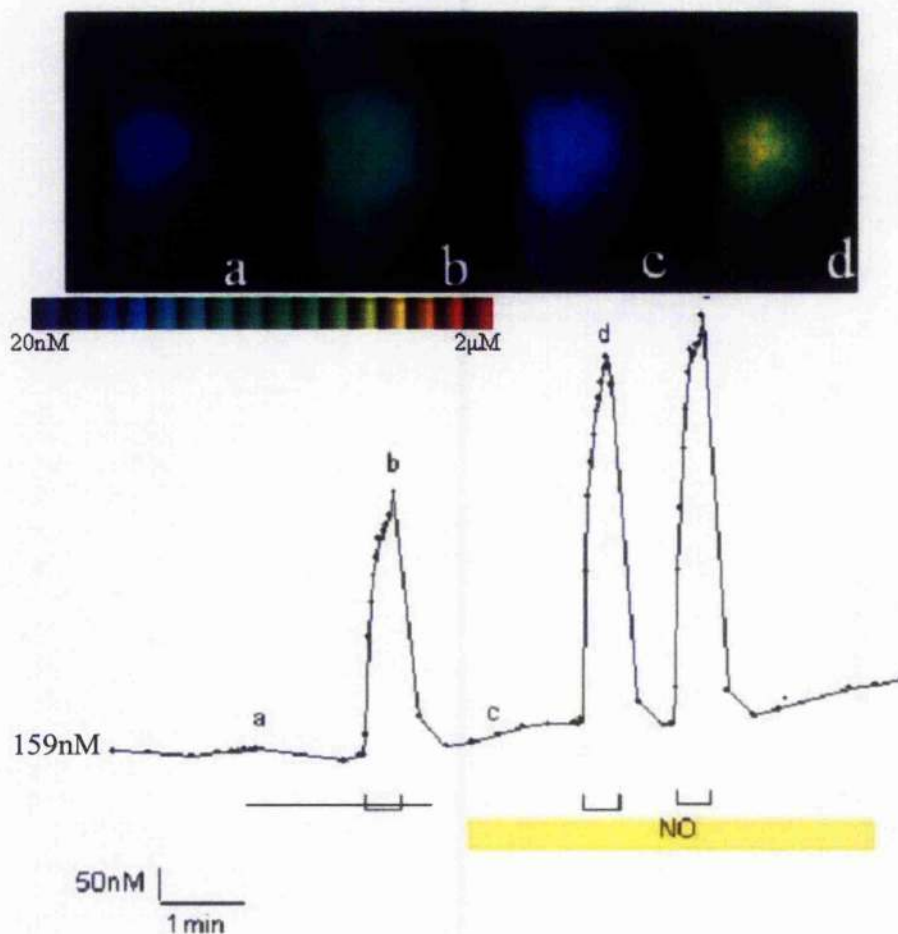
550nM, which was increased to a maximum just above 800nM in the presence of 10 $\mu$ M SNAP (Fig. 3.7). Recovery to baseline  $[Ca^{2+}]_{cyt}$  was complete within about 1min, similar to the recovery time in the absence of NO. To examine the effect of NO on the rise kinetics of the  $Ca^{2+}$  signal, data were fitted to single exponential function. The fits gave an initial rate of rise of  $42 \pm 15 \text{ nM s}^{-1}$  in the absence of NO which rose to  $86 \pm 16 \text{ nM s}^{-1}$  in the presence of NO. Thus the rate of rise is effectively doubled in the presence of NO. However, the time taken for the rise in  $[Ca^{2+}]_{cyt}$  to initiate did not alter in the presence of NO. The lag times derived from fitting the first few points to an exponential function were  $1.3 \pm 0.1 \text{ s}$  and  $1.4 \pm 0.1 \text{ s}$  in the absence and presence of NO respectively. The rate of rise and the lag time of the rise are indicative of changes of  $Ca^{2+}$  release from internal stores and  $Ca^{2+}$  entry across the plasma membrane. Therefore, these data support a role for enhanced release of  $Ca^{2+}$  from internal stores in the presence of NO.

Figure 3.7 summarises the statistics for data obtained in the measurement of  $[Ca^{2+}]_{cyt}$ . The mean evoked rise in  $[Ca^{2+}]_{cyt}$  in the absence of NO was  $452 \pm 31$  ( $n = 6$ ), rising to  $741 \pm 70$  in the presence of NO, which represents a significant enhancement of the  $Ca^{2+}$  signal. There was also a significant increase in the resting  $[Ca^{2+}]_{cyt}$ , and increase from  $159 \pm 15 \text{ nM}$  in the absence of NO to  $262 \pm 31 \text{ nM}$  in the presence of NO. The increase in resting  $[Ca^{2+}]_{cyt}$  strengthens release of  $Ca^{2+}$  from internal stores as the site of action for NO.

### 3.3.4. NO does not promote $\text{Ca}^{2+}$ channel gating at the plasma membrane

In order to dissect the contribution of  $\text{Ca}^{2+}$  entry across the plasma membrane to the increased  $[\text{Ca}^{2+}]_{\text{cyt}}$  with NO, Fura2 loaded cells were subjected to 93 second voltage ramps from  $-50$  to  $-200\text{mV}$ . The voltage threshold for activation of the increase in  $[\text{Ca}^{2+}]_{\text{cyt}}$  gives an insight into the behaviour of the plasma membrane hyperpolarisation activated  $\text{Ca}^{2+}$  channel (see Grabov and Blatt, 1998). Figure 3.8 shows data recorded from one cell, expressed as a kymograph with associated images at time intervals. Data for the kymograph were taken from a transect of the fluorescence in a band from the perinuclear region to periphery of the cell. The kymograph shows that the fluorescence increase was initiated by negative going voltage, with increase seen first at the cell periphery close to the plasma membrane, then propagating through the cytosol. In the presence of NO, a similar sequence of events can be seen though the final  $[\text{Ca}^{2+}]_{\text{cyt}}$  is clearly higher. The voltage threshold for activation of the  $\text{Ca}^{2+}$  signal was determined for several different cells. In the absence of NO, a threshold value of  $-133 \pm 7\text{mV}$  was determined, showing a slight negative shift in the presence of NO to  $-145 \pm 6\text{mV}$ , though the shift was not significant. These data suggest that the activity of the plasma membrane  $\text{Ca}^{2+}$  channel is not significantly altered by NO.

In order to obtain direct evidence for the effect of NO on the plasma membrane hyperpolarisation activated  $\text{Ca}^{2+}$  channel, whole cell and single channel activity was recorded in guard cell protoplasts. Figure 3.9 shows data from one representative whole cell and one representative cell attached recording. Single channel recordings in the cell attached configuration revealed single channel events with a mean amplitude of



**Figure 3.6. NO promotes evoked  $[Ca^{2+}]_{cyt}$  increases without affecting  $[Ca^{2+}]_{cyt}$  recovery.** (Lower)  $[Ca^{2+}]_{cyt}$  recorded from one guard cell clamped to -50 mV and stepped to -200 mV at time periods indicated ([unionsq]) before and after adding 10  $\mu$ M SNAP. (Lower Left)  $[Ca^{2+}]_{cyt}$  basal level. Fura 2 fluorescence images taken at 2-s intervals. (Upper) Selected ratio images (a–d) correspond to the time points indicated on trace below.

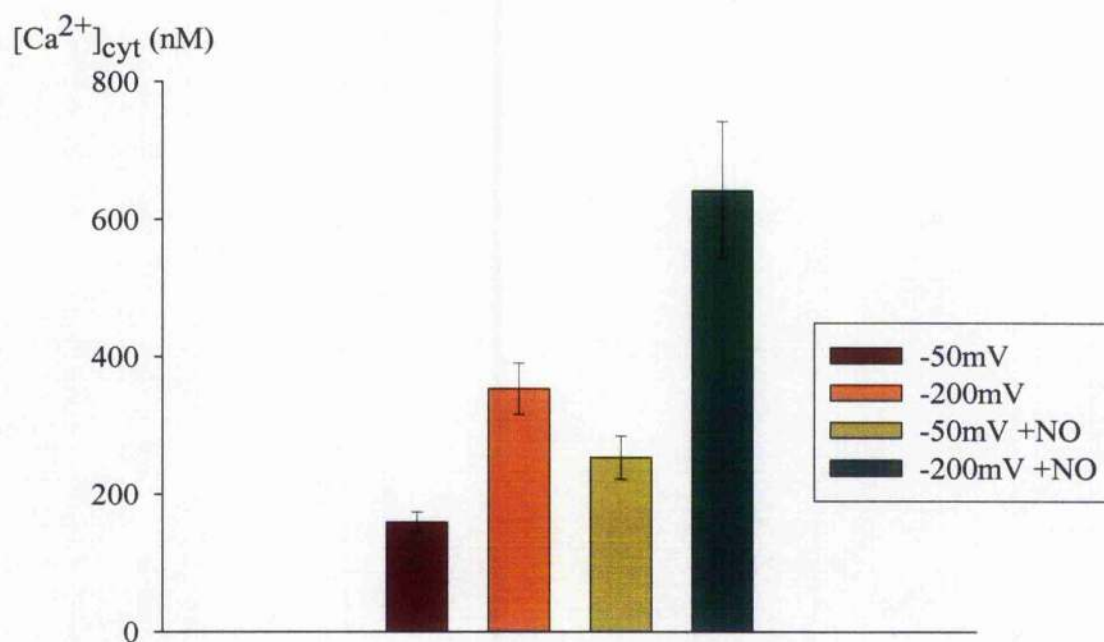


**Figure 3.7. Summary of the effect of NO on  $Ca^{2+}$  signalling.** Figure shows data for  $[Ca^{2+}]_{\text{cyt}}$  measurements both at resting voltage (-50mV) and after evoking a rise in  $Ca^{2+}$  by clamping to -200mV for 20 seconds. Data are expressed as mean  $\pm$  SE.

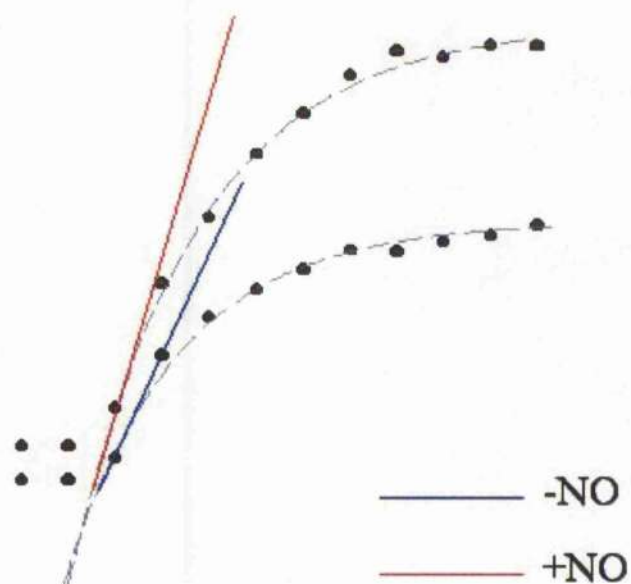


**Figure 3.8. NO increases rate of  $Ca^{2+}$  release.** Data from a single guard cell. Voltage was stepped from  $-50mV$  to  $-200mV$  for 30s. Graph shows the time dependent rise in  $[Ca^{2+}]_{cyt}$  both with and without  $10\mu M$  SNAP. Data are fitted to single exponential functions with the tangent to the initial rise plotted (coloured lines).



1.8±0.2pA and a conductance of about 13pS at -150mV ( $n = 6$ ). These characteristics are similar to those previously reported for this channel in *Vicia* (Hamilton *et al.*, 2000; Kohler and Blatt, 2002). Treatment of the protoplasts with 10µM SNAP changed the open probability of the channel from 0.104±0.004 before treatment to 0.049±0.003 after 2 minutes treatment ( $n = 6$ ). Single channel conductance remained unchanged after 2 minutes treatment. In the whole cell configuration, channel activity was assayed using voltage ramps in the presence and absence of NO. After 2 minutes treatment with 10µM SNAP, whole cell currents were significantly reduced by 1.9±0.4 fold. However, the apparent  $V_{1/2}$  for channel activation was unchanged implying no change in the voltage sensitivity of channel gating. These data imply that in fact NO slightly inhibits  $Ca^{2+}$  channel activity at the plasma membrane. Thus it is clear that the enhancement of the voltage induced increase in  $[Ca^{2+}]_{cyl}$  is due to release from internal stores.

### **3.3.5. $[Ca^{2+}]_{cyl}$ rise and $I_{K,in}$ inactivation by NO are sensitive to antagonists of guanylyl cyclase and cADPR mediated $Ca^{2+}$ release**

There are many possible pathways for the release of  $Ca^{2+}$  into the cytosol from internal stores that may be possible targets for NO. In animals, it is established that in neuronal cells NO targets guanylyl cyclase (Ahern *et al.*, 2002). Guanylyl cyclase synthesises the production of cGMP, which triggers synthesis of cADPR, a compound that gates  $Ca^{2+}$  channels of internal stores (Lee, 2001). In guard cells there is evidence that such

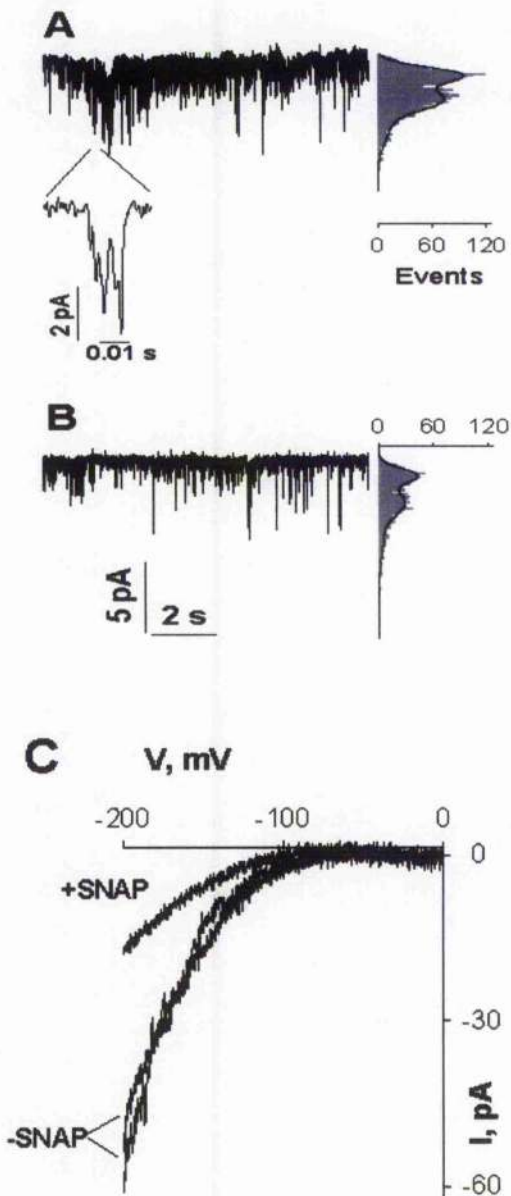


**Figure 3.9. Patch clamp analysis of  $\text{Ca}^{2+}$ -channel activity at the plasma membrane.** Cell-attached, single  $\text{Ca}^{2+}$ -channel records from one guard cell protoplast before (A) and 2 min after (B) adding 10  $\mu\text{M}$  SNAP. (Middle) Expanded time scale showing single opening events. [Scale: horizontal, 1 s (50 ms, Middle); vertical, 2 pA.] Point-amplitude histograms (Right), which plot the number of openings and their mean amplitude (the vertical axis is scaled to traces) for 10-s periods, including segments shown, indicate an  $\approx$  2-fold decrease in opening events. (C) Whole-cell  $\text{Ca}^{2+}$  currents recorded during voltage ramps before and 2 min after adding 10  $\mu\text{M}$  SNAP. Data from Dr. Sergei Sokolovski



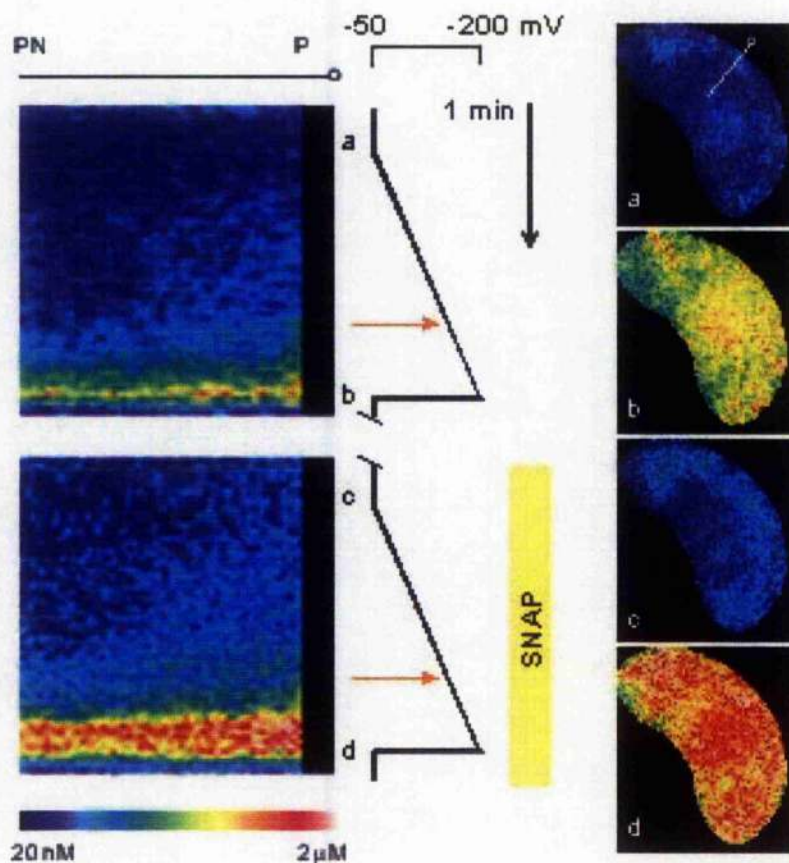


**Figure 3.10. NO enhances evoked  $[Ca^{2+}]_{cyt}$  increases without promoting  $Ca^{2+}$ -channel activity at the plasma membrane.**  $[Ca^{2+}]_{cyt}$  rise in one intact guard cell recorded by fura-2 fluorescence ratio at 2-s intervals before and 2 min after adding 10  $\mu$ M SNAP. The time line (*Centre*) runs top to bottom with voltage scale and ramps as indicated. Selected ratio images (*Right*, a–d) correspond to time points indicated. The kymograph was constructed from successive ratio images averaged over a 2-pixel-wide band (line in *Right*, a) from cell exterior and periphery (P) to the perinuclear region (PN). Voltage ramps from -50 mV to -200 mV over 93 s. The threshold for  $[Ca^{2+}]_{cyt}$  rise was determined as time of  $[Ca^{2+}]_{cyt}$  rise 1 SD above the pre-ramp level to a depth of 3 pixel units ( $\approx 2 \mu$ m). Thresholds are marked (red arrows).

pathways exist (Allen and Sanders, 1995; Leckie *et al.*, 1998; Neill *et al.*, 2003). Furthermore both cGMP and cADPR have been placed in the NO pathway in guard cells (Durner *et al.*, 1998). Therefore, the hypothesis that a cGMP / cADPR pathway is responsible for the NO enhanced voltage induced  $\text{Ca}^{2+}$  release and  $I_{K,in}$  inactivation was tested using a pharmacological approach.

Cells impaled with double-barrelled microelectrodes were pre-treated for 1-2minutes with either guanylyl cyclase inhibitor ODQ or the cADPR gated channel inhibitor ryanodine before challenging with NO. Table 3.10 summarises the data obtained. Treatment with 20 $\mu\text{M}$  ODQ completely removed the inactivation of  $I_{K,in}$  normally seen in response to NO. Mean current at -200mV before treatment was  $-517 \pm 53 \text{ pA}$ , decreasing to  $-151 \pm 35 \text{ pA}$  in response to 10 $\mu\text{M}$  SNAP ( $n = 27$ ). However, in cells treated with ODQ the mean current decreased only slightly to  $-443 \pm 36$  ( $n = 5$ ), which is not significantly different from the current before treatment with NO. Similar treatment with 1 $\mu\text{M}$  ryanodine gave  $I_{K,in}$  currents of  $-535 \pm 72 \text{ pA}$ , essentially unchanged from the amplitude of the control. These data suggest that the NO effect on  $I_{K,in}$  is via a cGMP / cADPR dependent pathway.

To confirm that the effect of both ODQ and ryanodine were due to inhibition of the  $\text{Ca}^{2+}$  signal and not some direct effect on  $I_{K,in}$ , experiments with ryanodine and ODQ were performed in cells loaded with Fura-2. As shown in table 3.10, pre-treatment of cells with either 1 $\mu\text{M}$  ryanodine or 20 $\mu\text{M}$  ODQ reduced not only the NO induced rise in  $[\text{Ca}^{2+}]_{\text{cyt}}$ , but also the  $[\text{Ca}^{2+}]_{\text{cyt}}$  before NO treatment. This suggests that the cGMP / cADPR

triggered pathway is the dominant pathway voltage-dependent release for the release of  $\text{Ca}^{2+}$  into the cytosol in guard cells, and that the same pathway is utilised in the NO response.

| Treatment                  | $I_{K,in}$ (pA)    | $[\text{Ca}^{2+}]_{\text{cyt}}$ resting (nM) | $[\text{Ca}^{2+}]_{\text{cyt}}$ evoked (nM) |
|----------------------------|--------------------|--|---|
| Control                    | $-517 \pm 53$ (27) | $159 \pm 15$ (6)                             | $452 \pm 31$ (6)                            |
| 10 $\mu\text{M}$ SNAP      | $-151 \pm 35$ (27) | $262 \pm 31$ (6)                             | $741 \pm 70$ (6)                            |
| +1 $\mu\text{M}$ ryanodine | $-535 \pm 72$ (5)  | $171 \pm 11$ (3)                             | $200 \pm 12$ (3)                            |
| +20 $\mu\text{M}$ ODQ      | $-443 \pm 36$ (5)  | $106 \pm 26$ (4)                             | $303 \pm 68$ (4)                            |

**Table 3.11. Summary of the effects of cGMP / cADPR pathway antagonists on  $I_{K,in}$  and  $\text{Ca}^{2+}$  signalling.** Data are expressed as mean  $\pm$  SE of (*n*) measurements.  $I_{K,in}$  amplitude was calculated at  $-200\text{mV}$  as for other figures. Resting  $[\text{Ca}^{2+}]_{\text{cyt}}$  is given as concentration before evoking a rise in  $\text{Ca}^{2+}$ , and evoked  $[\text{Ca}^{2+}]_{\text{cyt}}$  as the maximal  $[\text{Ca}^{2+}]_{\text{cyt}}$  upon clamping to  $-200\text{mV}$  for 30s.

### **3.4. Discussion.**

#### **3.4.1. Introduction**

The last ten years has seen growing interest in NO in plants. Now it is clear that there is an important role for NO in both promotion and inhibition of growth and development responses, as a pro- and antioxidant, and as a signalling molecule in plants (Neill *et al.*, 2003; Lamattina *et al.*, 2003). However, whilst the general effects of NO on various physiological processes have been described, data on the mechanistic basis for NO responses is still lacking. It is clear that NO signalling shares common themes with those seen in animals, and information gained on the mechanistic basis of NO action has drawn on these common themes (Delledonne *et al.*, 1998; Durner *et al.*, 1998). The discovery of a role for NO in ABA induced stomatal closure has provided the means to study NO effects in a system that is amenable to experimentation. Guard cell signalling has already received much attention, giving an opportunity to build on knowledge already gained from 20 years of intensive research.

#### **3.4.2. NO: component of ABA signalling in guard cells**

Data presented here show that treating guard cells with NO lead to inhibition of  $I_{K,in}$  and increase of  $I_{Cl}$ , but does not change  $I_{K,out}$  activity. It is shown that ABA induced regulation of  $I_{K,in}$  and  $I_{Cl}$  was abolished by cPTIO, an NO specific scavenger. Investigation of the basis for the NO effect revealed a central role for  $Ca^{2+}$ , since  $I_{K,in}$  and  $I_{Cl}$  were not modulated by NO when  $[Ca^{2+}]_{cyt}$  was buffered. Furthermore, NO was shown to enhance the voltage induced  $Ca^{2+}$  signal. Measurement of the voltage threshold and single channel activity of the plasma membrane hyperpolarisation activated  $Ca^{2+}$  channel,

along with pharmacological evidence confirmed that NO targeted  $\text{Ca}^{2+}$  release from internal stores, via a cGMP / cADPR dependent pathway.

The ABA response of guard cells effectively changes the poise of the plasma membrane from a state that promotes solute uptake to a state of solute efflux, which allows loss of turgor and stomatal closure (Schroeder *et al.*, 2001; Blatt, 2002). The downstream effectors of this process are  $I_{K,in}$ , which decreases, and  $I_{Cl}$  and  $I_{K,out}$  which increase (Blatt, 1990a; Armstrong *et al.*, 1995; Grabov and Blatt, 1997a; Pei *et al.*, 1997). The effect of NO on  $I_{K,in}$  and  $I_{Cl}$  is similar to the effect seen when cells are treated with ABA alone. Both ABA and NO decrease  $I_{K,in}$  and affect the voltage dependence and activation kinetics of the current, which are indicators of altered gating properties at the single channel level. Indeed, the effect of NO on  $I_{K,in}$  is so similar to that of ABA that it could be suggested that NO alone can account for the effect of ABA on  $I_{K,in}$ . A similar explanation could also be given for the effect of NO on  $I_{Cl}$ .

The fact that NO doesn't have an ABA-type effect on  $I_{K,out}$  suggests that NO is not solely responsible for all the downstream effects seen in response to ABA. The NO effect seems to be limited to those ion channels known to be  $\text{Ca}^{2+}$  sensitive. However, there are other known ABA-triggered signals that are able to regulate  $I_{K,out}$ . Cytosolic pH ( $\text{pH}_{\text{cyt}}$ ) rises up to 0.3 units in guard cells treated with ABA. Irving *et al.* (1992) and Blatt and Armstrong (1993) were able to show that the  $\text{pH}_{\text{cyt}}$  rise is essential for the effect of ABA on  $I_{K,out}$ . The fact that  $\text{pH}_{\text{cyt}}$  regulation of  $I_{K,out}$  is membrane delimited indicates a simple mechanism of protons binding to the channel or closely associated proteins (Blatt and

Armstrong, 1993; Miedema and Assmann, 1996). Whether or not NO has an effect on  $\text{pH}_{\text{cyt}}$  remains to be determined.

### **3.4.3. NO signalling in guard cells: a central role for $\text{Ca}^{2+}$ .**

In animals the activation of guanylyl cyclase and production of cGMP are prerequisites for the transmission of the NO signal (Ahern *et al.*, 2002). The results of the  $\text{Ca}^{2+}$  signalling experiments show that NO targets  $\text{Ca}^{2+}$  release via cGMP and cADPR. The presence of cGMP in plants was initially a controversial issue, though reliable data have now been gathered from a number of tissues via a number of methods (Newton *et al.*, 1999). In animals, cGMP stimulates the production of cADPR via activation of a cGMP dependent protein kinase (Wendehenne *et al.*, 2001). Elements of the cADPR triggered  $\text{Ca}^{2+}$  release pathway have been demonstrated in plants. In fact, cADPR has already been placed in ABA signalling leading to stomatal closure. Use of cADPR antagonist and synthesis inhibitors has shown that flux of  $\text{Ca}^{2+}$  from the vacuole into the cytosol occurs in response to ABA, and that cADPR is essential for stomatal closure (Leckie *et al.*, 1998; MacRobbie, 2000). The data using the cGMP and cADPR antagonists strongly suggest that not only is the cGMP / cADPR pathway important for the NO induced  $\text{Ca}^{2+}$  response, but that this pathway alone is sufficient for the response of guard cells to NO. Other known pathways that exist for  $\text{Ca}^{2+}$  release include voltage dependent channels such as SV, and  $\text{IP}_3$  activated pathways (Gilroy *et al.*, 1990; Ward and Schroeder, 1994). Data presented here suggests that either these pathways are not important for the NO response, or that their contribution comes 'downstream' of the cGMP pathway. When comparing ABA and NO, there are differences in the response of the  $\text{Ca}^{2+}$  signalling

systems that are worthy of discussion. ABA is known to stimulate the activity of the plasma membrane  $\text{Ca}^{2+}$  channel in guard cells (Grabov and Blatt 1998; Hamilton *et al.*, 2002; Pei *et al.*, 2000). In both patch clamp and impalement experiments performed in this study, no such effect was seen in response to NO. This suggests an NO-independent mechanism by which ABA regulates the plasma membrane channel. Furthermore, the kinetics of the  $\text{Ca}^{2+}$  signature in NO and ABA differ. The hyperpolarisation induced  $\text{Ca}^{2+}$  increase in ABA shows a slower recovery than with NO, typically 3-5 minutes. In NO the recovery kinetics are similar to those seen in the absence of NO and ABA. Whilst it would seem that the NO-enhanced  $\text{Ca}^{2+}$  signal is sufficient to account for the ABA action on  $\text{I}_{\text{K, in}}$  and  $\text{I}_{\text{Cl}}$ , the difference in signal may mean that later events in ABA induced stomatal closure such as changes in gene expression might require this prolonged elevation. The  $\text{Ca}^{2+}$  required for the prolonged  $\text{Ca}^{2+}$  increase might arise from any one of a number of other pathways, including  $\text{IP}_3$  receptors, voltage gated channels.

#### **3.4.4. NO signalling in guard cells: common themes with animal cells?**

From these experiments, it is not possible to distinguish the mechanism by which NO is perceived in guard cells. Common themes with animal systems may provide pointers. Soluble guanylyl cyclase essentially acts as an NO receptor in animals. The enzyme contains a prosthetic heme group that is essential for NO activation (Ahern *et al.*, 2002). It is also known that the uncharged radical form of NO, ( $\text{NO}^\bullet$ ), is the active form, with both the positively and negatively charged forms ( $\text{NO}^+$  and  $\text{NO}^-$  respectively) having no effect (Dierks and Burstyn, 1996). Another possible mechanism for NO action could be by direct modulation of the ion channels by S-nitrosylation. BK  $\text{Ca}^{2+}$  activated  $\text{K}^+$

channels show increased activity in response to NO. In some cases, the effect of NO on BK channels has been demonstrated to be membrane delimited, suggesting an S-nitrosylation of the channel or closely associated protein (Bolotina *et al.*, 1994; Lang and Watson, 1998). Of particular interest to the data presented here is the effect of NO on ryanodine receptors, which are cADPR sensitive ion channels. NO is known to modulate ryanodine receptors by S-nitrosylation. There are 80-100 cysteine residues in ryanodine receptors (Takeshima *et al.*, 1989). In cardiac muscle ryanodine receptors, 12 of these cysteines are accessible and able to be nitrosylated (Xu *et al.*, 1998). In contrast, a single cysteine is responsible for NO modulation of the skeletal muscle isoform of the receptor (Sun *et al.*, 2001).

#### 3.4.5. Summary

The effect of NO on guard cell ion channels studied here show that NO can bring about changes in ion transport which can lead to changes in the bias of the plasma membrane towards solute efflux and stomatal closure. In the presence of NO,  $I_{Cl}$  is stimulated and  $I_{K,in}$  inhibited by increase  $[Ca^{2+}]_{cyt}$ . Increased  $I_{Cl}$  drives the membrane potential positive, thus favouring  $K^+$  efflux. The data presented show NO as an essential component of ABA mediated control of  $Ca^{2+}$  sensitive ion channels in guard cells.



**CHAPTER 4**

**PROTEIN KINASES AND NITRIC OXIDE  
SIGNAL TRANSDUCTION IN GUARD  
CELLS**

#### 4.1. Introduction.

Phosphorylation and dephosphorylation events are known to be a central feature in cell signalling. Pharmacological evidence for the involvement of protein phosphatases in regulation of guard cell  $K^+$  channels came initially from pharmacological studies with okadaic acid (Li *et al.*, 1994; Luan *et al.*, 1993; Thiel and Blatt, 1994). The action of phosphatases in ABA induced stomatal closure was shown by work on mutants defective in ABA-induced stomatal closure (Koornneef *et al.*, 1984). Both the *abi1-1* and *abi2-1* mutants are known to be dominant mutations in type 2C protein phosphatases (Leung *et al.*, 1994; Leung *et al.*, 1997; Meyer *et al.*, 1994). The ABA insensitive stomata of *abi1-1* and *abi2-1* plants may in part be due to altered signalling, leading to altered ion channel responses to ABA. In transgenic *N. benthamiana* plants expressing *abi1-1* showed 20-fold less sensitivity of  $I_{K,in}$  and  $I_{K,out}$  to 20 $\mu$ M ABA compared to wild type plants (Armstrong *et al.*, 1995). Moreover there are changes in anion channel behaviour. In *Arabidopsis* *abi1-1* and *abi2-1* plants, ABA induced activation of the slow anion channel is abolished (Pei *et al.*, 1997). In the transgenic *abi1-1* *N. benthamiana* plants no such inhibition of the ABA response of the anion current was seen (Grabov *et al.*, 1997). Pharmacological studies have also implicated protein phosphatases in anion channel control (Schmidt *et al.*, 1995; Schwarz and Schroeder, 1998). More recently data from radiotracer flux analysis has revealed a role for a protein tyrosine phosphatase in the release of  $K^+$  across the tonoplast during stomatal closure in response to a variety of stimuli, including ABA (MacRobbie, 2002).

In addition, several ion channels in guard cells are known to be modulated by protein kinases. The protein kinase antagonist K252a inhibits normal S-type anion channel

activity and ABA induced stomatal closure (Schmidt *et al.*, 1995). In studies using the protein kinase inhibitor staurosporine in intact plants, no changes in anion channel activity were seen either in the presence or absence of ABA (Grabov *et al.*, 1997a). Pharmacological evidence has also been given for phosphorylation by a  $\text{Ca}^{2+}$  dependent protein kinase (CDPK) as being important for inactivation of  $\text{I}_{\text{K,in}}$  by  $\text{Ca}^{2+}$ . Heterologous coexpression of CDPK with the guard cell expressed inward rectifier KAT1 leads to reduced  $\text{K}^+$  currents (Kamasani *et al.*, 1997). From biochemical studies it is also known that CDPK can phosphorylate the KAT1 protein in a  $\text{Ca}^{2+}$  manner, though whether this interaction is possible *in vivo* is not clear (Li *et al.*, 1998). Recently, protein phosphorylation has been shown to be important in the activation of the *Vicia* plasma membrane  $\text{Ca}^{2+}$  channel. Isolated patches from *Vicia* guard cells have a requirement for hydrolysable ATP to prevent decay of channel activity. Furthermore, protein phosphatase antagonists lead to an ABA type shift in the activation threshold of the channel, implying a role for a type 1/2A protein phosphatase at the plasma membrane (Kohler and Blatt, 2002).

Further clues as to possible ion channels that might be regulated by phosphorylation come from studies on  $\text{Ca}^{2+}$  signalling in animal cells. By cloning and sequencing animal ion channels, it has been possible to identify potential phosphorylation sites, and to test their function *in vivo* and *in vitro*. Ryanodine receptors, for example, have many putative phosphorylation sites (Takeshima *et al.*, 1989). Both protein kinases and phosphatases can modulate ryanodine receptors at the single channel level, though the effects are highly variable, with both activation and deactivation of the receptors reported (Cheng *et al.*, 1995; Hain *et al.*, 1995; Igami *et al.*, 1999; Sonnleitner *et al.*, 1997; Valdivia *et al.*, 1995). Phosphorylation of  $\text{IP}_3$  receptors has

also been demonstrated to modulate their activity (Jiang *et al.*, 2000; Komalavilas and Lincoln, 1994; Komalavilas and Lincoln, 1996). Indeed protein kinases and phosphatases form an interacting functional unit with  $IP_3$  receptors in some cases (deSouza *et al.*, 2002; Tang *et al.*, 2003).

Parallels with  $Ca^{2+}$  signalling components in animal cells suggest that there may be other guard cell ion channels whose regulation by phosphorylation has yet to be explored. Since the data presented in the previous chapter suggest  $Ca^{2+}$  release from internal stores as the target of NO in guard cells, it was decided to investigate whether phosphorylation is important for transmission of the NO signal. A pharmacological approach was taken using protein kinase inhibitors. Results show that phosphorylation is important for the transmission of the NO signal. The broad range protein kinase antagonist staurosporine blocked the NO induced decrease in  $I_{K,in}$  and increase in  $I_{Cl}$ . The NO enhanced release of  $[Ca^{2+}]_{cyt}$  was inhibited in the presence of staurosporine, implying a role for protein kinase(s) in regulation of  $Ca^{2+}$  dynamics in NO signalling.

## **4.2. Materials and methods.**

All  $K^+$  channel and  $Ca^{2+}$  imaging experiments were carried out as described in Chapter 2 and in section 3.2 of Chapter three, with the following exceptions. As for Chapter 3, both  $K^+$  channel measurements and  $Ca^{2+}$  imaging experiments, cells were bathed in the standard buffer (5mM Ca-MES (pH 6.1), 10mM KCl). The standard buffer was supplemented where necessary with 10 $\mu$ M SNAP, 20 $\mu$ M c-PTIO, 1 $\mu$ M staurosporine, 25 $\mu$ M phenylarsine oxide (PAO) and 10 $\mu$ M genistein. All compounds were added to the standard buffer from concentrated stocks. SNAP and c-PTIO were prepared as stocks in EtOH (1:1 EtOH water for SNAP). Genistein, staurosporine and PAO were prepared as stocks in DMSO. Fresh stocks of SNAP were prepared daily and kept in the freezer to slow NO release. Stock solutions containing SNAP were discarded after 5 hours and fresh stocks prepared. Final concentrations of EtOH and DMSO in solutions used for experiments  $\leq 0.1\%$  in all cases. For  $Ca^{2+}$  imaging experiments, only voltage step protocols were used in this chapter, since data in Chapter 3 show that NO does not significantly alter the voltage threshold.

### 4.3. Results.

#### 4.3.1. Staurosporine blocks the effect of NO on $I_{K,in}$ and $I_{Cl}$ .

The effect of the broad range protein kinase inhibitor staurosporine on the NO induced inhibition of  $I_{K,in}$  and  $I_{Cl}$  in intact *Vicia faba* cells was assayed. Epidermal strips were perfused with solutions containing 10 $\mu$ M SNAP either in the presence or absence of 1 $\mu$ M staurosporine ( $n = 10$ , and  $n = 22$  respectively) and currents recorded by voltage clamp using double-barrelled microelectrodes. Figure 4.1 shows data from one representative cell treated first with 1 $\mu$ M staurosporine for 2 minutes, followed by 2 minutes treatment with 1 $\mu$ M staurosporine and 10 $\mu$ M SNAP. Both original current traces and steady-state IV curves show that 1 $\mu$ M staurosporine effectively blocked the inhibition of  $I_{K,in}$  normally seen in response to 10 $\mu$ M SNAP. The effect of staurosporine could be seen even after 5 minutes, indicating that the effect was a total inhibition and not simply a delayed response. Fitting of Boltzmann functions to all  $I_{K,in}$  records showed that the half-maximal activation voltage ( $V_{1/2}$ ) did not show the 18mV negative displacement which is characteristic of the response of  $I_{K,in}$  to NO (see chapter 3).

Figure 4.2A summarises the effect of staurosporine and NO on  $I_{K,in}$  and  $I_{K,out}$ . Mean  $I_{K,in}$  amplitude at -200mV before treatment as described in the previous chapter was  $-0.52 \pm 0.08$ nA, decreasing to  $-0.15 \pm 0.05$ nA in response to 10 $\mu$ M SNAP ( $n = 22$ ). However, in cells treated with 1 $\mu$ M staurosporine, mean current amplitude in response to 10 $\mu$ M SNAP was virtually unchanged at  $-0.65 \pm 0.12$ nA ( $n = 10$ ), which is not significantly different from the mean amplitude before treatment. In control cells treated with staurosporine alone the mean current amplitude was  $-0.61 \pm 0.13$ nA ( $n =$

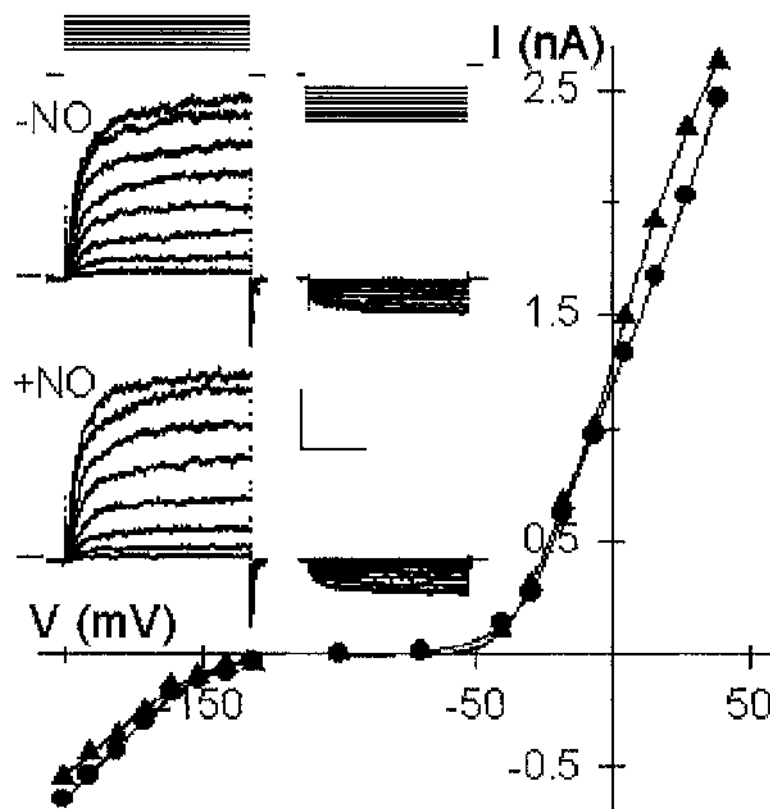


**Figure 4.1. The effect of NO on  $I_{K,in}$  is inhibited by staurosporine .** Voltage-clamp recordings from a single intact *Vicia* guard cell are shown. Steady-state current-voltage curves determined from voltage-clamp steps before (●), and after 2 min of exposure to 10  $\mu$ M SNAP + 1  $\mu$ M staurosporine (▲).  $K^+$ -channel currents were obtained by subtracting instantaneous current from steady-state current at each voltage. Data for  $I_{K,in}$  and  $I_{K,out}$  are shown with fitted Boltzmann functions. (Inset) Current traces for  $I_{K,out}$  (Left) and  $I_{K,in}$  (Right) before (Middle) and during (Bottom) NO + staurosporine treatment. Zero current is indicated on the left. Voltage protocols (Top) of steps between -200 and +50 mV from holding voltage of -100 mV are shown. (Scale: horizontal, 2 s; vertical, 1 nA.)

10), which represents a small but insignificant increase compared to the amplitude in the absence of staurosporine. A similar insignificant increase is also seen in cells treated with both SNAP and staurosporine may reflect some minor indirect effect of staurosporine on  $I_{K,in}$  amplitude. Therefore, these results demonstrate the involvement of protein kinase(s) in the regulation of  $I_{K,in}$  by NO.

Treatment of *Vicia* guard cells with NO alone produces a dramatic slowing of the activation kinetics of  $I_{K,in}$  at  $-200\text{mV}$  from  $314 \pm 35\text{ms}$  before treatment to  $538 \pm 72\text{ms}$  following treatment with  $10\mu\text{M}$  SNAP. The effect of staurosporine on the ability of NO to slow the activation kinetics of  $I_{K,in}$  was examined. In cells treated with both staurosporine and SNAP, no such effects on kinetics were observed. Mean half activation times in cells treated with either  $1\mu\text{M}$  staurosporine alone or with  $10\mu\text{M}$  SNAP gave a mean  $I_{K,in}$  half activation time at  $-200\text{mV}$  of  $298 \pm 23\text{ms}$  and  $306 \pm 26\text{ms}$  respectively, which are not significantly different from control values.

The ability of staurosporine to block the effect of NO on the anion currents was examined. Figure 4.2B shows the response of  $I_{Cl}$  to NO both in the presence and absence of  $1\mu\text{M}$  staurosporine, where  $I_{Cl}$  was determined as in Chapter 3. As already described, NO gives rise to a significant increase in  $I_{Cl}$ , from a mean amplitude of  $-44 \pm 6\text{pA}$  to  $-96 \pm 11\text{pA}$  ( $n = 22$ ), an effective doubling of the current amplitude. However, in the presence of  $1\mu\text{M}$  staurosporine the mean  $I_{Cl}$  amplitude in response to  $10\mu\text{M}$  SNAP was  $-40 \pm 7\text{pA}$  ( $n = 10$ ), which is not significantly different from control levels. In cells treated with  $1\mu\text{M}$  staurosporine alone  $I_{Cl}$  amplitude was  $-42 \pm 6\text{pA}$  ( $n = 10$ ), which shows that protein kinases are not required to maintain steady normal  $I_{Cl}$



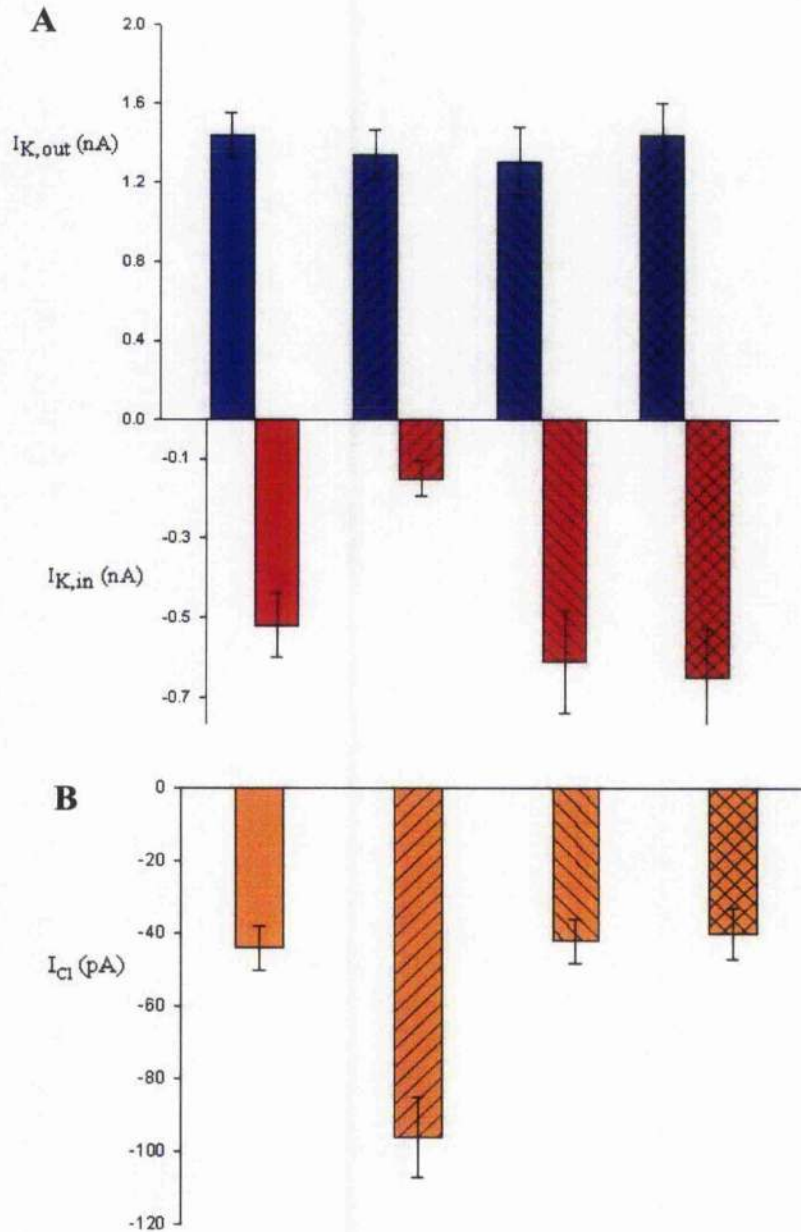


**Figure 4.2. Summary of staurosporine on the action of NO on  $I_{K,in}$ ,  $I_{K,out}$  and  $I_{Cl}$ .** Steady-state current determined as described in main text for  $I_{K,out}$  at +30 mV and  $I_{K,in}$  at -200 mV (**A**), and  $I_{Cl}$  at -70 mV (**B**). Figure shows mean  $\pm$  SE for current amplitude for control -NO (plain bars), + NO (left diagonal lines), + staurosporine (right diagonal lines), and + NO + staurosporine (crossed bars) for each current.

activity, as seen by (Grabov *et al.*, 1997a). These results demonstrate that protein kinase action is also important in the regulation of  $I_{Cl}$  by NO.

#### **4.3.2. Protein kinase(s) are essential to the NO-induced enhancement of $Ca^{2+}$ release from internal stores.**

The effect of staurosporine is to block the action of NO on the downstream targets of NO signalling in guard cells. However, from the results described in chapter 3 it is known that NO acts upstream of  $I_{K,in}$  and  $I_{Cl}$  and targets  $Ca^{2+}$  release from internal stores. Since staurosporine blocks the effect of NO on both the  $Ca^{2+}$  dependent ion channels it was hypothesised that the action of staurosporine might be to interfere with the NO induced enhanced release of  $Ca^{2+}$  from internal stores. To test this hypothesis, cells were impaled with triple barrelled microelectrodes and loaded with Fura-2 to image voltage induced dynamics in  $[Ca^{2+}]_{cyt}$ . Following impalement the membrane voltage was clamped to  $-50mV$  and the cells loaded with Fura-2. After stabilisation of the resting  $[Ca^{2+}]_{cyt}$  level, cells were treated for 2 minutes with  $1\mu M$  staurosporine and stimulated by a 20s voltage step to  $-200mV$ . Further treatment was then carried out with solutions containing both  $1\mu M$  staurosporine and  $10\mu M$  SNAP together. Figure 4.3 shows data from one representative cell. The resting level of  $[Ca^{2+}]_{cyt}$  was about  $200nM$ , which is within the range of values measured in chapter 3. In the presence of  $1\mu M$  staurosporine, stepping the voltage to  $-200mV$  evoked a rise in  $[Ca^{2+}]_{cyt}$  to  $446nM$ , similar to that without staurosporine, indicating that staurosporine does not affect the normal voltage induced increase in  $[Ca^{2+}]_{cyt}$ . When perfused with both  $1\mu M$  staurosporine and  $10\mu M$  SNAP the voltage induced  $[Ca^{2+}]_{cyt}$  was  $453nM$ , essential the same as the level seen with staurosporine alone. This

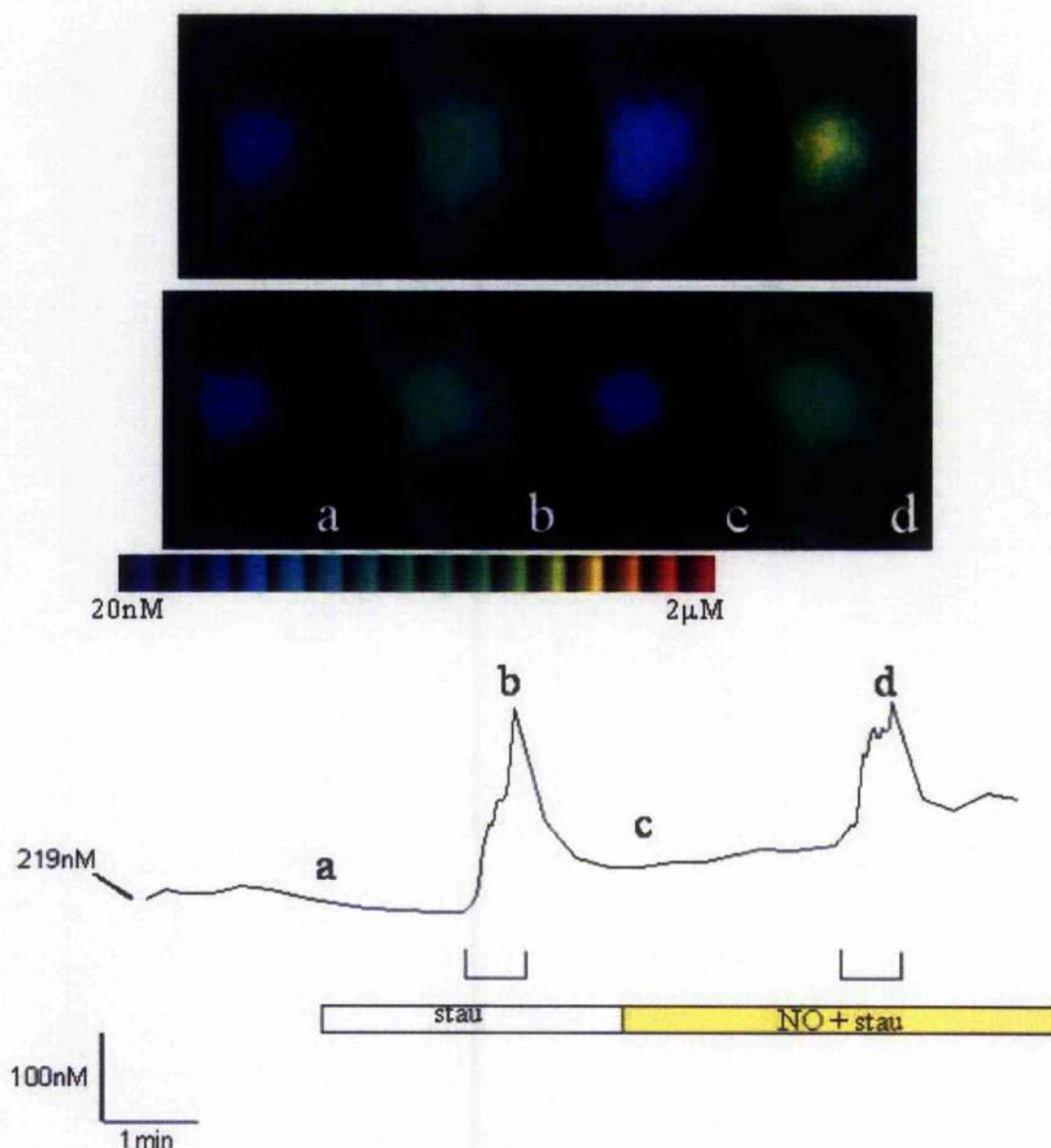


**Figure 4.3. Staurosporine blocks the normal effect of NO on promotes evoked  $[Ca^{2+}]_{cyt}$ .** (Lower)  $[Ca^{2+}]_{cyt}$  recorded from one guard cell clamped to -50 mV and stepped to -200 mV at time periods indicated ([unionsq]) in the presence of 1  $\mu$ M staurosporine before and after adding 10  $\mu$ M SNAP. (Lower Left)  $[Ca^{2+}]_{cyt}$  basal level in nM. Fura 2 fluorescence images taken at 2-s intervals. (Upper) Selected ratio images (a-d) correspond to the time points indicated on trace below, and are shown with similar images from a cell without staurosporine for comparison.

indicates that treatment with staurosporine compromises the ability of NO to stimulate release of  $\text{Ca}^{2+}$  from internal stores.

Figure 4.4 summarises the statistics for data obtained in the measurement of  $[\text{Ca}^{2+}]_{\text{cyt}}$ . The mean evoked rise in  $[\text{Ca}^{2+}]_{\text{cyt}}$  in the absence of treatment was  $378 \pm 20 \text{ nM}$  ( $n = 10$ ). In the presence of  $1 \mu\text{M}$  staurosporine the mean evoked maximal was  $406 \pm 25 \text{ nM}$  ( $n = 6$ ). In the presence of both staurosporine and SNAP, the mean  $[\text{Ca}^{2+}]_{\text{cyt}}$  was  $400 \pm 20 \text{ nM}$  compared with  $741 \pm 70 \text{ nM}$  ( $n = 6$ ) in the presence of NO alone, which represents significant inhibition of the normal NO stimulation of the  $\text{Ca}^{2+}$  signal. Resting levels of  $[\text{Ca}^{2+}]_{\text{cyt}}$  in both control measurements and with  $1 \mu\text{M}$  staurosporine were also compared. Control measurements gave mean resting level of  $171 \pm 10 \text{ nM}$  ( $n = 8$ ) whilst treatment with staurosporine alone gave a mean resting value of  $178 \pm 15 \text{ nM}$  ( $n = 6$ ), which is not significantly different from the control level. When treated with both staurosporine and NO together, the resting level showed a slight increase when compared to the control level, being  $215 \pm 31 \text{ nM}$  ( $n = 6$ ). However, this value is not significantly different from the control level, indicating that staurosporine lead to a partial inhibition of the increase in resting level normally seen upon treatment with NO.

#### **4.3.3. The protein tyrosine phosphatase inhibitor PAO promotes release of $\text{Ca}^{2+}$ from internal stores.**

Since the broad range protein kinase inhibitor staurosporine inhibits the NO enhancement of  $\text{Ca}^{2+}$  release from internal stores, it was decided to ascertain whether a more specific inhibitor might assist in identifying the protein kinase(s) involved. Previously, a protein tyrosine phosphatase has been shown to be implicated in the

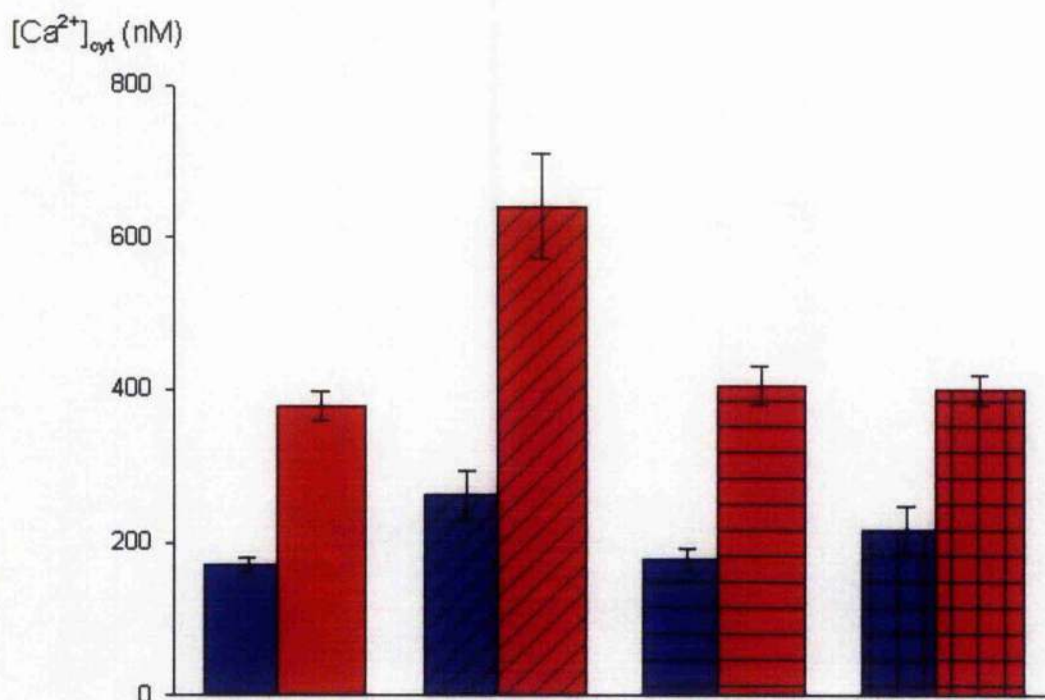


**Figure 4.4. Summary of the effect staurosporine on the NO enhanced  $Ca^{2+}$  signal.** Figure shows data for  $[Ca^{2+}]_{cyt}$  measurements both at resting voltage ( $-50mV$ ) (blue bars) and after evoking a rise in  $Ca^{2+}$  by clamping to  $-200mV$  for 30 seconds (red bars) for control measurements (plain bars), + NO (diagonal lines), + staurosporine (horizontal lines), + NO + staurosporine (crossed lines). Data are expressed as mean  $\pm$  SE.

control of ion release from the vacuole (MacRobbie, 2002). By using the protein tyrosine phosphatase inhibitor phenyl arsine oxide (PAO), showed an inhibition flux of  $^{86}\text{Rb}^+$  from the vacuole in response to a number of stimuli. Given these data, it was decided to explore a possible role for protein tyrosine phosphatase / kinase activity in regulating release of  $\text{Ca}^{2+}$  from internal stores. Preliminary experiments were carried out to examine whether PAO had any effect on the voltage induced increase in  $[\text{Ca}^{2+}]_{\text{cyt}}$ . Guard cells were impaled and loaded with Fura-2. Cells were clamped to  $-50\text{mV}$  as before and the voltage induced  $[\text{Ca}^{2+}]_{\text{cyt}}$  was examined in the absence and presence of  $25\mu\text{M}$  PAO. Figure 4.5 summarises the data obtained. Mean resting  $[\text{Ca}^{2+}]_{\text{cyt}}$  before treatment with PAO was  $163\pm 13\text{nM}$  ( $n = 11$ ). Upon voltage clamping to  $-200\text{mV}$  the level of  $[\text{Ca}^{2+}]_{\text{cyt}}$  increased to a mean value of  $377\pm 18\text{nM}$  ( $n = 11$ ). After 2 minutes of treatment with  $25\mu\text{M}$  PAO there was a significant increase in the resting level, from  $163\pm 13\text{nM}$  before PAO treatment to  $319\pm 106\text{nM}$  ( $n = 4$ ) with PAO. Clamping the cells to  $-200\text{mV}$  lead to massive increases in  $[\text{Ca}^{2+}]_{\text{cyt}}$ . Mean  $[\text{Ca}^{2+}]_{\text{cyt}}$  in the presence of PAO was  $1016\pm 159\text{nM}$  ( $n = 4$ ), almost  $750\text{nM}$  greater than without PAO. Following clamping to  $-200\text{mV}$  in the presence of PAO, no recovery of the levels of  $[\text{Ca}^{2+}]_{\text{cyt}}$  was seen during the time-course of the experiments. These results suggest a role for a protein tyrosine phosphatase or a PAO-sensitive in regulating the release of  $\text{Ca}^{2+}$  from internal stores.

#### **4.3.4. The protein tyrosine kinase inhibitor genistein does not block the inhibition of $\text{I}_{\text{K,In}}$ by NO.**

Since PAO enhances the release of  $\text{Ca}^{2+}$  from internal stores, a protein tyrosine kinase seemed a possible candidate kinase in the NO mediated release of  $\text{Ca}^{2+}$  from



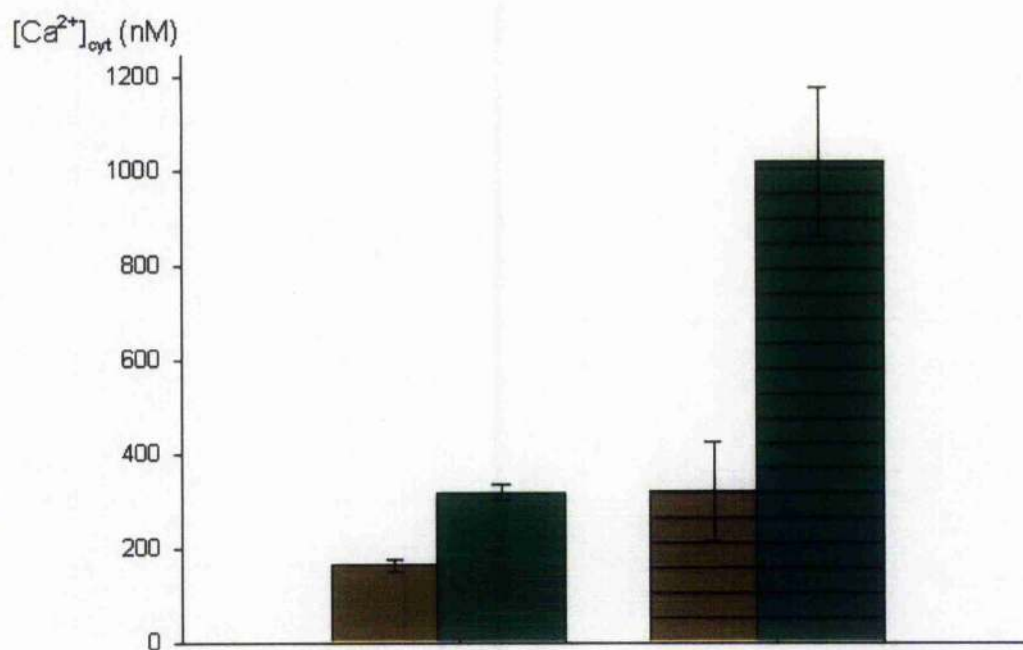


**Figure 4.5. PAO enhances Ca<sup>2+</sup> release from internal stores.** Figure shows data for [Ca<sup>2+</sup>]<sub>cyt</sub> measurements both at resting voltage (-50mV) (dark yellow bars) and after evoking a rise in Ca<sup>2+</sup> by clamping to -200mV for 30 seconds (green bars) for control measurements (plain bars), and with 25μM PAO (horizontal lines). Data are expressed as mean ± SE.

internal stores. Experiments were carried out using the protein tyrosine kinase inhibitor genistein, which was predicted to have an effect in blocking the effect of NO on  $I_{K,in}$  and  $I_{Cl}$  by inhibiting the release of  $Ca^{2+}$  from internal stores.

Figure 4.6 shows data from one representative cell treated first with  $10\mu M$  SNAP, then followed by treatment with  $10\mu M$  genistein both in the presence and absence of  $10\mu M$  SNAP. Treatment with SNAP alone led to a characteristic NO response in  $I_{K,in}$  whereby current amplitude decreased significantly within 2 minutes of treatment. This was fully washed out prior to treatment with genistein. After 2 minutes treatment with genistein alone,  $I_{K,in}$  showed little change compared to the control. After two minutes treatment with both genistein and SNAP together,  $I_{K,in}$  showed a significant decrease which was similar to the response seen with SNAP alone, indicating that it is unlikely that a protein tyrosine kinase is involved in the response of  $I_{K,in}$  to NO.

The effect of genistein on  $I_{K,in}$  is summarised in Figure 4.7. Mean  $I_{K,in}$  amplitude at  $-200mV$  before treatment was  $-0.9\pm0.2nA$  ( $n = 12$ ), decreasing to  $-0.17\pm0.01nA$  ( $n = 12$ ) in response to  $10\mu M$  SNAP. The control current amplitude in these cells was much higher than described in chapter 3. This may reflect variation in plant material. However, current amplitude in response to  $10\mu M$  SNAP is comparable to the value reported in the previous chapter. In cells treated with  $10\mu M$  genistein mean current amplitude in response to  $10\mu M$  SNAP was  $-0.24\pm0.08nA$  ( $n = 7$ ), which is not significantly different from the mean amplitude in response to  $10\mu M$  SNAP alone. In control cells treated with  $10\mu M$  genistein alone the mean current amplitude was  $-0.92\pm0.19nA$  ( $n = 11$ ), which is essentially the same as the amplitude in the absence



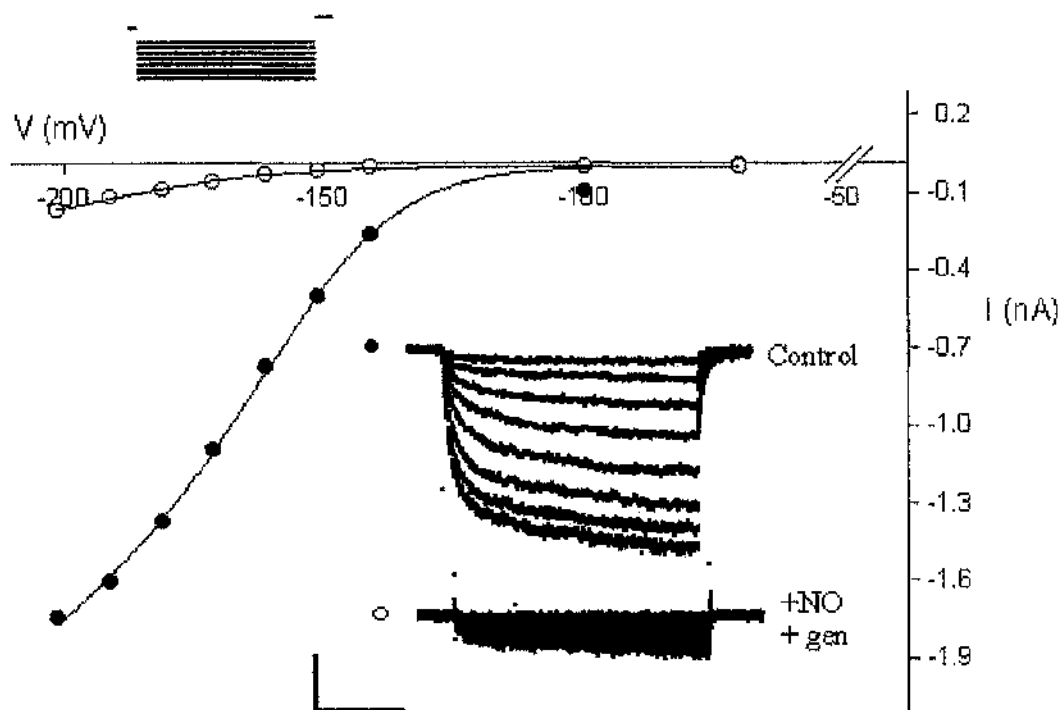


**Figure 4.6. Genistein does not affect the NO induced inhibition of  $I_{K,in}$ .** Voltage-clamp recordings from an intact *Vicia* guard cell are shown. Steady-state current-voltage curves determined from voltage-clamp steps before (●) and after 2 min of exposure to 10  $\mu$ M SNAP and 10  $\mu$ M genistein (○).  $K^+$ -channel currents were obtained by subtracting instantaneous current from steady-state current at each voltage. Data for  $I_{K,in}$  are shown with fitted Boltzmann functions. (Inset) Current traces for  $I_{K,in}$  before (upper) and during (lower) NO + genistein treatment. Voltage protocols (Top) of steps between -200 and -120 mV from holding voltage of -100 mV are shown. (Scale: horizontal, 2 s; vertical, 0.5 nA.)

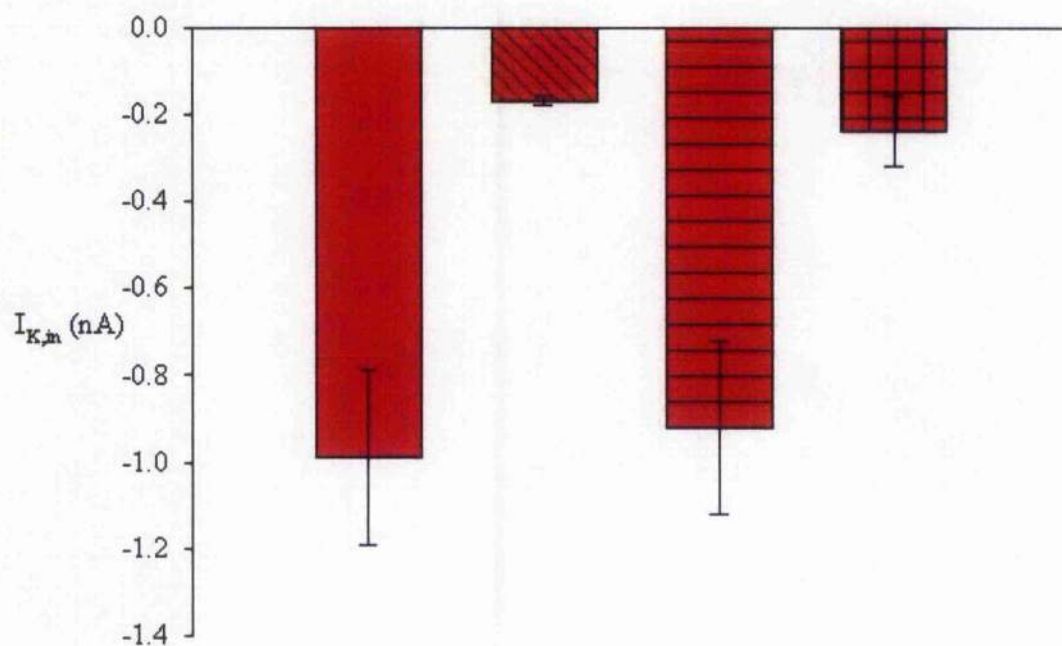


**Figure 4.7. Summary of genistein on the action of NO on  $I_{K,in}$ .** Steady-state current determined as described in main text for  $I_{K,in}$  at -200 mV. Figure shows mean  $\pm$  SE for current amplitude for control -NO (plain bars), +NO (diagonal lines), + genistein (horizontal lines) and + NO + genistein.

of genistein. These data suggest that genistein has no effect on  $I_{K,in}$  either in the presence or absence of genistein. Thus it is unlikely that a protein tyrosine kinase is involved in the transmission of the NO signal.

#### **4.3.5. Genistein does not inhibit the effect of NO on the voltage evoked increase in $[Ca^{2+}]_{cyt}$ .**

Whilst there was no effect of genistein on the response of  $I_{K,in}$  and  $I_{Cl}$  to NO, the possibility of some effect on the response of the  $Ca^{2+}$  signal to NO remained. Therefore, the effect of genistein on the voltage evoked increase in  $[Ca^{2+}]_{cyt}$  and the associated NO enhancement was investigated. Figure 4.8 summarises the data obtained. The mean evoked rise in  $[Ca^{2+}]_{cyt}$  before treatment was  $353 \pm 38 \text{ nM}$  ( $n = 11$ ), comparable to previous data sets outlined in this study. In the presence of  $10 \mu\text{M}$  genistein alone, the mean evoked rise was  $424 \pm 52 \text{ nM}$  ( $n = 7$ ), which represents an increase compared to the control level, but this is not significant. Treatment with NO alone gave a mean evoked rise to  $682 \pm 42 \text{ nM}$  ( $n = 11$ ). When treated with both NO and genistein, mean evoked  $[Ca^{2+}]_{cyt}$  was  $830 \pm 75 \text{ nM}$  ( $n = 7$ ), which is significantly higher than with NO alone. The higher evoked  $[Ca^{2+}]_{cyt}$  in the presence of both genistein and NO together may represent a real effect of the genistein treatment, or prolonged exposure to NO or a combination of both. However it is clear that genistein does not act to inhibit the NO enhancement of the voltage evoked  $[Ca^{2+}]_{cyt}$ .

Resting levels of  $[Ca^{2+}]_{cyt}$  in both control measurements and with  $10 \mu\text{M}$  genistein were also compared. Control measurements gave mean resting level of  $163 \pm 13 \text{ nM}$  ( $n = 11$ ), whilst treatment with genistein alone gave a mean resting value of  $162 \pm 20 \text{ nM}$

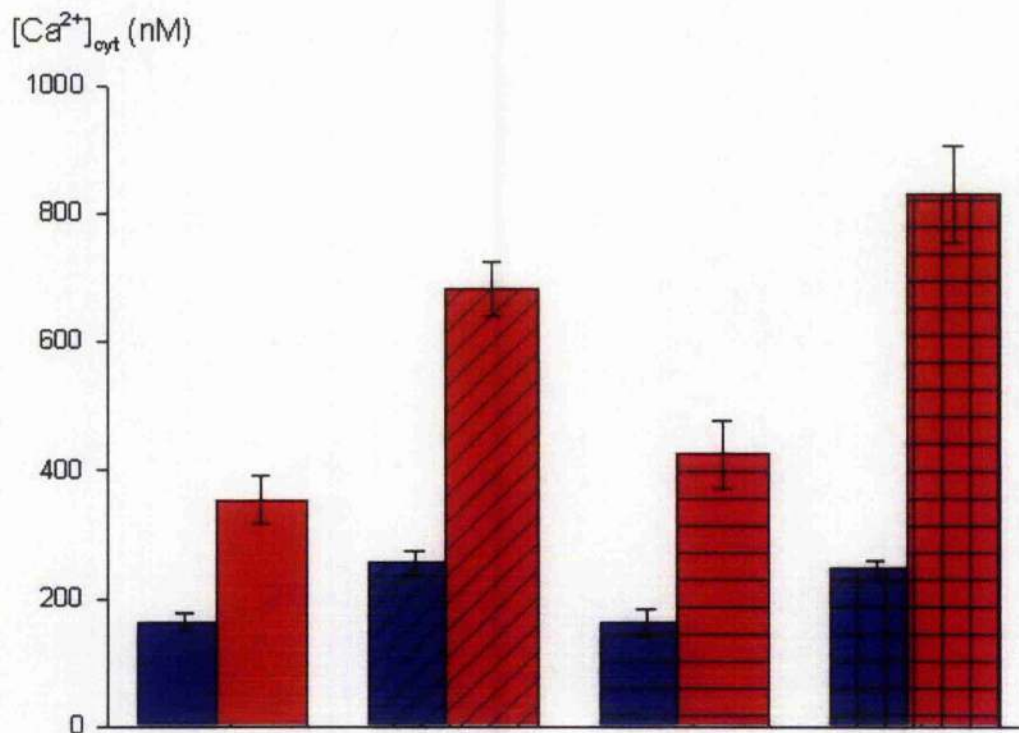


**Figure 4.8. Summary of the effect of genistein on the NO enhanced  $Ca^{2+}$  signal.** Figure shows data for  $[Ca^{2+}]_{cyt}$  measurements both at resting voltage (-50mV) (blue bars) and after evoking a rise in  $Ca^{2+}$  by clamping to -200mV for 30 seconds (red bars) for control measurements (plain bars), + NO (diagonal lines), + genistein (horizontal lines), + NO + genistein (crossed lines). Data are expressed as mean  $\pm$  SE.

( $n = 6$ ), which is not significantly different from the control level. When treated with both staurosporine and NO together, the resting level showed a slight increase when compared to the control level of  $246 \pm 13 \text{ nM}$  ( $n = 6$ ). This value is significantly higher than the control level. This difference, as for the difference at  $-200 \text{ mV}$ , may be due to the amount of time spent in the presence of NO rather than any real enhancement effect of genistein treatment.

## 4.4. Discussion.

### 4.4.1. Introduction

Phosphorylation and dephosphorylation are key events in cell signalling and metabolism. Protein kinases and phosphatases often act as molecular on and off switches, triggering changes in the addition and removal of phosphate groups on proteins acting as molecular on and off switches. In guard cells, proteins involved in phosphorylation events have already been shown to be involved in the regulation of ion channels. Plasma membrane  $K^+$  channels  $Ca^{2+}$  channels, and vacuolar channels have all been shown to be sensitive to phosphatase and kinase inhibitors (Allen and Sanders, 1995). Further insights have come from studying *abil* mutant and dominant negative plants, which have revealed a role for phosphatases in regulation of anion channels,  $K^+$  channels and  $Ca^{2+}$  signalling (Allen *et al.*, 1999; Murata *et al.*, 2001).

The data outlined here provide evidence of a role for protein kinase(s) in NO signalling in guard cells. Cells were treated with the protein kinase inhibitor staurosporine both in the presence and absence of NO. Staurosporine alone did not alter the properties of either  $I_{K,in}$  or  $I_{Cl}$ . However, staurosporine could block the normal effect of NO on both  $I_{K,in}$  and  $I_{Cl}$ , such that  $I_{K,in}$  was not inhibited and  $I_{Cl}$  not stimulated. The effect of staurosporine on the enhancement of the  $Ca^{2+}$  signal by NO was examined. Whilst staurosporine alone had no effect on the voltage induced increase in  $[Ca^{2+}]_{cyt}$ , the inhibitor blocked the NO enhancement of the signal, indicating that protein kinase(s) are part of the signal cascade which targets the release of  $Ca^{2+}$  from internal stores. The possible role of a protein tyrosine kinase / phosphatase system was investigated using genistein and PAO. PAO alone dramatically enhanced the voltage induced increase in  $[Ca^{2+}]_{cyt}$ . However, genistein

did not inhibit the effect of NO on  $I_{K,in}$ ,  $I_{Cl}$  or the voltage induced increase in  $[Ca^{2+}]_{cyt}$ . These data suggest that whilst protein tyrosine phosphatases might regulate release of  $Ca^{2+}$  from internal stores, protein tyrosine kinases are not important for the propagation of the NO signal leading to control of  $I_{K,in}$ ,  $I_{Cl}$  and the voltage induced increase in  $[Ca^{2+}]_{cyt}$ .

#### **4.4.2. Protein kinases and guard cell signalling.**

The data on the action on staurosporine provide interesting information on the action of protein kinases in guard cells. Previous studies such as those of have taken a pharmacological approach to examine the role of phosphorylation events in guard cells. However, such studies have been unable to identify the targets of phosphorylation. More recent work including and the genetic approach of have been better able to pin down possible targets and their positions. Placing NO in the context of ABA signalling and ion channel control has opened new avenues in which to explore phosphorylation signalling in guard cells.

The data suggest the action of protein kinase(s) somewhere in the pathway between NO perception and the stimulation of  $Ca^{2+}$  release from external stores. Data from the previous chapter provided evidence that this pathway involves *de novo* synthesis of NO, and transduction of the signal via cGMP and cADPR. Thus the action of the kinase might be at some point on this pathway. However, since staurosporine is a broad range kinase inhibitor, the data do not provide information about the kinase involved. A number of protein kinases have been identified that are known to be involved in signalling in guard cells. Of these, the most extensively studied are the  $Ca^{2+}$  dependent protein kinases (CDPK), of which there are 34 known in the

*Arabidopsis* genome (Hrabak *et al.*, 2003). Purified CDPK has been shown to interact and activate a chloride channel on the tonoplast of *V. faba* guard cells (Pei *et al.*, 1996). Furthermore, CDPK has been shown to phosphorylate KAT1 *in vitro*, and to promote KAT1 currents in oocytes co-injected with KAT1 and CDPK. Interestingly, other possible components of NO signalling in guard cells are regulated by protein kinases. One such example is the enzyme nitrate reductase (NR), which is one of the candidate NOS activities in guard cells (Desikan *et al.*, 2002; Garcia-Mata and Lamattina, 2003). Examining the role of protein kinases and phosphatases might help in unravelling the source of NO in the future.

#### **4.4.3. What is the identity of the protein kinase involved in NO signal transmission?**

From studies in animal cells, it is known that NO signalling proceeds via a cGMP / cADPR pathway to facilitate  $\text{Ca}^{2+}$  release from internal stores (Friebe and Koesling, 2003; Lee, 1997). A key to this process is the action of protein kinase G, which is activated by cGMP (Carvajal *et al.*, 2000; Piltz and Casteel, 2003). Activation of protein kinase G is essential for the production of cADPR further downstream (Galione *et al.*, 1993; Graeff *et al.*, 1998; Willmott *et al.*, 1996). Results in the previous chapter show that NO signalling in guard cells also proceeds via cGMP and cADPR, which was demonstrated by inhibition of the NO effect by inhibitors of guanylate cyclase and the ryanodine receptor. Thus it can be speculated that a possible target for staurosporine might be a protein kinase G homologue, which is responsible for activating the production of cADPR. Inhibitors of protein kinase G are available that different modes of action, such as KT5823, which competes for the ATP binding site on the enzyme, and cGMP analogues such as Rp-8pCPT-cGMP, which competes



for the cGMP binding site (Butt *et al.*, 1994; Kase *et al.*, 1987). The existence of such tools allows for a more detailed examination of the action of protein kinase G in future studies.

#### **4.4.4. Summary**

The data presented here show that protein kinase activity is essential for the transmission of the NO signal to bring about changes in  $I_{K,in}$ ,  $I_{Cl}$  and  $Ca^{2+}$  release from internal stores. The protein kinase action is probably located upstream of  $Ca^{2+}$  release from internal stores. Animal models of NO signalling show the requirement of a protein kinase G to stimulate cADPR synthesis to gate  $Ca^{2+}$  release from internal stores. Such a mechanism might exist in plants, and data in this chapter suggest that experiments using protein kinase G inhibitors might in future help to identify the underlying mechanism.

## **CHAPTER 5**

### **INTEGRATION OF MEMBRANE TRAFFIC AND CELL VOLUME WITH ION CHANNELS AND $\text{Ca}^{2+}$ SIGNALLING**

### 5.1. Introduction.

There are two essential processes that occur during stomatal movements. The first is the modulation of ion transport so as to allow net solute efflux or influx to respectively control stomatal closure and stomatal opening. The second process is the regulation of cell volume. In *Vicia faba*, guard cell volume is typically 3pl when the cell is flaccid and the aperture is closed, increasing to up to 9pl when the cell is turgid and the aperture is open (Blatt *et al.*, 1999a). The stretching of the lipid bilayer can only accommodate a 2% change in surface area before shearing (Wolfe and Steponkus, 1983). Thus some exo- and endocytotic events must be involved in driving the changes in cell surface area required during stomatal movement. Use of the patch clamp technique to measure membrane capacitance (which is related to membrane surface area) has helped advance our understanding of membrane dynamics in guard cells (Homann and Tester, 1998). Membrane capacitance changes in response to hypo- and hyperosmotic conditions, leading respectively to increased and decreased membrane capacitance (Homann, 1998). Using capacitance measurements in combination with styryl dye labelling, it has been possible to show that there can be both rapid and constitutive endocytosis in guard cells (Kubitscheck *et al.*, 2000). A pool of membrane material has also been observed close to the plasma membrane which might be available for re-incorporation (Kubitscheck *et al.*, 2000; Hurst *et al.*, 2004).

There is evidence, though limited, which points to a link between control of membrane traffic and regulation of ion channels. One such example is *Era1*, which encodes a protein farnesyl transferase, which is responsible for addition of lipid

anchor moieties to small GTPases (Cutler *et al.*, 1996). Small GTPases are known to be important at various stages in membrane trafficking in plants (Batoko *et al.*, 2000; Rutherford and Moore, 2002). Mutant *eral* plants show a ABA hypersensitive response, which in guard cells may be attributed to enhanced ABA sensitivity of  $\text{Cl}^-$  channels (Pei *et al.*, 1998). Whilst the results of this study hint at the possible regulation of ion channels by components of membrane trafficking, further evidence on the possible mechanism is lacking. In both animals and yeast, the production of phosphatidic acid by phospholipase D (PLD) is strongly linked to vesicle formation and budding (Siddhanta and Shields, 1998; Martin, 1997). In guard cells, phospholipase D has been identified and shown to be essential in normal stomatal movements and  $\text{K}^+$  channel regulation, though data further linking phosphatidic acid production and membrane traffic in guard cells is lacking (Jacob *et al.*, 1999).

One potential point of interaction between ion channels and cell volume / membrane traffic is via actin filaments. Guard cells are known to possess actin filaments that can undergo changes in distribution. When stomata are turgid and the pore is open, the actin filaments show a radial distribution, and these filament reorganise in response to stimuli which lead to stomatal closure (Kim *et al.*, 1995; Eun and Lee, 1997). Reorganisation is not simply a chance event, and regulatory factors have now been identified which include  $\text{Ca}^{2+}$ , ABA, protein kinases and phosphatases (Hwang and Lee, 2001; Eun *et al.*, 2001). Using actin antagonists it has been possible to correlate actin filament integrity with levels of  $\text{K}^+$  channel activity (Hwang *et al.*, 1997; Liu and Luan, 1998). In both cases, the investigators have interpreted the role of actin as a mechanosensor, which is linked directly to ion channels. However, it is now clear that actin plays a role in vesicle trafficking in plants, such that Golgi vesicles move around

the cell on actin cables, using an actin / myosin interactions (Boevink *et al.*, 1998; Nebenfuhr *et al.*, 1999). In the light of such evidence there is a need to revisit the role of actin in the regulation of ion channels in guard cells.

A further development in exploring the regulation of volume in guard cells came with the identification of a syntaxin, NtSyr1, which is involved in the regulation of guard cell ion channels (Leyman *et al.*, 1999). The role of syntaxins as components of membrane fusion and vesicle trafficking in all eukaryotes is well documented (see chapter 1). However, the cloning of NtSyr1 raised fundamental questions as to the possible links between vesicle trafficking and regulation of ion channels. Syntaxins are known to interact directly with ion channels in animal cells, forming part of a 'signalosome' which is essential for co-localising ion channels and secretion events (Wiser *et al.*, 1996; Wiser *et al.*, 1999). Disruption of normal NtSyr1 function in guard cells also leads to uncoupling of the normal response of  $I_{K,in}$ ,  $I_{K,out}$  and  $I_{Cl}$  to ABA . Whilst some progress has been made in understanding the mode of action of NtSyr1 in secretion (Geelen *et al.*, 2002), it is still relatively unclear as to how its function might relate to guard cell ion channels and stomatal movements, and any possible interaction between the two. With this in mind, it was decided to take a multi-disciplinary approach to examining possible interactions between secretion, cell volume control and the regulation of ion channels in guard cells.

Studies were carried out to examine the effect of the secretion inhibitors brefeldin A (BFA) and Latrunculin B (LATB) on ion channel control and stomatal movements. Furthermore, the role of NtSyr1 in guard cell  $Ca^{2+}$  signalling and stomatal closure was examined using transgenic plants expressing the cytosolic fragment of NtSyr1 under

the control of a dexamethasone inducible promoter. Results show that both LATB and BFA inhibit  $I_{K,in}$ , but only LATB inhibits  $I_{K,out}$ . In addition, LATB induces stomatal closure and BFA inhibits stomatal opening. Analysis of  $Ca^{2+}$  signalling and ABA in dexSP2-14 transgenic plants revealed that expression of the SP2 fragment of NtSyr1 induces a negative shift in the threshold for voltage induced increases in  $[Ca^{2+}]_{cyt}$ . Plants expressing the SP2 protein were defective in ABA induced stomatal closure and showed a time-dependent increase in osmotic content. SP2 expressing also showed a delayed stomatal closure response in response to NO. Together, these results suggest that membrane trafficking and its machinery are involved in the regulation of  $K^+$  channels and  $Ca^{2+}$  signalling leading to changes in stomatal aperture in guard cells.

## 5.2. Materials and methods

Electrophysiological and imaging experiments were performed as described in chapter 2 with the following exceptions. All experiments in this chapter were carried out using *Nicotiana tabacum* plants.  $K^+$  channel measurements were carried out in 5mM Ca-MES (pH6.1), 10mM KCl supplemented with brefeldin A (BFA) and Latrunculin B as indicated in the text. Both BFA and LATB prepared as stock solutions in DMSO and diluted as required (final DMSO concentration < 0.1%). Transgenic plants (designated dexSP2-14) expressing the cytosolic portion of the tobacco syntaxin NtSyr1 under the control of a dexamethasone-inducible promoter (Aoyama and Chua, 1997) were used (see Geelen *et al.*, 2002). Untreated dexSP2-14, wild type and empty vector (C2) plants were also used as controls. SP2 expression was induced by treatment with 10 $\mu$ M water-soluble dexamethasone by application to the soil and foliar spray.

Stomatal aperture measurements were carried out by preparing epidermal peels, and attaching them to microscope slides with small quantities of pressure sensitive adhesive (see chapter 2). Apertures were measured by eye with the aid of a calibrated eyepiece. All aperture measurements were carried out in 5mM Ca-MES (pH6.1), 10mM supplemented with BFA and LATB as required. Leaf tissue osmotic strength analysis was carried out using a vapour pressure osmometer (Westcor, Utah, USA). A known weight of leaf tissue was ground in water (1:1 w/v), and then spun at 13,000 rpm for 3 minutes. The supernatant was removed and analysed.

*N. tabacum* guard cells were generally more delicate than *V. faba*, with only the small guard cells giving satisfactory currents. Thus it was necessary to manufacture finer

tipped double and triple barrelled electrodes than for *V. faba* so as to improve the impalement success rate. Voltage clamp protocols were as used in previous chapters. However, since  $I_{K,in}$  activation occurred at a more negative voltage in *N. tabacum* compared with *V. faba*, clamp steps to  $-250\text{mV}$  were used. Clamping to positive voltages was often difficult, since the smaller tip diameter required for delicate *N. tabacum* cells compromised the current passing ability of the electrodes. Thus,  $I_{K,out}$  voltage steps were adjusted as required. Single voltage protocols were used to examine the effect of BFA on  $I_{K,in}$ , and are described in section 5.3.



## 5.3 Results 1: Pharmacology

### 5.3.1 Brefeldin A inhibits $I_{K,in}$ in a concentration dependent manner, but does not inhibit $I_{K,out}$

The effect of BFA on  $I_{K,in}$  and  $I_{K,out}$  currents in intact *Nicotiana tabacum* cells was examined. Currents were recorded under voltage clamp in cells perfused with solutions either with or without micromolar concentrations of BFA. The measurements shown in figure 5.1 are taken from one representative cell treated with 7nM BFA. Original IV curves show currents recorded immediately prior to and after 5 minutes treatment with BFA. It can be seen that  $I_{K,in}$  shows a marked decrease in response to 7nM BFA after 5 minutes treatment, but that  $I_{K,out}$  showed little change. Indeed,  $I_{K,out}$  failed to show a consistent response at any of the BFA concentrations examined. All cells showed a similar response of  $I_{K,in}$  to BFA. Following treatment, the BFA solution was removed by perfusion with standard buffer solution (5mM Ca-MES (pH6.1), 10mM KCl). Within the time-course of the experiments  $I_{K,in}$  currents failed to recover, and thus was essentially irreversible. The results of fitting IV curves to a Boltzmann function showed that the half-maximal activation voltage ( $V_{1/2}$ ) was not displaced in the presence of BFA, remaining at about -200mV, indicating that the voltage dependence of  $I_{K,in}$  was not altered. However, fitting of the Boltzmann function revealed that BFA significantly decreased the maximal conductance ( $G_{max}$ ). In the absence of BFA, the mean  $G_{max}$  was  $0.8 \pm 0.3 \mu S \text{ cm}^{-2}$ , decreasing to  $0.3 \pm 0.1 \mu S \text{ cm}^{-2}$  in the presence of BFA ( $n = 8$ ). Relative mean  $I_{K,in}$  at -220mV was significantly lower in the presence of 7nM BFA after 5 minutes treatment with BFA, effectively half the value of the control.

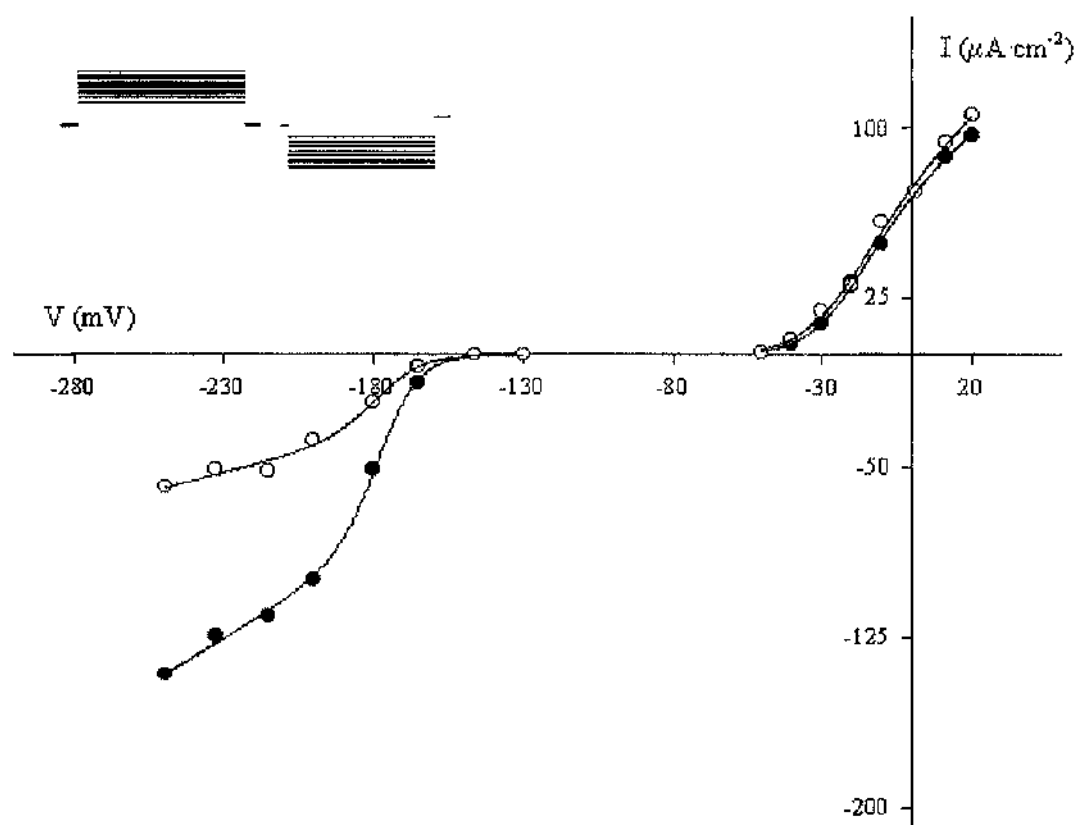


**Figure 5.1. BFA inhibits  $I_{K,in}$  but not  $I_{K,out}$ .** Voltage-clamp recordings from an intact *N. tabacum* guard cell are shown. Steady-state current–voltage curves determined from voltage-clamp steps before (●) and after 5 min of exposure to 7nM BFA (○).  $K^+$ -channel currents were obtained by subtracting instantaneous current from steady-state current at each voltage. Voltage protocols (*Top*) of steps between -250 and +20 mV from holding voltage of -100 mV are shown.

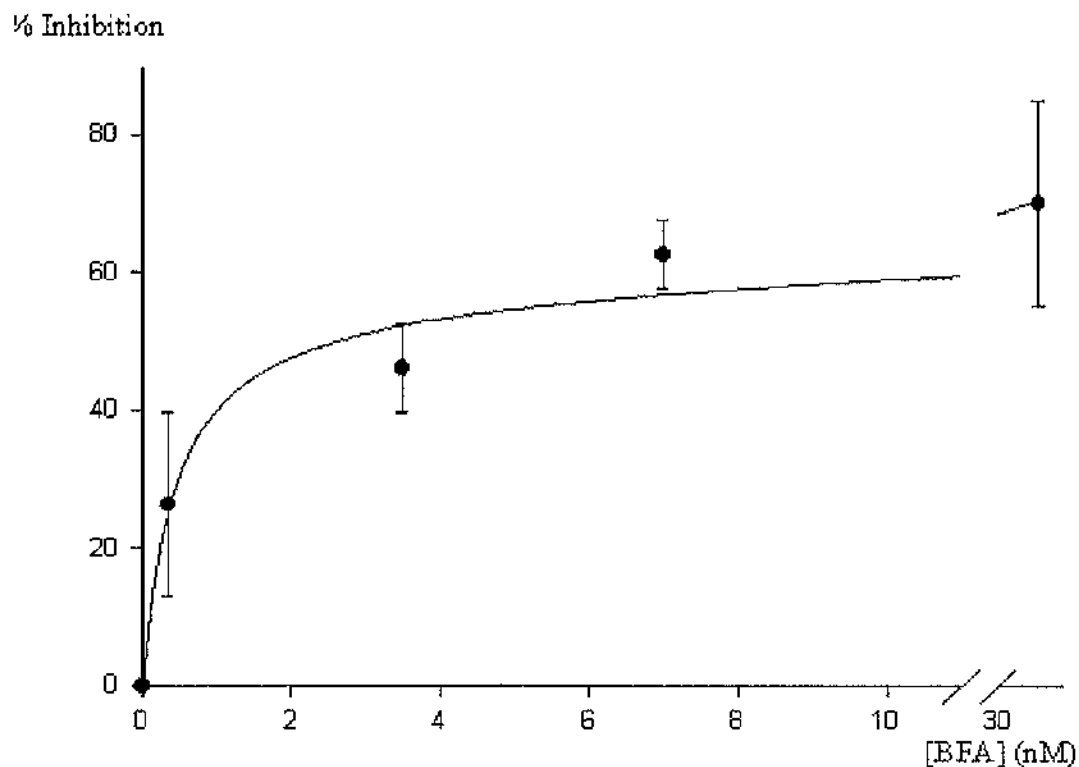


**Figure 5.2. BFA inhibition of  $I_{K,in}$  is dose-dependent.** Figure shows percentage inhibition of  $I_{K,in}$  in response to increasing concentrations of BFA (expressed as mean  $\pm$  SE). Percentage inhibition was calculated from the steady-state current at  $-200\text{mV}$  following subtraction of the instantaneous current. Data are shown with fitted Michaelis-Menten equation, which yielded a  $K_i$  of  $0.75 \pm 0.3\text{nM}$  ( $r^2=0.96$ ).

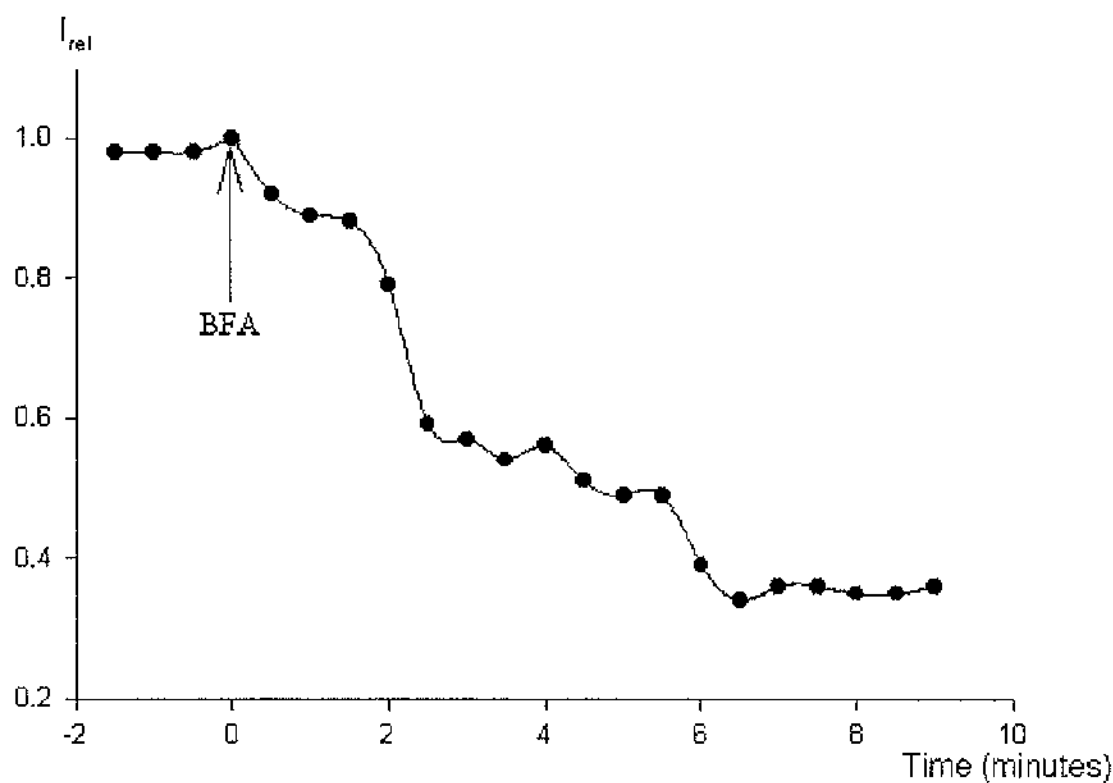


**Figure 5.3. Time-course of  $I_{K,in}$  inhibition by BFA.** Data from one representative cell.  $K^+$ -channel currents were obtained by subtracting instantaneous current from steady-state current. Data were obtained using a single step protocol from a holding potential of  $-100\text{mV}$  to  $-220\text{mV}$ .  $30\text{nM}$  BFA was added at the time-point indicated.

### 5.3.2 BFA inhibition of $I_{K,in}$ is dose-dependent

Concentration series experiments were performed on single cells at BFA concentrations from 0.35nM up to 30nM. Measurements were taken moving from the lowest to highest concentration, ensuring that currents had stabilised before progressing to the next concentration. Figure 5.2 shows mean percentage inhibition of  $I_{K,in}$  in response to increasing BFA concentration at  $-220\text{mV}$  ( $n = 5$ ).  $I_{K,in}$  is highly sensitive to BFA, with  $26 \pm 13\%$  inhibition seen at only 0.35nM BFA. The maximal inhibition was  $70 \pm 15\%$  at a BFA concentration of 30nM. Data could be described by a Michaelis-Menten function ( $r^2=0.96$ ), yielding a value of half-maximal inhibition ( $K_i$ ) of  $0.75 \pm 0.3\text{nM}$ .

The time-course of BFA inhibition of  $I_{K,in}$  was examined by application of a single voltage clamp step at  $-220\text{mV}$ , repeated at 30s intervals. Figure 5.3 shows data from a representative cell treated with 30nM BFA. It can be seen that  $I_{K,in}$  was relatively stable prior to BFA treatment, then decreases with time. Decrease in  $I_{K,in}$  was most pronounced after two minutes of treatment. Current amplitude reached a new steady after 7 minutes. As with all other experiments in this study, the effects were not reversible upon washout of the BFA solution.

### 5.3.3 Latrunculin B inhibits both $I_{K,in}$ and $I_{K,out}$ .

The effect of the actin antagonist LATB on  $I_{K,in}$  and  $I_{K,out}$  was also examined. As for BFA, currents were recorded under voltage clamp before and after LATB treatment. The measurements shown in figure 5.4 are taken from one representative cell treated

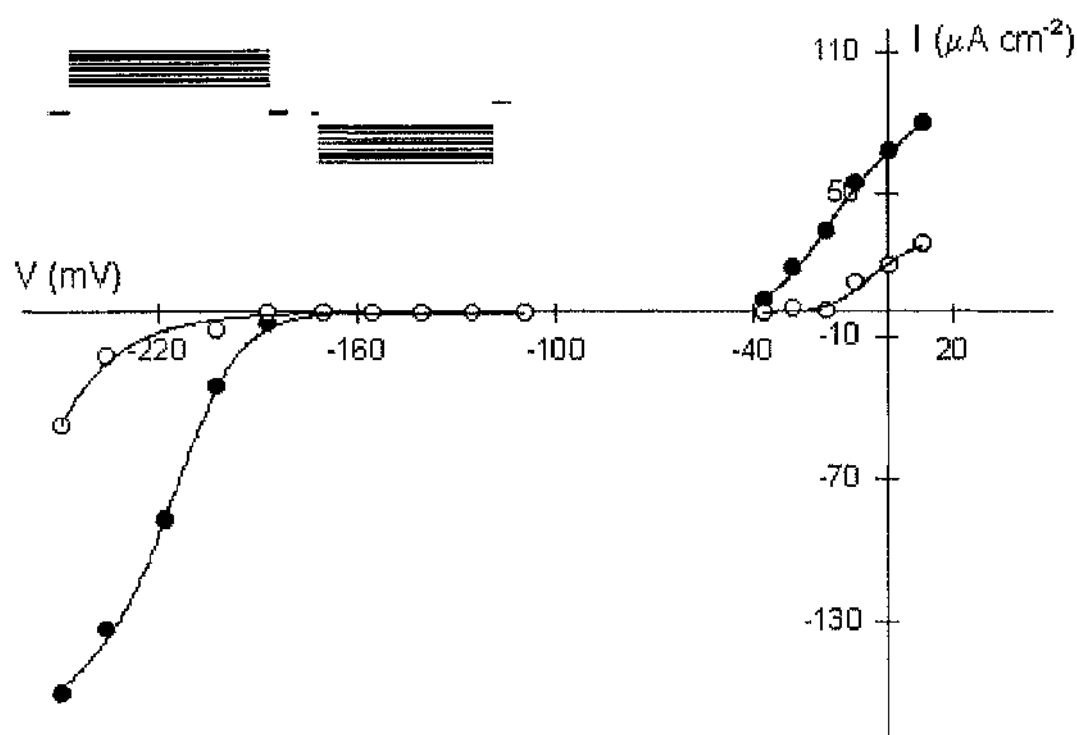


**Figure 5.4. LATB inhibits  $I_{K,in}$  and  $I_{K,out}$ .** Voltage-clamp recordings from an intact *N. tabacum* guard cell are shown. Steady-state current-voltage curves determined from voltage-clamp steps before (●) and after 2 min of exposure to 30nM LATB (○).  $K^+$ -channel currents were obtained by subtracting instantaneous current from steady-state current at each voltage. Voltage protocols (*Top*) of steps between -250 and +10 mV from holding voltage of -100 mV are shown.

with 30nM LATB. IV curves show currents recorded prior to and after 5 minutes treatment with LATB. Both  $I_{K,in}$  and  $I_{K,out}$  show strong inhibition by LATB. The inhibition of  $I_{K,in}$  by LATB was stronger than by BFA, indeed some cells showing complete inhibition. Following treatment, the LATB solution was removed by perfusion with standard buffer solution (5mM Ca-MES (pH6.1), 10mM KCl). Within the time-course of the experiments neither  $I_{K,in}$  nor  $I_{K,out}$  showed signs of recovery, indicating that the effects of LATB were essentially irreversible within the time-course of the experiment. IV curves from cells where there was not complete inhibition of  $I_{K,in}$  and  $I_{K,out}$  were fitted to a Boltzmann function. Parameters from the fits showed that the half-maximal activation voltage ( $V_{1/2}$ ) for both  $I_{K,out}$  and  $I_{K,in}$  was displaced in the presence of LATB. Before treatment,  $V_{1/2}$  for  $I_{K,out}$  was  $-14 \pm 1$  mV, shifting to  $-7.9 \pm 3$  mV in the presence of 30nM LATB. Before treatment,  $V_{1/2}$  for  $I_{K,in}$  was  $-207 \pm 1$  mV, shifting to  $-225 \pm 1$  mV in the presence of 30nM LATB. Fitting of the Boltzmann function revealed that LATB also significantly decreased the maximal conductance ( $G_{max}$ ). In the absence of LATB, the mean  $G_{max}$  for  $I_{K,in}$  was  $4.8 \pm 0.9 \mu S$   $cm^{-2}$ , decreasing to  $0.7 \pm 0.01 \mu S$   $cm^{-2}$  in the presence of 30nM LATB ( $n = 5$ ). For  $I_{K,out}$ ,  $G_{max}$  was  $0.9 \pm 0.2 \mu S$   $cm^{-2}$ , decreasing to  $0.6 \pm 0.1 \mu S$   $cm^{-2}$  upon treatment with LATB. Mean relative  $I_{K,in}$  calculated at  $-220$  mV after 5 minutes treatment with 30nM LATB was  $14 \pm 2\%$  ( $n = 5$ ). Mean relative  $I_{K,out}$  at  $+20$  mV after 5 minutes treatment was  $27 \pm 12\%$  ( $n = 3$ ).

#### **5.3.4 LATB inhibition of $I_{K,in}$ and $I_{K,out}$ is dose-dependent**

Concentration series experiments were performed on single cells with concentrations of 0.1, 0.5, 1 and 30nM LATB. As for the BFA treatments, currents were allowed to

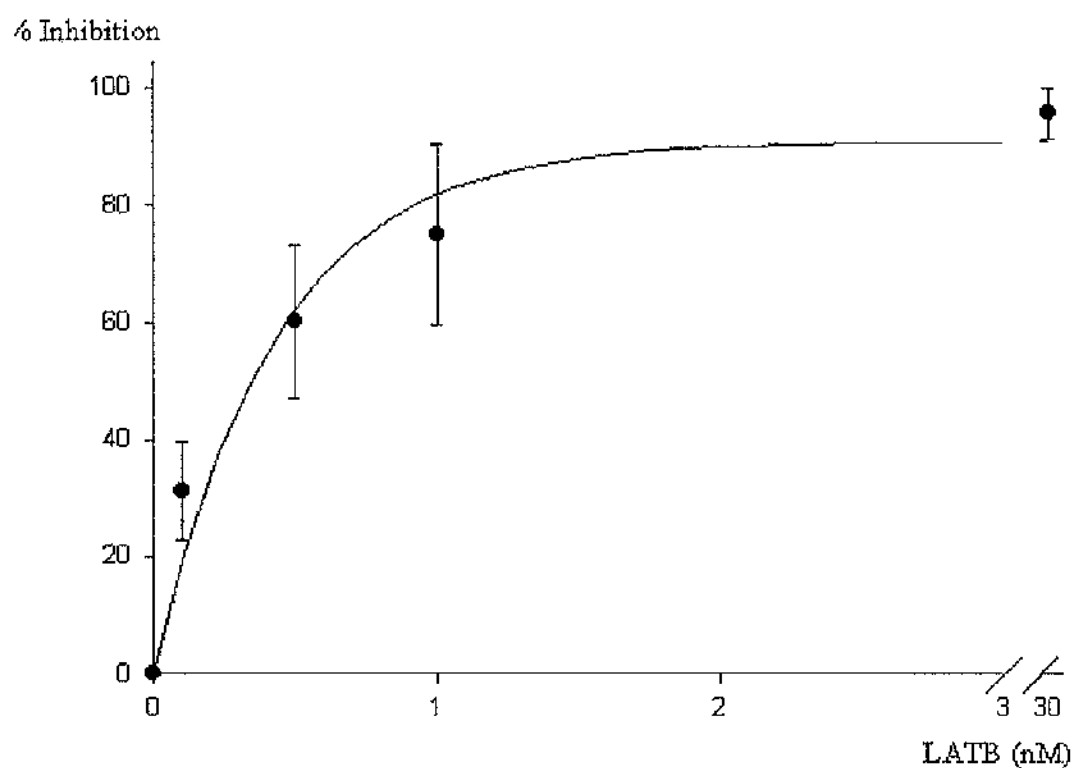


**Figure 5.5. LATB inhibition of  $I_{K,in}$  is dose-dependent.** Figure shows percentage inhibition of  $I_{K,in}$  in response to increasing concentrations of LATB (expressed as mean  $\pm$  SE). Percentage inhibition was calculated from the steady-state current at  $-200\text{mV}$  following subtraction of the instantaneous current. Data are shown with fitted Michaelis-Menten equation, which yielded a  $K_i$  of  $0.25 \pm 0.03\text{nM}$  ( $r^2=0.995$ ).



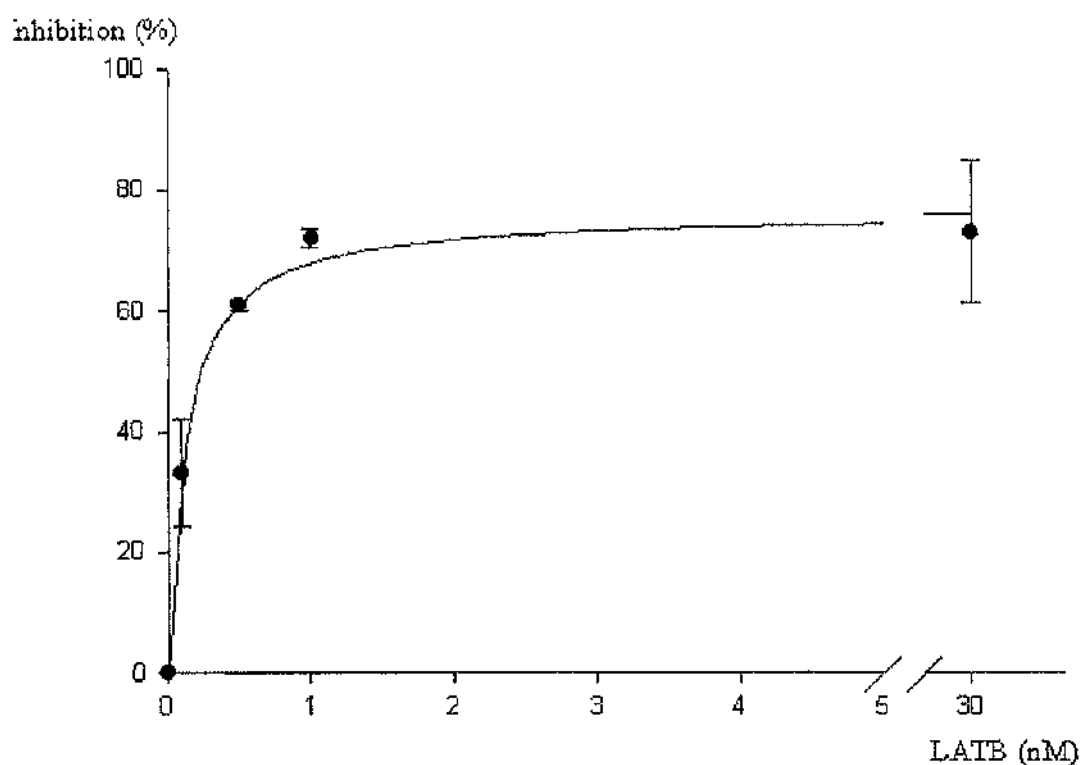


**Figure 5.6. LATB inhibition of  $I_{K,out}$  is dose-dependent.** Figure shows percentage inhibition of  $I_{K,out}$  in response to increasing concentrations of LATB (expressed as mean  $\pm$  SE). Percentage inhibition was calculated from the steady-state current at  $-200\text{mV}$  following subtraction of the instantaneous current. Data are shown with fitted Michaelis-Menten equation, which yielded a  $K_i$  of  $0.12 \pm 0.02\text{nM}$  ( $r^2=0.993$ ).

stabilise before stepping up in concentration. Both  $I_{K,in}$  (figure 5.5) and  $I_{K,out}$  (figure 5.6) showed increased inhibition with increased LATB concentrations. This dose-dependent inhibition by LATB could be described by fitting to a Michaelis-Menten equation ( $r^2=0.995$  and  $0.993$  respectively). Fits generated  $K_i$  values of  $0.25\pm0.03$ nM for  $I_{K,in}$  ( $n = 5$ ) and  $0.12\pm0.02$ nM for  $I_{K,out}$  ( $n = 3$ ).

### 5.3.5 BFA and LATB impair normal stomatal movements

Since both BFA and LATB have an effect on  $K^+$  channel activity at the plasma membrane, it was decided to assay their effects on stomatal movements. Aperture measurements were taken from epidermal strips of *N. tabacum* leaves. Results outlined above show that BFA only affects  $I_{K,in}$  and not  $I_{K,out}$ , and so it was decided to examine whether stomatal opening following ABA treatment was impaired in guard cells when treated with BFA. Figure 5.7 shows the results of aperture measurements from 5 epidermal strips ( $n = 39$ ). Upon addition of  $20\mu$ M ABA, a normal stomatal closure response to ABA was seen, with the aperture closing within about 1hr. The effect of BFA alone on stomatal apertures was also examined. Treatment with 7nM BFA alone for up to 1hr did not alter the normal stomatal aperture (data not shown). In cells treated with  $20\mu$ M ABA, washout with 7nM BFA, stomata showed only a partial reopening before reaching a static state at an aperture of about  $2\mu$ m, suggesting that BFA affects the normal opening response of guard cells.

Treatment with LATB leads to decreases in both  $I_{K,in}$  and  $I_{K,out}$ . Thus it was decided to examine whether LATB alone could bring about stomatal closure. Figure 5.8 shows

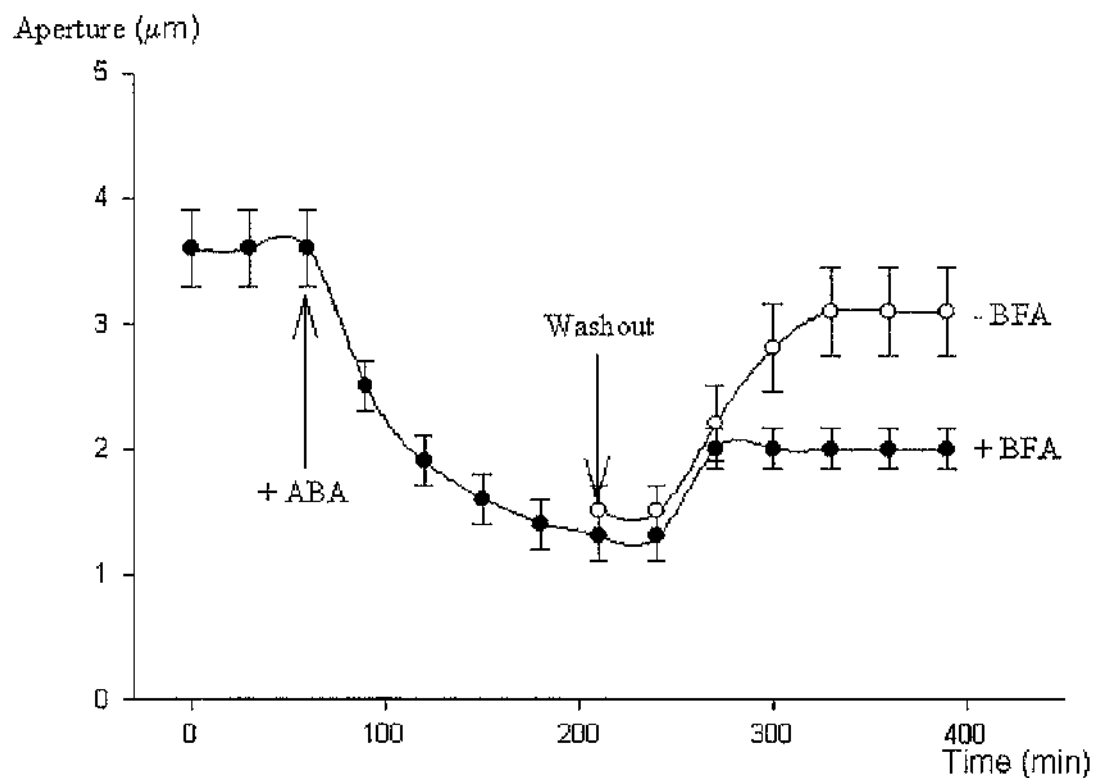


**Figure 5.7. BFA inhibits stomatal opening.** Stomatal apertures were measured at 30min intervals. Addition of  $20\mu\text{M}$  ABA is indicated, along with the time-point whereby washout with / without  $7\text{nM}$  BFA was commenced. Data are expressed as mean aperture ( $\mu\text{m}$ )  $\pm$  SE.

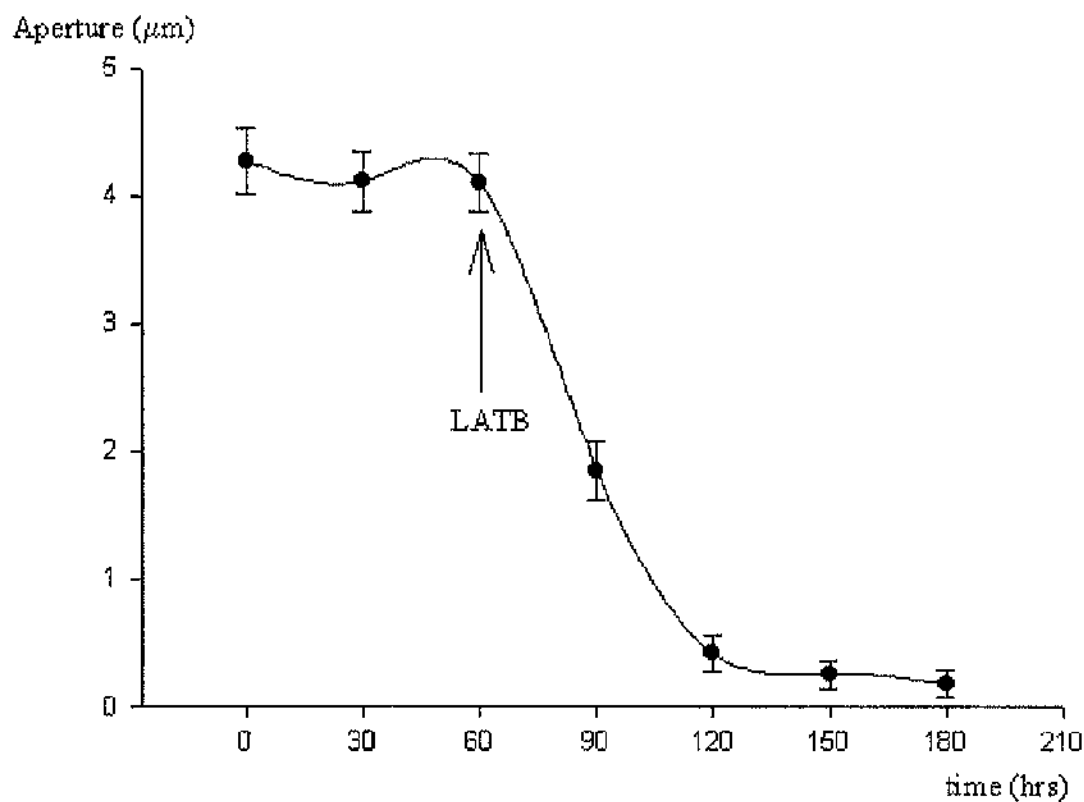


**Figure 5.8. LATB induces stomatal closure.** Stomatal apertures were measured at 30min intervals. Epidermal strips were treated with 30nM LATB at the time-point indicated. Data are expressed as mean aperture ( $\mu\text{m}$ )  $\pm$  SE.

the results of aperture measurements from 3 epidermal strips ( $n = 20$ ). Upon addition of 30nM LATB, stomatal closure was seen. The response of stomata could be seen after 30 minutes in LATB, and was complete within 60 minutes of treatment. The response was notably different from that of BFA, which alone could not bring about stomatal closure.

## **5.4 Results II: Analysis of SP2 transgenic plants**

### **5.4.1 Expression of the SP2 fragment of NtSyr1 causes a negative shift in the threshold for voltage induced $\text{Ca}^{2+}$ induced $\text{Ca}^{2+}$ release**

The SP2 fragment leads to an insensitivity of  $\text{K}^+$  channels and  $\text{I}_{\text{Cl}}$  to ABA and also leads to an ABA insensitive phenotype with respect to stomatal closure. From data in this study, and from previous studies, it is known that ABA signalling and stomatal closure involve  $\text{Ca}^{2+}$  signalling events (Blatt, 2000; Ng *et al.*, 2001; Evans *et al.*, 2001). One of the ways in which ABA interacts with  $\text{Ca}^{2+}$  signalling is by causing a positive shift in the voltage threshold for  $\text{Ca}^{2+}$  induced  $\text{Ca}^{2+}$  release in guard cells (Grabov and Blatt, 1998). Thus it was decided to examine whether expression of the SP2 protein had any effect on the voltage threshold for  $\text{Ca}^{2+}$  induced  $\text{Ca}^{2+}$  release.

In order to examine the effect of SP2 expression on the voltage threshold for  $\text{Ca}^{2+}$  induced  $\text{Ca}^{2+}$  release, cells were loaded with fura-2, and were subjected to 93 second voltage ramps from  $-50$  to  $-230\text{mV}$ . Figure 5.9 shows data recorded from two separate cells, expressed as a kymograph, with associated images at time intervals for a cell from a wild type plant and a dexSP2-14 plant 14hrs post induction with dexamethasone. Data for the kymographs were taken from transects of the fluorescence in a band from the perinuclear region to periphery of the cell. The

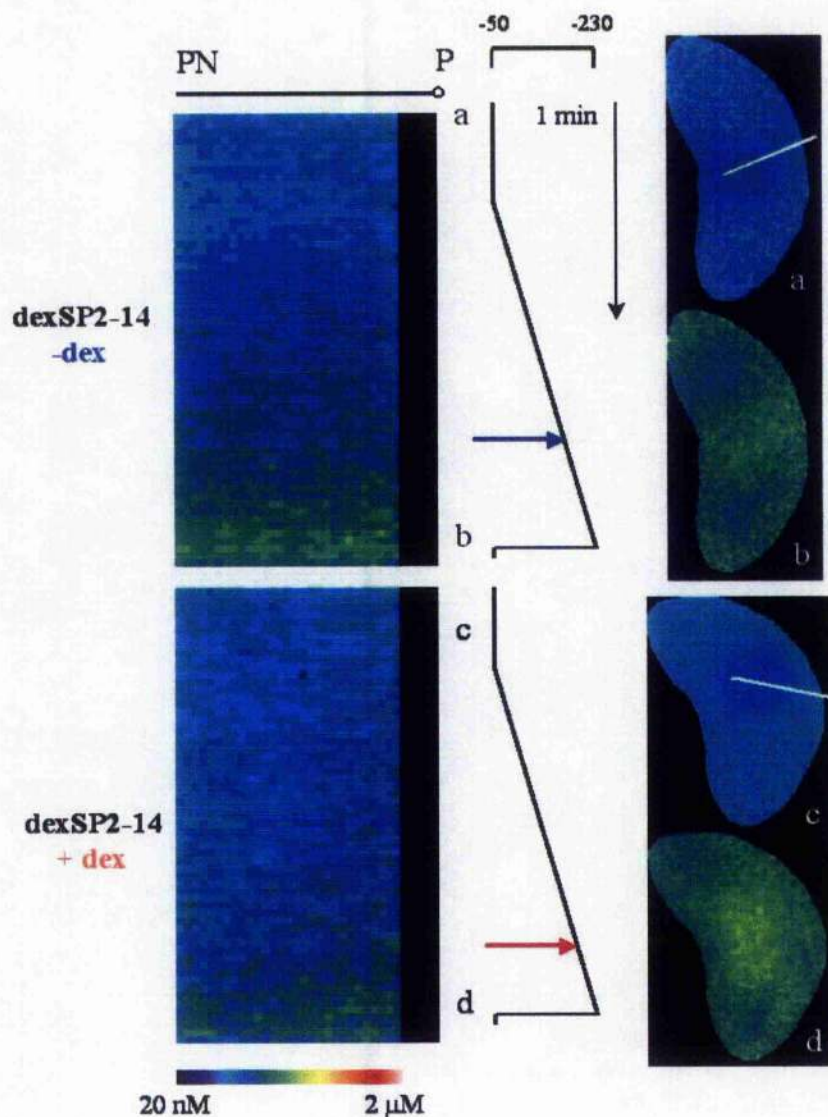


**Figure 5.9. Expression of the SP2 fragment of NtSyr1 induces a negative shift in the threshold for voltage evoked increases in  $[Ca^{2+}]_{\text{cyt}}$ .**  $[Ca^{2+}]_{\text{cyt}}$  rise from two dexSP2-14 guard cells, one from a plant not treated with dexamethasone and another 12hrs after dexamethasone treatment. Images were recorded by fura-2 fluorescence ratio at 2-s intervals. The time line (*Centre*) runs top to bottom with voltage scale and ramps as indicated. Selected ratio images (*Right*, a–d) correspond to time points indicated. The kymograph was constructed from successive ratio images averaged over a 2-pixel-wide band (white line in *Right*, a and c) from cell exterior and periphery (P) to the perinuclear region (PN). Voltage ramps from -50 mV to -230 mV over 93 s. The threshold for  $[Ca^{2+}]_{\text{cyt}}$  rise was determined as time of  $[Ca^{2+}]_{\text{cyt}}$  rise 1 SD above the pre-ramp level to a depth of 3 pixel units ( $\approx 2 \mu\text{m}$ ). Thresholds are marked (red and blue arrows).

kymograph shows that the fluorescence increase was initiated by negative going voltage, with increase seen first at the cell periphery close to the plasma membrane, then propagating through the cytosol. The voltage threshold for activation of the  $\text{Ca}^{2+}$  signal was determined by defining the threshold as the point where the  $[\text{Ca}^{2+}]_{\text{cyt}}$  crossed over 1SD of the mean resting level at  $-50\text{mV}$  before beginning the ramp. In both wt and dexamethasone treated empty vector plants (dexC2), the threshold was  $-169 \pm 6\text{mV}$  ( $n = 4$ ). Notably, the value obtained for the threshold in *N. tabacum* is significantly negative of the threshold determined for *V. faba* in this study. In cells from dexSP2-14 plants 12-24hrs post induction with dexamethasone, the threshold was determined to be  $-200 \pm 1\text{mV}$  ( $n = 5$ ) which is a significant negative shift of  $30\text{mV}$ . This suggests that one function of NtSyr1 leads to maintenance of the voltage threshold for  $\text{Ca}^{2+}$  induced  $\text{Ca}^{2+}$  release.

#### **5.4.2 Expression of the SP2 fragment of NtSyr1 inhibits ABA-induced stomatal closure**

The tobacco syntaxin NtSyr1 is known to be involved in ABA signalling in stomatal guard cells. Indeed, loading guard cells with the cytosolic fragment (SP2) of NtSyr1 or with syntaxin antagonists leads to uncoupling of the normal response of both  $\text{K}^+$  channels and  $\text{I}_{\text{Cl}}$  to ABA . It is also known that NtSyr1 is located to the plasma membrane, and is important for normal secretion and growth in tobacco (Leyman *et al.*, 2000). Since the function of NtSyr1 is important both in secretion and in ion channel control it was decided to investigate its function in ABA induced stomatal closure.

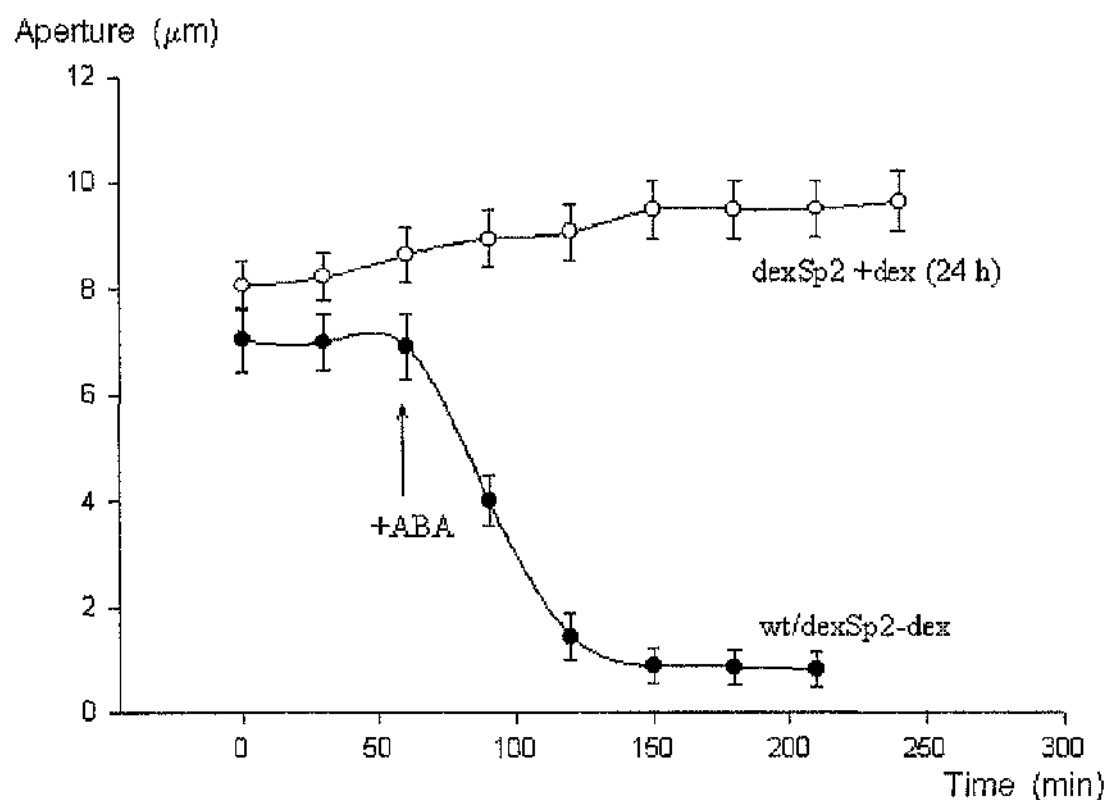


**Figure 5.10. Expression of the SP2 fragment of NtSyr1 inhibits ABA-induced stomatal closure.** Stomatal apertures were measured at 30min intervals for both wt/dexSP2-14 untreated plants (●) and dexSP2-14 plants 24hrs post dexamethasone treatment (○). Data are expressed as mean aperture ( $\mu\text{m}$ )  $\pm$  SE.



Stomatal aperture measurements were carried out to compare ABA-induced stomatal closure in both wild-type and dexSP2-14 plants. Figure 5.10 shows combined measurements from separate experiments (5 experiments with dexamethasone induced dexSP2-14 cells, 3 experiments with wild-type cells and 2 experiments with non-induced dexSP2-14 cells, total  $n = 60$  for each curve). Wild-type plants showed typical ABA induced stomatal closure. Apertures started closure 30 minutes following application of  $20\mu\text{M}$  ABA, and stomatal closure was essentially complete within 60-90 minutes. In contrast, induced dexSP2-14 plants did not show stomatal closure in response to ABA. In fact during the time-course of ABA treatment, mean stomatal aperture slightly increased.

#### **5.4.3 Expression of the SP2 protein leads to solute accumulation in leaf tissue**

As a way of further examining the effect of SP2 expression on membrane transport, the osmotic content of leaves was analysed (figure 5.11). Osmotic content of wild type and dexSP2-14 plants (with and without dexamethasone) was examined. At 48hrs post dexamethasone induction dexSP2-14 leaf tissue showed significantly higher osmotic content than both wild type and un-induced dexSP2-14 plants (Figure 5.11A). Closer examination of the time-course for this increase in osmotic strength (Figure 5.11B) revealed that even 24hrs post induction, dexSP2-14 plants already showed a significant increase in solute content, increasing to almost double the initial osmotic content by 96hrs. These results suggest that there may be changes in membrane transport, which lead to increased solute content in the leaf cells.

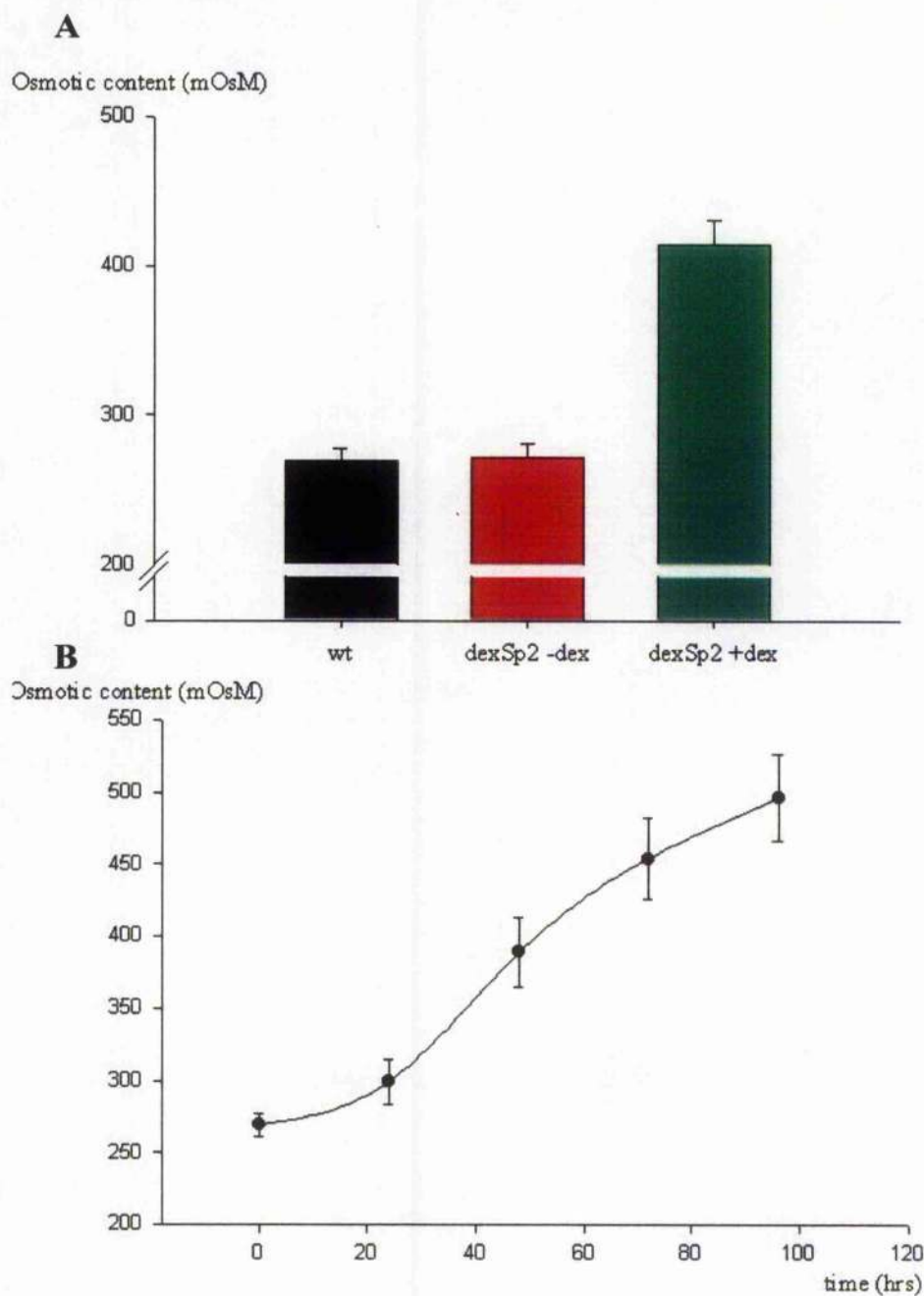


**Figure 5.11. Expression of the SP2 protein increases the osmotic content of dexSP2-14 plants.** Measured leaf tissue osmotic content in wt and dexSP2-14 plants after 48hrs with or without dexamethasone induction (**A**). Increase in osmotic strength with time in dexamethasone induced dexSP2-14 plants (**B**). Data are expressed as mean  $\pm$  SE.

#### 5.4.4 Expression of the SP2 protein inhibits NO mediated stomatal closure

Treatment of epidermal strips with NO donor compounds such as SNAP and SNP leads to stomatal closure in a number of species (Garcia-Mata and Lamattina, 2001). Furthermore, synthesis of NO *in vivo* is an essential component of ABA induced stomatal closure (Garcia-Mata and Lamattina, 2002; Neill *et al.*, 2002). Data from previous chapters has shown a link between NO and regulation of ion channels by ABA. Data from this chapter have shown a link between secretion and ion channel control. Thus, it was decided to explore whether there are any possible links between NO and secretory / volume regulation processes in guard cells.

The possible link between NO and the NtSyr1 protein was examined by performing stomatal closure assays. Figure 5.12 shows data from a series of experiments where the effect of SP2 expression on NO induced stomatal closure was examined. Both wt and dexamethasone treated dexC2 plants showed stomatal closure in response to NO. Treatment with 10 $\mu$ M SNAP led to stomatal closure with similar kinetics to ABA induced stomatal closure (figure 5.10) ( $n = 18$ ). Apertures started closure 30 minutes following application of 10 $\mu$ M SNAP, and stomatal closure was essentially complete within 90 minutes, slightly delayed when compared with ABA. However, in induced dexSP2-14 plants stomatal closure in response to NO was much reduced, though not completely abolished, as with ABA. Stomatal apertures gradually decreased and reached a steady state level about 2 ½ to 3hrs following treatment with SNAP ( $n = 14$ ). These results suggest that normal SP2 function may be important for NO signalling leading to stomatal closure in guard cells.

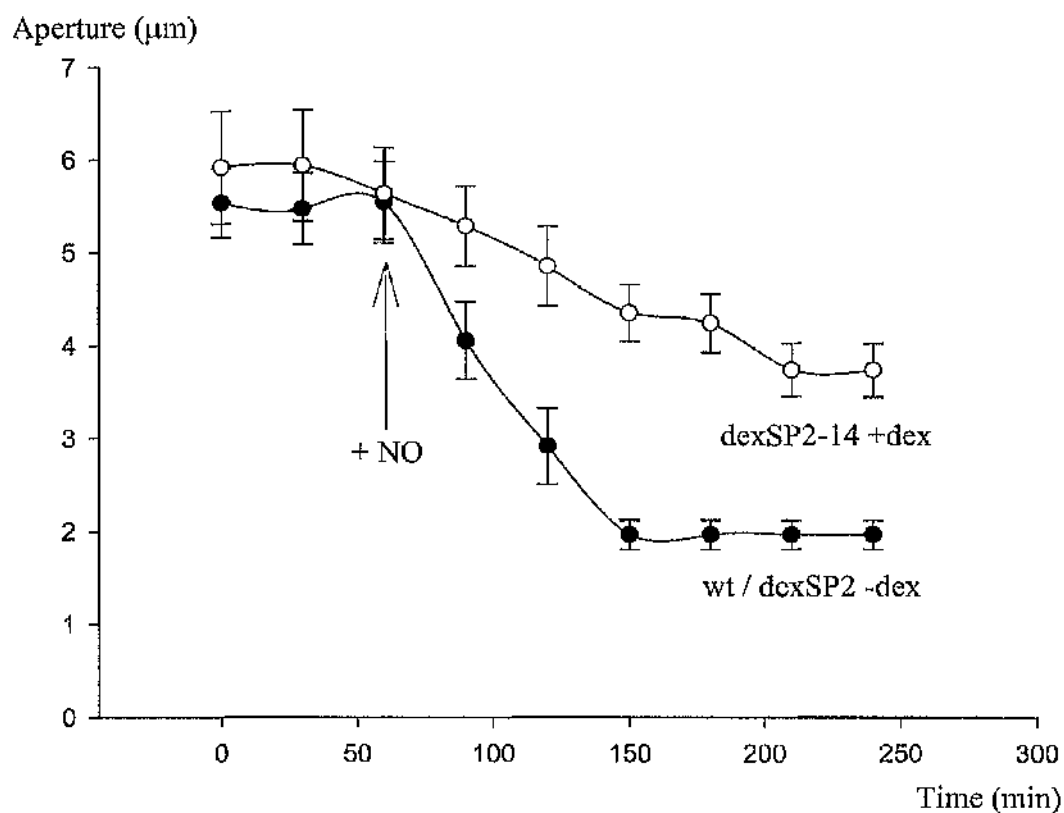


**Figure 5.12. Expression of the SP2 fragment of NtSyr1 inhibits NO-induced stomatal closure.** Stomatal apertures were measured at 30min intervals for both wt/dexSP2-14 untreated plants (●) and dexSP2-14 plants 24hrs post dexamethasone treatment (○). Epidermal strips were treated with 10 $\mu\text{M}$  SNAP at the time-point indicated. Data are expressed as mean aperture ( $\mu\text{m}$ )  $\pm$  SE.

## 5.5. Discussion

### 5.5.1. Introduction

The process of membrane trafficking in guard cells has received much attention in the last few years (Blatt, 2002). This attention has been sparked in part by a renewed interest in understanding how guard cells swell and shrink during stomatal opening and closing. Research has traditionally focussed on pathways for ion transport and their regulation, but now interest has now developed into understanding the membrane dynamics involved in stomatal opening and closing, and how this might be integrated with ion channel control. Data presented in this chapter an attempt to further explore the regulation of guard cell ion channels and signalling processes by membrane trafficking using inhibitors of secretion and transgenic plants expressing the cytosolic fragment of the tobacco syntaxin NtSyr1. Results show that treating guard cells with the secretion inhibitor brefeldin A (BFA) led to a decrease in  $I_{K,in}$  but did not affect  $I_{K,out}$ . The effect of BFA was scalar, and no change in gating and voltage dependence was seen, suggesting that the effect of BFA could be to reduce the number of active channels in the plasma membrane. Experiments further examining the effect of BFA on  $I_{K,in}$  showed that BFA inhibition was dose-dependent. In contrast, the effect of the actin antagonist latrunculin B (LATB) induced a decrease of both  $I_{K,in}$  and  $I_{K,out}$ . Unlike BFA, LATB shifted the voltage dependence of both channels, inducing a shift in the half-maximal activation voltage from  $-200\text{mV}$  to  $-225\text{mV}$ . The change in  $V_{1/2}$  suggests that the LATB effect was not merely a simple change in the number of active channels on the membrane. Like BFA, the effect of LATB on both  $I_{K,in}$  and  $I_{K,out}$  was dose-dependent. Treatment with BFA led to partial inhibition of ABA induced stomatal closure and subsequent reopening. Treatment

with LATB alone was sufficient to induce stomatal closure, suggesting that actin filaments are essential part of maintaining an open stomatal aperture.

Experiments were also performed using transgenic (dexSP2-14) plants expressing the cytosolic fragment (SP2) of the tobacco syntaxin NtSyr1. Voltage ramp experiments were performed in Fura2 loaded cells to examine the voltage threshold for  $\text{Ca}^{2+}$  induced  $\text{Ca}^{2+}$  release (CICR). Results showed that the voltage threshold was shifted negative from mV to mV in dexamethasone induced dexSP2-14 plants. Furthermore, guard cells in dexSP2-14 plants failed to close the stomatal aperture 24hrs after induction of SP2 expression. Measurements of the plant solute content revealed a time-dependent increase in leaf tissue solute content in transgenic SP2, suggesting other effects of the SP2 protein on membrane transport. Dexamethasone induced dexSP2-14 plants also showed reduced stomatal closure in response to NO, suggesting a possible link between NO signalling and membrane trafficking in guard cells.

### **5.5.2. The mechanism of BFA action.**

For some time, BFA has also been used to probe membrane traffic and protein transport in plant cells (SatiatJeunemaitre *et al.*, 1996; Neumann *et al.*, 2003). As in animal cells, treatment with BFA in plants also leads to a redistribution of certain Golgi enzymes into the ER (Boevink *et al.*, 1998; Lee *et al.*, 2002; Ritzenthaler *et al.*, 2002; Saint-Jore *et al.*, 2002). Curiously, in plants BFA also causes massive changes in Golgi morphology, including the formation of ER-Golgi fusion hybrids. (Satiat-Jeunemaitre *et al.*, 1996; Nebenfuhr *et al.*, 2002).

The action of BFA at the molecular level is now reasonably well characterised. In mammals, BFA binds to a subset of sec7-type GTP exchange factors, causing inhibition of their function. These sec7 GTP exchange factors are responsible for activation of small GTPase proteins called Arf1p (Jackson and Casanova, 2000). The activity of Arf1 is essential for the recruitment of vesicle coat proteins such as COPI and clathrin, which are required for the formation of transport vesicles (Scales *et al.*, 2000). The macroscopic effect of BFA is to block the movement of transport vesicles from the ER to the Golgi, causing a blockage of secretion. At the biochemical level, some redistribution of Golgi enzymes into the ER is also seen (Sciaky *et al.*, 1997).

There is evidence that BFA has a similar primary mode of action in plants. It is clear that formation of COPI coat proteins and vesicles is sensitive to BFA. Cells that are not treated with BFA show strong labelling by  $\alpha$ -COPI antibodies at the Golgi, a labelling pattern that completely disappears after 5 minutes treatment with BFA . These results not only point to the mode of action of BFA in plants, but also indicate that BFA is able to rapidly alter the normal function of the endomembrane system.

*Arabidopsis* contains GNOM, an Arf GEF that is homologous to the BFA sensitive Sec7 like proteins (Steinmann *et al.*, 1999). Interestingly GNOM is involved in controlling the polar localisation of an auxin transporter, PIN1, which is important for polar transport of auxin during embryo development . The fact that an Arf GEF system in plants has been shown to be involved in regulating the distribution of a membrane transporter suggests that it is entirely feasible that  $I_{K,in}$  trafficking and localisation might also be regulated by such an Arf GEF system. In their study, show that PIN1 can re-localise within 5 minutes of BFA treatment. Data in this chapter

reveal that BFA had a similarly rapid effect on  $I_{K,in}$  amplitude, and indicate that there might be a rapid turnover of  $I_{K,in}$  channel proteins as seen for PIN1. Furthermore, the fact that the effect of BFA on  $I_{K,in}$  is purely scalar provides strong evidence for changes in the number of active channels in the plasma membrane. Such changes could be due to decreased trafficking and incorporation of new channels into the plasma membrane in response to BFA. Under such circumstances, if the removal of channels from the plasma membrane was to continue at a normal rate, then a gradual decrease in  $I_{K,in}$  activity would be seen.

Interestingly, BFA had an effect both on stomatal closure in ABA and on stomatal opening following washout of ABA. From the effect of BFA on  $I_{K,in}$  it is not surprising that stomatal opening is compromised upon ABA washout, since  $I_{K,in}$  is essential for uptake of  $K^+$  during stomatal opening. However, the reduced stomatal closure in response to ABA cannot be accounted for by the effect on  $I_{K,in}$ . It is possible that other transporters that are important for stomatal closure might be affected by BFA, such as vacuolar  $K^+$  channels (MacRobbie, 2000). A role for vesicle trafficking in the transport of ions across the tonoplast has previously been suggested (MacRobbie, 1999).

### **5.5.3. LATB and control of cell volume via actin.**

In recent years there have been several reports of a role for actin in various developmental processes in plants. Several studies have utilised LATB as their actin antagonist. Treatment with LATB causes a dose-dependent inhibition of pollen tube germination and growth (Gibbon *et al.*, 1999). Indeed, pollen tube growth was completely blocked by low nanomolar concentrations of LATB, similar to those used in



this study. Pollen tube growth is inhibited by LATB, but cytoplasmic streaming is not, which raises questions as to the role of actin in vesicle trafficking in pollen tubes since cytoplasmic streaming and long distance movement of vesicles are thought to be linked (Vidali *et al.*, 2001). In root hairs, actin is involved in guiding transport vesicles to the growing tip of the hair, where they are deposited in a pool ready for fusion (Ketelaar *et al.*, 2003). There is also evidence for an involvement of actin filaments in endocytosis in plants. Uptake of cell wall pectins and fluorescent endocytosis markers into Maize root cells is inhibited by LATB (Baluska *et al.*, 2002; Baluska *et al.*, 2004).

There are many examples of ion channels whose regulation is linked in some way to actin. Regulation of ATP gated  $K^+$  channels ( $K_{ATP}$ ) as at least in some part due to actin filaments, which are physically coupled to the channel protein (Yokoshiki *et al.*, 1997; Korchhev *et al.*, 2000). Access of other modulatory factors is prevented when actin is linked to the channel as filaments (Yoshiki *et al.*, 1997). Ryanodine receptor channels, which provide a pathway for release of  $Ca^{2+}$  from internal stores are also linked to actin filaments via ankyrin. Binding of ankyrin prevents ryanodine binding to the receptor (Bourguignon *et al.*, 1995). Thus, the traditional view that actin links to ion channels were simply a mechanism to mechanically alter channel gating seems to have been slightly oversimplified. In most cases, it would seem that the role of actin in regulating ion channels is poorly understood.

The results presented in this chapter give an extra insight into the role of actin in guard cell ion channel control. Unlike BFA, the effect of LATB has not only a scalar, but also an effect on the voltage dependence of channel gating. The effect on voltage

dependence would argue against a role for actin filaments as being important for trafficking and insertion of ion channels into the plasma membrane, since it is likely that LATB would have caused a scalar effect similar to BFA. Actin filaments might provide a means of linking channel regulation directly to cell volume, thus providing a mechanism for fine-tuning channel activity.

The results on stomatal aperture measurements with LATB suggest that actin might indeed be linked to the maintenance of cell volume. Since LATB causes inhibition of both  $I_{K,in}$  and  $I_{K,out}$ , it is unlikely that its effect on the stomatal aperture was due to these changes in ion channel activity. The effect of LATB is to depolymerise actin filaments, and so it is conceivable that this might lead to partial collapse of cell structure over time, which might account for the stomatal closure response.

#### **5.5.4. Probing the link between ion channel regulation and membrane trafficking: Experimental approaches.**

The patch clamp technique has been used as a way of probing the link between ion channel activity and membrane trafficking. The advantage of patch clamping as approach, is that both ion channel activity and membrane surface area may be measured simultaneously (Homann, 1998). From studies using patch clamp to measure exo- and endocytotic events in guard cells, it has now been shown that there is indeed a coupling between membrane surface area and the level of ion channel activity. The membrane surface area of guard cell protoplasts increases and decreases in response to increased and decreased osmotic and hydrostatic pressure (Homann, 1998; Homann and Thiel, 1999). Furthermore, changes in membrane surface area are mirrored by changes in both  $I_{K,in}$  and  $I_{K,out}$  currents, which both increase with

membrane surface area (Homann and Thiel, 2002). Indeed,  $I_{K,in}$  has been shown to reside in vesicles close to the plasma membrane which are incorporated and removed when triggered by changes in hydrostatic pressure (Hurst *et al.*, 2004).

Whilst such results have shown the coupling between ion channel activity and membrane surface area in guard cells, the significance of this process as a mechanism of ion channel regulation is still unanswered. Whilst patch clamping provides a powerful tool with which to probe the link between ion channel regulation and membrane traffic, the technique comes with drawbacks. Isolation of protoplasts can sometimes be difficult. Furthermore, use of protoplasts may give a slightly distorted view of membrane trafficking processes, since they lack a cell wall and thus the cell is not subject to turgor pressure. Clearly combining data from intact cells and patch clamp studies is key to future progress.

#### **5.5.5. Syntaxins, $Ca^{2+}$ signalling and stomatal closure.**

Data presented in this chapter show a possible link between voltage induced  $Ca^{2+}$  increases and syntaxin function. The negative shift in the voltage threshold for evoked  $[Ca^{2+}]_{cyt}$  seen in plants expressing the SP2 fragment of NtSyr1 suggests that normal functioning of this protein is required to maintain the voltage dependence of the plasma membrane  $Ca^{2+}$  channel. Physical interactions between  $Ca^{2+}$  channels and syntaxins have been demonstrated in animal cells. The binding of syntaxins and other SNARE proteins can modulate  $Ca^{2+}$  channel activity (Sheng *et al.*, 1997; Zhong *et al.*, 1999; Degtiar *et al.*, 2000). It has been suggested that the physical coupling between syntaxins, their SNARE partners and  $Ca^{2+}$  channels is important in forming localised functional units to regulate exocytosis (Rettig *et al.*, 1997). Similar interactions might

be important in guard cells, and could form the coupling point between ion channel regulation and membrane traffic in guard cells. Leyman *et al.* (1999) and (Blatt, 2002) have hinted at a similar role for NtSyr1 in forming similar complexes with components of ABA signalling.

The ABA-insensitive stomatal closure phenotype seen in SP2-expressing dexSP2-14 plants, suggests some effect of the SP2 protein on membrane transport in guard cells. showed that guard cell  $K^+$  and  $Cl^-$  channels are insensitive to ABA in cells injected with the SP2 protein. The data presented in this chapter suggest that this effect might possibly be partly accounted for by defective  $Ca^{2+}$  signalling upstream. A possible explanation of the ABA insensitivity of stomatal closure caused by SP2 might be that the negative shift in the threshold for  $Ca^{2+}$  release affects the ability of ABA to depolarise the threshold and allow  $Ca^{2+}$  influx. Influx of  $Ca^{2+}$  is an essential in the regulation of  $I_{K,in}$  and  $I_{Cl}$  with ABA, whose changes in activity allow membrane depolarisation and shift the balance between solute gain and solute loss (Grabov and Blatt, 1998; Grabov and Blatt, 1999; Blatt *et al.*, 2002)

Data in this chapter show that NO-induced stomatal closure is also blocked by expression of the SP2 protein. This raises possible questions as to the interaction between NO signalling and syntaxin function in guard cells. In animals, NO is known to modulate the interactions of syntaxins with their cognate SNARE partners (Meffert *et al.*, 1996). It is now know that proteins that contain cysteine residues that are available for nitrosylation form part of the consensus sequence (Stamler *et al.*, 1997). The NtSyr1 protein sequence does not contain any nitrosylation motifs, however the

possibility that the tertiary structure might allow the consensus amino acids to reside in close proximity cannot be discounted.

#### **5.5.6. Summary**

The results presented in this chapter show a link between membrane trafficking, SNARE machinery and regulation of  $K^+$  channels and  $Ca^{2+}$  signalling in guard cells. Data suggest that  $I_{K,in}$  is regulated by turnover of channel proteins. Furthermore, both  $I_{K,in}$  and  $I_{K,out}$  activity require intact actin filaments to maintain normal channel activity. Actin filaments might provide a means of coupling ion channel activity to cell volume. Experiments examining stomatal apertures in dexSP2-14 plants showed that SP2 expression leads to an ABA-insensitive stomatal closure phenotype. Analysis of the voltage-induced  $Ca^{2+}$  signal showed that SP2 expression lead to a negative shift in the threshold for voltage-evoked  $Ca^{2+}$  release. The negative shift in the threshold for  $Ca^{2+}$  release might explain the ABA-insensitivity of guard cells in SP2 expressing plants. Stomatal aperture measurements also hint at a possible interaction between the function of NtSyr1 and NO signal transduction in guard cells.

## **CHAPTER 6**

### **GENERAL DISCUSSION**

## 6.1 Introduction

Guard cells respond to a variety of environmental cues. These environmental cues perceived, communicated via signal transduction pathways and translated into changes in stomatal aperture. Regulation of the stomatal aperture is brought about by changes in ion transport which lead to net solute influx and efflux to respectively open and close the stomatal aperture (Blatt, 2000a; Blatt *et al.*, 2002; Schroeder *et al.*, 2001a). There are also concurrent changes in membrane surface area and cell volume, which are brought about net exocytosis and endocytosis (Blatt, 2002). The principal players involved in ion transport across the plasma membrane are the inward and outward rectifier  $K^+$  channels ( $I_{K,in}$  and  $I_{K,out}$ ) and the anion channel ( $I_{Cl}$ ) (Blatt, 2000; Blatt, 2000b; Schroeder *et al.*, 2001b). Factors that regulate these currents, along with  $Ca^{2+}$  signalling systems are summarised below (Table 6.1).

$I_{K,in}$ ,  $I_{K,out}$  and  $I_{Cl}$  are regulated by ABA, which increases  $I_{K,out}$  and  $I_{Cl}$  and decreases  $I_{K,in}$ , thus shifting the balance of the membrane from solute uptake to solute efflux (Blatt, 1990; Grabov *et al.*, 1997; Pei *et al.*, 1997). Changes in these ion channel currents by ABA are brought about by a series of signalling events, one of which is  $Ca^{2+}$ . Upon perception of the ABA signal, changes in the activity of the plasma membrane  $Ca^{2+}$  channel ( $I_{Ca}$ ) and release of  $Ca^{2+}$  from internal stores lead to elevated  $[Ca^{2+}]_{cyt}$  (Allen *et al.*, 1999; Grabov and Blatt, 1998; Hamilton *et al.*, 2000). Elevated  $[Ca^{2+}]_{cyt}$  brings about changes in  $I_{K,in}$  and  $I_{Cl}$ , which are  $Ca^{2+}$  sensitive (Grabov and Blatt, 1999; Hedrich *et al.*, 1990; Schroeder and Hagiwara, 1989). Regulation of  $I_{K,out}$  by ABA seems to be at least in part due to changes in  $pH_{cyt}$  (Blatt and Armstrong, 1993). Other factors involved in the regulation of  $I_{K,in}$ ,  $I_{K,out}$  and  $I_{Cl}$  include protein kinases and phosphatases. Indeed, the activity of protein phosphatases seems

|                        | $I_{K,in}$ | $I_{K,out}$ | $I_{Cl}$ | $I_{Ca}$ | $[Ca^{2+}]_{cyt}$ | References           |
|------------------------|------------|-------------|----------|----------|-------------------|----------------------|
| $[Ca^{2+}]_{cyt}$      | -          | 0           | +        | -        | N/A               | 1,2,3,4,13           |
| $[Ca^{2+}]_{ext}$      | -          | 0           | +        | +        | +                 | 5,6,7,8              |
| ABA                    | -          | +           | +        | +        | +                 | 9,10,11,12,13,14     |
| Protein kinases /PPase | +/-        |             | +/-      | +        | +                 | 10,11,15,16,17,18,34 |
| NO                     | -          | 0           | +        | 0        | +                 |                      |
| pH <sub>ext</sub>      | +          | 0           |          |          |                   | 19,20,21,22          |
| pH <sub>cyt</sub>      | 0          | +           |          |          |                   | 23,24,25             |
| G proteins             | +          |             | +        |          |                   | 26,27,28             |
| Actin                  | +          | +           |          |          |                   | 29,30                |
| Membrane trafficking   | +          | 0           |          |          |                   | 31,32                |
| Syntaxin               | +          | +           | +        | +        | +                 | 33                   |

**Table 6.1 Summary of factors affecting  $I_{K,in}$ ,  $I_{K,out}$ ,  $I_{Cl}$ ,  $I_{Ca}$  and  $[Ca^{2+}]_{cyt}$ .** Known effects on the channels or  $[Ca^{2+}]_{cyt}$  that have been published are written as + for positive regulation and - for negative regulation. No effect is represented by 0. Unknown effects are left as blank cells. Areas yet to be explored are represented by a question mark, and N/A represents not applicable. Contributions this study has made to existing knowledge are marked (red characters). The key to the references is provided below<sup>a</sup>

<sup>a</sup> 1: Schroeder and Hagiwara, 1989; 2: Grabov and Blatt, 1999; 3: Schroeder and Hagiwara, 1990a; 4: Allen *et al.*, 1999; 5: Hedrich *et al.*, 1990; 6: Grabov and Blatt, 1999; 7: Hamilton *et al.*, 2001; Grabov and Blatt, 1998; 9: Blatt, 1990; 10: Grabov *et al.*, 1997; 11: Pei *et al.*, 1997; 12: Allen *et al.*, 2001; 13: Hamilton *et al.*, 2001; 14: Pei *et al.*, 2000; 15: Luan *et al.*, 1993; 16: Kamasani *et al.*, 1997; 18: Li *et al.*, 1998a; 19: Blatt, 1992; 20: Ilan *et al.*, 1996; 21: Hoth *et al.*, 1997; 22: Hoth *et al.*, 2001; 23: Blatt and Armstrong, 1993; 24: Miedema and Assmann, 1996; 25: Grabov and Blatt, 1997; 26: Fairley and Assmann, 1991; 27: Armstrong and Blatt, 1995; 28: Wang *et al.*, 2001; 29: Hwang *et al.*, 1997; 30: Liu and Luan, 1998; 31: Homann and Thiel, 2002; 32: Hurst *et al.*, 2004; 33: Leyman *et al.*, 1999; 34: Kohler and Blatt, 2002



to be a key component of the regulation of several guard cell ion channels by ABA (Armstrong *et al.*, 1995; Grabov *et al.*, 1997; Pei *et al.*, 1997; Allen *et al.*, 1999a; Murata *et al.*, 2001).

Regulation of  $I_{K,in}$  by G-proteins via a 7TMS receptor has been explored, though only recently have G-proteins been shown to be important as a component of ABA signalling, not only of  $I_{K,in}$  but also of  $I_{Cl}$  (Armstrong and Blatt, 1995; Fairley and Assmann, 1991; Wang *et al.*, 2001). A possible link between ABA regulation of ion channels and membrane traffic was uncovered during a screen for ABA signalling components, which led to the cloning of NtSyr1, a syntaxin protein involved in ABA regulation of  $I_{K,in}$ ,  $I_{K,out}$  and  $I_{Cl}$  (Leyman *et al.*, 1999). Data on the mechanistic basis of syntaxin regulation of these channels is still lacking.

Data presented in this thesis explore (i) regulation of ion channels by NO, which was recently implicated in ABA induced stomatal closure (Garcia-Mata and Lamattina, 2002; Neill *et al.*, 2002) and (ii) the interaction between ion channel /  $Ca^{2+}$  signalling regulation and membrane trafficking in guard cells. The main findings are summarised below.

Cells treated with NO showed inhibition of  $I_{K,in}$  and an increase in  $I_{Cl}$ , but no changes in  $I_{K,out}$ . The NO induced changes in  $I_{K,in}$  and  $I_{Cl}$  were  $Ca^{2+}$  dependent, as revealed by  $Ca^{2+}$  buffering effects. Measurements of voltage induced changes in  $[Ca^{2+}]_{cyt}$  revealed that NO enhanced the release of  $Ca^{2+}$  from internal stores via a cGMP / cADPR pathway, but did not promote  $Ca^{2+}$  channel activity at the plasma membrane. The effect of NO on  $I_{K,in}$  and  $I_{Cl}$  was abolished by the broad range protein kinase inhibitor

staurosporine, but not by the protein tyrosine kinase inhibitor genistein. The effect of staurosporine could be attributed to a blocking of the NO induced enhancement of  $\text{Ca}^{2+}$  release from internal stores, suggesting that protein kinases are essential for the transmission of the NO signal to facilitate  $\text{Ca}^{2+}$  release from internal stores. These data provide information on the mechanistic basis of NO action in guard cells.

Both pharmacological and transgenic approaches were taken to examine the role of membrane trafficking in the regulation of guard cell ion channels. Cells treated with the secretion inhibitor BFA led to decreased  $I_{K,in}$  but not  $I_{K,out}$ . The effect of BFA on  $I_{K,in}$  was scalar, suggesting that the inhibition might be due to a decreased number of  $I_{K,in}$  channels in the plasma membrane. BFA also inhibited ABA induced stomatal closure and subsequent reopening. In contrast the actin antagonist LATB inhibited both  $I_{K,in}$  and  $I_{K,out}$ . Both channels showed a change in voltage dependence as well as a scalar decreases in current, suggesting that actin filaments regulate  $I_{K,in}$  and  $I_{K,out}$  by means other than vesicle trafficking. LATB alone was sufficient to induce stomatal closure, suggesting that actin filaments are important for maintaining cell structure when guard cells are turgid.

Transgenic plants expressing the cytosolic fragment (SP2) of the tobacco syntaxin NtSyr1, which competitively impairs normal NtSyr1 function (Geelen *et al.*, 2002), were used as a tool to examine interactions between NtSyr1 and ion channel regulation. Twenty-four hours after induction of SP2 expression, plants showed an ABA insensitive phenotype with respect to stomatal closure. Analysis of  $\text{Ca}^{2+}$  signalling showed a significant negative shift in the threshold for voltage induced CICR, suggesting that the cells might be defective in the normal response of the

plasma membrane  $\text{Ca}^{2+}$  channel to ABA. Plants expressing the SP2 protein also showed increased osmotic content over time, suggesting that disruption of normal NtSyr1 function causes other changes in membrane transport. The function of NtSyr1 was also shown to be linked to NO signalling, since NO induced stomatal closure was impaired in plants expressing SP2.

## **6.2 NO and its place in guard cell signalling**

### **6.2.1 ABA signalling - NO is not the whole story**

The recent surge in interest in the role of NO in plants was started by work on plant – pathogen interactions in the latter part of the last decade (Delledonne *et al.*, 1998; Durner *et al.*, 1998). Following this, discovery of the effect of NO on stomatal closure and its placing as an essential component of ABA induced stomatal closure opened a whole new aspect of guard cell signalling, and the possibility that NO might regulate guard cell ion channels. Results in this study clearly demonstrate a central role for NO in ABA mediated ion channel control, but clearly show that NO is not the whole story.

An important effect of ABA in guard cells is to activate  $I_{K,out}$  and thus promote net  $\text{K}^+$  efflux from the cell (Blatt, 1990; MacRobbie, 1995). This crucial step cannot be accounted for by NO, since  $I_{K,out}$  activity does not change in response to  $10\mu\text{M}$  SNAP. However, the activation of  $I_{K,out}$  by ABA can be sufficiently accounted for by other ABA signals, such as  $\text{pH}_i$  changes. ABA causes a significant alkalisation of the cytosol (Gehring *et al.*, 1990; Irving *et al.*, 1992). Cytoplasmic alkalisation leads to an increase in  $I_{K,out}$  activity, possibly through changes in the level of protonation of binding sites on  $I_{K,out}$  channel proteins, or other proteins that reside at the plasma

membrane (; Miedema and Assmann, 1996). It is also possible that other unknown second messengers are responsible for increasing  $I_{K,out}$  activity in response to ABA. Experiments to investigate whether NO can induce any changes in  $pH_i$  might help clarify the role of the  $pH$  signal in ABA mediated ion channel control.

Results in this study show that the plasma membrane  $Ca^{2+}$  channel ( $I_{Ca}$ ) characteristics were not greatly altered by NO. This is quite a contrast to the effect of ABA on  $I_{Ca}$  in both patch clamp experiments and in whole cell impalements. Voltage ramp experiments in the presence and absence of ABA show that there is a significant positive shift in the voltage threshold for  $I_{Ca}$  activation with ABA, both in intact cells and in protoplasts . Furthermore, in patch clamp experiments,  $I_{Ca}$  activity is increased up to 260 fold in excised patches . Since NO does not mimic the effect of ABA on  $I_{Ca}$ , it is likely that the target for NO in guard cells is downstream. Interestingly, Hamilton *et al.* (2000) reported that changes in  $I_{Ca}$  through ABA are membrane delimited, with the site for ABA perception on the cytosolic face of the membrane. Thus it is likely that the effect of ABA on  $I_{Ca}$  can be accounted for in the absence of cytoplasmic signalling systems. It is important to note that measurements of the effect of NO on the voltage induced CICR and patch clamp studies of  $I_{Ca}$  activity were carried out using only exogenous application of SNAP. Further experiments using a combination of ABA and the NO scavenger cPTIO would provide useful support to the argument that NO is not important for  $I_{Ca}$  regulation by ABA.

### **6.2.2 NO enhancement of $Ca^{2+}$ release from internal stores**

Data in this study suggest that NO enhances  $Ca^{2+}$  release from internal stores via a cGMP / cADPR pathway. Indeed, the data suggest that this pathway is essential for

voltage induced CICR both in the presence and absence of NO. The data do not shed any light on the possible mechanism by which NO enhances the release of  $\text{Ca}^{2+}$  via the cGMP / cADPR pathway. However, paradigms from animal systems provide useful hints. In animals, soluble guanylate cyclase acts as an NO receptor, and binds NO to bring about a 100-fold increase in cGMP synthesis (Fricbe and Koesling, 2003). A similar mechanism might operate in guard cells, though the only cloned plant guanylate cyclase cloned to date, AtGC1, is insensitive to NO *in vitro* (Ludidi and Gehring, 2003). However, AtGC1 has little homology to guanylate cyclase protein in other organisms, so other proteins with NO sensitive guanylate cyclase activity may await discovery.

Animal cells also have mechanisms of NO action, which proceed independently of cGMP. One such mechanism is S-nitrosylation (Ahern *et al.*, 2002; Stamler, 1994). The experiments performed in this study suggest that the cGMP / cADPR pathway operates to propagate the NO signal. However, the possibility of the operation of a S-nitrosylation pathway in parallel cannot be discounted. Ryanodine receptors in both cardiac muscle and skeletal muscle contain cysteine residues, which are available for nitrosylation. Interestingly, the different isoforms are nitrosylated to a different extent by NO (Sun *et al.*, 2001; Xu *et al.*, 1998). The molecular identity of plant ryanodine receptors is not currently known. However, screening for nitrosylated proteins *in vitro*, or by searching for nitrosylation consensus sequences *in silico* might be a useful tool to discover the identity of plant ryanodine receptors, along with other NO targets (Hess *et al.*, 2001; Stamler *et al.*, 1997).

### **6.2.3 Protein kinase activity and NO enhanced $\text{Ca}^{2+}$ release**

There is evidence at the pharmacological, biochemical and molecular level for the operation of a variety of protein kinases and phosphatases in guard cell ion channel regulation, including CDPK, AAPK, PP1/2A (Li *et al.*, 1998; Li *et al.*, 2000; Li *et al.*, 1994; Luan *et al.*, 1993; Thiel and Blatt, 1994). Interestingly, staurosporine only affected the NO enhancement of the  $\text{Ca}^{2+}$  signal, with the normal voltage induced signal remaining unaffected. Several candidate protein kinase targets could be affected by staurosporine, including cGMP dependent kinase (PKG) as already discussed (see chapter 4). In animal cells there are also many other possible target kinases that are involved in  $\text{Ca}^{2+}$  release from internal stores. Production of the  $\text{IP}_3$  precursor phosphatidyl inositol 4,5, diphosphate requires two separate protein kinases, namely phosphatidyl inositol 4 kinase and type I phosphatidyl inositol phosphate kinase (Irvine, 2003). In addition  $\text{IP}_3$  receptors can be modulated by kinases that include  $\text{Ca}^{2+}$  / calmodulin-dependent protein kinase II, PKG, protein kinase C and protein kinase A (Carafoli *et al.*, 2001). Identification of the kinase(s) involved in NO-enhanced release of  $\text{Ca}^{2+}$  from internal stores would be a complex process, and may be beyond the scope of the pharmacological toolbox currently available. Future progress might be aided by analysis of *Arabidopsis* kinase mutant / dominant negative plants, though improvements in impalement techniques would be required to allow use of *Arabidopsis* as a model plants in such studies.

## **6.3. Coordinating membrane traffic and ion channel control**

### **6.3.1. SNARE protein function – more than membrane fusion?**

Interactions between ion channels and SNARE proteins are now well documented. The interactions between SNAREs and neuronal  $\text{Ca}^{2+}$  channels have been widely

studied, and are now thought to form part of a secretosome complex, localising  $\text{Ca}^{2+}$  channel proteins to sites of  $\text{Ca}^{2+}$  dependent vesicle fusion events (Leveque *et al.*, 1994; O' Connor *et al.*, 1993; Sheng *et al.*, 1994; Sheng *et al.*, 1996; Sheng *et al.*, 1997). However, there are other ion channels and transporters that interact with SNARE proteins, whose interaction is not directly related to vesicle fusion (Cormet-Boyaka *et al.*, 2002; Fili *et al.*, 2001; Naren *et al.*, 1997; Naren *et al.*, 1998; Quick, 2002). Such interactions open the possibility of other functions for the interaction of syntaxins and other SNARE and membrane fusion related proteins with membrane transport proteins.

In plants, the only published example of the interaction between syntaxins and ion channels is that of NtSyr1. Expression of the SP2 fragment of NtSyr1 leads to an ABA insensitivity of  $I_{K,in}$ ,  $I_{K,out}$  and  $I_{Cl}$ , an effect which is mimicked by treatment with syntaxin cleaving botulinum toxins (Leyman *et al.*, 1999). Further to this, results from experiments presented in this thesis suggest a role for syntaxin function in maintaining plasma membrane  $\text{Ca}^{2+}$  channel activity ( $I_{Ca}$ ). It is not clear as to how NtSyr1 interacts with any of these channels. However, this interaction might provide the crucial link between membrane traffic and ion channel control in guard cells, with NtSyr1 serving a role in both membrane fusion and signal transduction. Discovery of NtSyr1 binding partners may help unravel these interactions in future. Other, unrelated, functions have been found for NtSyr1 orthologues in both *Arabidopsis* (AtSyp121) and barley (HvSyp121) (Collins *et al.*, 2003). In both species, syntaxins are involved in defence against fungal penetration. Mutations in both syntaxins lead to an accumulation of reactive oxygen species filled vesicles at the site of fungal penetration, which are unable to fuse. Whether or not any signalling function is also

performed by these proteins is as yet unclear, however these data and those of Leyman *et al.* (1999) point to a wide range of functions for syntaxins in plants.

### **6.3.2. Evidence for coupling of membrane traffic and ion channel control in plants.**

To date the most convincing evidence for the interaction between ion channels and membrane traffic comes from studies which have combined patch clamp measurements of membrane capacitance and currents with GFP tagging of channel proteins. Initially, it was shown that changes of both  $I_{K,in}$  and  $I_{K,out}$  occurred in parallel with changes in membrane capacitance, such that the activity of both channels increased with increased membrane surface area (Homann and Thiel, 2002). The examination of the kinetics of both  $I_{K,in}$  and  $I_{K,out}$  indicated that the increases in currents were scalar, suggesting that the number of ion channels in the membrane was altered. A more detailed analysis of the trafficking of a GFP tagged KAT1, a cloned  $K^+$  inward rectifier has recently been carried out (Hurst *et al.*, 2004). They extended previous observations by reporting the presence of clusters of small KAT1::GFP rich vesicles, containing as many as 50 KAT1 channel, in close proximity to the plasma membrane. The authors also suggest that KAT1 channels may cluster in the plasma membrane (Hurst *et al.*, 2004). The observations presented in both studies provide strong evidence for coupling of ion channels with changes in membrane surface area. However, there is as yet no evidence that changes in membrane surface area provides a way of regulating ion transport in guard cells.



### **6.3.2. Coupling guard cell membrane traffic and ion channel control – future prospects**

Future progress in unravelling the links between membrane traffic and ion channels in guard cells will require a multi-disciplinary approach. Combining patch clamp measurements of ion channel activity and membrane capacitance with fluorescent dyes and GFP tagging has already yielded promising results (Kubitschcek *et al.*, 2000; Homann and Thiel, 2002; Hurst *et al.*, 2004). However, much of the work to date has been carried out in protoplasts, and there is a need to study trafficking of ion channels in intact cells so as to get a more realistic view of channel trafficking *in planta*. Use of GFP tagged channels expressed under their native promoter in intact tissue might enable testing of the effects of, for example, ABA, on the localisation of channel. The availability of GFP variants such as YFP and CFP might also allow tracking of a number of different channels simultaneously.

The recent completion of the *Arabidopsis* genome sequence, (*Arabidopsis* genome initiative, 2000), has provided a powerful resource to explore new aspects of membrane transport and membrane traffic. Analysis of the genome *in silico* has revealed a large number of the SNARE proteins, along with other important membrane trafficking proteins such as Rab GTPases (Rutherford and Moore, 2002; Sanderfoot *et al.*, 2000). Similar information is also available for plant membrane transporters (Barbier-Brygoo *et al.*, 2001; Ward, 2001). The sequence information available should allow screening for protein-protein interactions using the yeast two hybrid system, or co-immunoprecipitation to discover ways in which membrane trafficking proteins and ion channels interact.

## REFERENCES

**Ahern, G.P., Klyachko, V.A., and Jackson, M.B.** (2002) cGMP and S-nitrosylation: two routes for modulation of neuronal excitability by NO. *Trends in Neurosciences* **25**:510-517.

**Allan, B.B., Moyer, B.D., and Balch, W.E.** (2000) Rab1 recruitment of p115 into a cis-SNARE complex: Programming budding COPII vesicles for fusion. *Science* **289**:444-448.

**Allen, G.J., Chu, S.P., Harrington, C.L., Schumacher, K., Hoffman, T., Tang, Y.Y., Grill, E., and Schroeder, J.I.** (2001) A defined range of guard cell calcium oscillation parameters encodes stomatal movements. *Nature* **411**:1053-1057.

**Allen, G.J., Chu, S.P., Schumacher, K., Shimazaki, C.T., Vafeados, D., Kemper, A., Hawke, S.D., Tallman, G., Tsien, R.Y., Harper, J.F., Chory, J., and Schroeder, J.I.** (2000) Alteration of stimulus-specific guard cell calcium oscillations and stomatal closing in *Arabidopsis det3* mutant. *Science* **289**:2338-2342.

**Allen, G.J., Kuchitsu, K., Chu, S.P., Murata, Y., and Schroeder, J.I.** (1999) *Arabidopsis* *abi1-1* and *abi2-1* phosphatase mutations reduce abscisic acid-induced cytoplasmic calcium rises in guard cells. *Plant Cell* **11**:1785-1798.

**Allen, G.J., Muir, S.R., and Sanders, D.** (1995) Release of  $\text{Ca}^{2+}$  from individual plant vacuoles by both *insp(3)* and cyclic ADP-ribose. *Science* **268**:735-737.

**Allen, G.J., Murata, Y., Chu, S.P., Nafisi, M., and Schroeder, J.I.** (2002) Hypersensitivity of abscisic acid-induced cytosolic calcium increases in the *Arabidopsis* farnesyltransferase mutant *era1-2*. *Plant Cell* **14**:1649-1662.

**Allen, G.J. and Sanders, D.** (1995) Calcineurin, a type 2B protein phosphatase, modulates the  $\text{Ca}^{2+}$ -permeable slow vacuolar ion channel of stomatal guard cells. *Plant Cell* **7**:1473-1483.

**Allen, G.J. and Sanders, D.** (1996) Control of ionic currents in guard cell vacuoles by cytosolic and luminal calcium. *Plant J.* **10**:1055-1069.

**Anderson, L. and Mansfield, T.A.** (1979) The effects of nitric oxide pollution on the growth of tomato. *Environ. Pollution* **20**:113-121.

**Aoyama, T. and Chua, N.H.** (1997) A glucocorticoid-mediated transcriptional induction system in transgenic plants. *Plant J.* **11**:605-612.

***Arabidopsis* genome initiative** (2000) Analysis of the genome sequence of the flowering plant *Arabidopsis thaliana*. *Nature* **408**:796-815.

**Arai, H., Hori, S., Aramori, I., Ohkubo, H., and Nakanishi, S.** (1990) Cloning and expression of a cDNA encoding an endothelin receptor. *Nature* **348**:730-732.

**Armstrong, F. and Blatt, M.R.** (1995) Evidence for  $K^+$  channel control in *Vicia* guard cells coupled by G-proteins to a 7TMS receptor. *Plant J.* **8**:187-198.

**Armstrong, F., Leung, J., Grabov, A., Brearley, J., Giraudat, J., and Blatt, M.R.** (1995) Sensitivity to abscisic acid of guard cell  $K^+$  channels is suppressed by *abi1-1*, a mutant *Arabidopsis* gene encoding a putative protein phosphatase. *Proc.Nat.Acad.Sci.USA* **92**:9520-9524.

**Assaad, F.F., Huet, Y., Mayer, U., and Jurgens, G.** (2001) The cytokinesis gene KEULE encodes a Sec1 protein that binds the syntaxin KNOLLE. *J.Cell Biol.* **152**:531-543.

**Assmann, S.M.** (1993) Signal transduction in guard cells. *Ann.Rev.Cell Biol.* **9**:345-375.

**Baluska, F., Hlavacka, A., Samaj, J., Palme, K., Robinson, D.G., Matoh, T., Mccurdy, D.W., Menzel, D., and Volkmann, D.** (2002) F-actin-dependent endocytosis of cell wall pectins in meristematic root cells. Insights from brefeldin A-induced compartments. *Plant Physiol.* **130**:422-431.

**Baluska, F., Samaj, J., Hlavacka, A., Kendrick-Jones, J., and Volkmann, D.** (2004) Actin-dependent fluid-phase endocytosis in inner cortex cells of maize root apices. *J.Exp.Bot.* **55**:463-473.

**Barroso, J.B., Corpas, F.J., Carreras, A., Sandalio, L.M., Valderrama, R., Palma, J.M., Lupianez, J.A., and del Rio, L.A.** (1999) Localization of nitric-oxide synthase in plant peroxisomes. *J.Biol.Chem.* **274**:36729-36733.

**Batoko, H., Zheng, H.Q., Hawes, C., and Moore, I.** (2000) A Rab1 GTPase is required for transport between the endoplasmic reticulum and Golgi apparatus and for normal Golgi movement in plants. *Plant Cell* **12**:2201-2217.

**Beligni, M.V., Fath, A., Bethke, P.C., Lamattina, L., and Jones, R.L.** (2002) Nitric oxide acts as an antioxidant and delays programmed cell death in barley aleurone layers. *Plant Physiol.* **129**:1642-1650.

**Beligni, M.V. and Lamattina, L.** (1999a) Is nitric oxide toxic or protective? *Trends Plant Sci.* **4**:299-300.

**Beligni, M.V. and Lamattina, L.** (1999b) Nitric oxide counteracts cytotoxic processes mediated by reactive oxygen species in plant tissues. *Planta* **208**:337-344.

**Beligni, M.V. and Lamattina, L.** (2002) Nitric oxide interferes with plant photo-oxidative stress by detoxifying reactive oxygen species. *Plant Cell And Environment* **25**:737-748.

**Bennett, M.K., Calakos, N., and Scheller, R.H.** (1992) Syntaxin - a synaptic protein implicated in docking of synaptic vesicles at presynaptic active zones. *Science* **257**:255-259.

**Berridge, M., Bootman, M. D., and Roderick, H. L.** Calcium signalling: dynamics, homeostasis and remodelling. *Nature Reviews Molecular Cell Biology* 4, 517-529. 2003.  
Ref Type: Generic

**Berridge, M.J.** (1998) Neuronal calcium signaling. *Neuron* 21:13-26.

**Berridge, M.J. and Dupont, G.** (1994) Spatial and temporal signaling by calcium. *Current Opinion In Cell Biology* 6:267-274.

**Bick, I., Thiel, G., and Homann, U.** (2001) Cytochalasin D attenuates the desensitisation of pressure- stimulated vesicle fusion in guard cell protoplasts. *European Journal of Cell Biology* 80:521-526.

**Blatt, M.R.** (1987) Electrical characteristics of stomatal guard cells: the ionic basis of the membrane potential and the consequence of potassium chloride leakage from microelectrodes. *Planta* 170:272-287.

**Blatt, M. R.** (1988a) Potassium channel gating in guard cells depends on external  $K^+$  concentration. *Plant Physiology* 86: 826.

**Blatt, M.R.** (1988b) Potassium-dependent bipolar gating of potassium channels in guard cells. *J.Membr.Biol.* 102:235-246.

**Blatt, M.R.** (1990) Potassium channel currents in intact stomatal guard cells: rapid enhancement by abscisic acid. *Planta* 180:445-455.

**Blatt, M.R.** (1991) A Primer in Plant Electrophysiological Methods. In *Methods in Plant Biochemistry*, K.Hostettmann, ed (London: Academic Press), pp. 281-321.

**Blatt, M.R.** (1992)  $K^+$  channels of stomatal guard cells: characteristics of the inward rectifier and its control by pH. *J.Gen.Physiol.* 99:615-644.

**Blatt, M.R.** (2000a)  $Ca^{2+}$  signalling and control of guard-cell volume in stomatal movements. *Current Opinion In Plant Biology* 3:196-204.

**Blatt, M.R.** (2000b) Cellular signaling and volume control in stomatal movements in plants. *Ann.Rev.Cell Dev.Biol.* 16:221-241.

**Blatt, M.R.** (2002) Toward understanding vesicle traffic and the guard cell model. *New Phytol.* 153:405-413.

**Blatt, M.R. and Armstrong, F.** (1993)  $K^+$  channels of stomatal guard cells: abscisic acid-evoked control of the outward rectifier mediated by cytoplasmic pH. *Planta* 191:330-341.

**Blatt, M.R. and Grabov, A.** (1997) Signal redundancy, gates and integration in the control of ion channels for stomatal movement. *J.Exp.Bot.* 48:529-537.

- Blatt, M.R., Grabov, A., Brearley, J., Hammond-Kosack, K., and Jones, J.D.G.** (1999) K<sup>+</sup> channels of *Cf-9* transgenic tobacco guard cells as targets for *Cladosporium fulvum* Avr9 elicitor-dependent signal transduction. *Plant J.* **19**:453-462.
- Blatt, M.R. and Gradmann, D.** (1997) K<sup>+</sup>-sensitive gating of the K<sup>+</sup> outward rectifier in *Vicia* guard cells. *J.Membr.Biol.* **158**:241-256.
- Blatt, M.R., Moore, I., Batoko, H., DiSansebastiano, G.P., Leyman, B., and Geelen, D.** (2002) Integrating control of ion channels and cell volume in guard cell signalling. *Biophysical Journal* **82**:3011.
- Blatt, M.R. and Thiel, G.** (1994) K<sup>+</sup> channels of stomatal guard cells: bimodal control of the K<sup>+</sup> inward-rectifier evoked by auxin. *Plant J.* **5**:55-68.
- Blatt, M.R., Thiel, G., and Trentham, D.R.** (1990) Reversible inactivation of K<sup>+</sup> channels of *Vicia* stomatal guard cells following the photolysis of caged inositol 1,4,5-trisphosphate. *Nature* **346**:766-769.
- Block, M.R., Glick, B.S., Wilcox, C.A., Wieland, F.T., and Rothman, J.E.** (1988) Purification of an n-ethylmaleimide-sensitive protein catalyzing vesicular transport. *Proc.Nat.Acad.Sci.USA* **85**:7852-7856.
- Boevink, P., Oparka, K., Cruz, S.S., Martin, B., Betteridge, A., and Hawes, C.** (1998) Stacks on tracks: the plant Golgi apparatus traffics on an actin/ER network. *Plant J.* **15**:441-447.
- Bolotina, V.M., Najibi, S., Palacino, J.J., Pagano, P.J., and Cohen, R.A.** (1994) Nitric-Oxide Directly Activates Calcium-Dependent Potassium Channels in Vascular Smooth-Muscle. *Nature* **368**:850-853.
- Bootman, M.D., Berridge, M.J., and Lipp, P.** (1997) Cooking with calcium: The recipes for composing global signals from elementary events. *Cell* **91**:367-373.
- Bourguignon, L.Y.W., Chu, A., Jin, H., and Brandt, N.R.** (1995) Ryanodine Receptor-Ankyrin Interaction Regulates Internal Ca<sup>2+</sup> Release in Mouse T-Lymphoma Cells. *J.Biol.Chem.* **270**:17917-17922.
- Brown, A.M. and Birnbaumer, L.** (1990) Ionic channels and their regulation by G-protein subunits. *Ann.Rev.Physiol.* **52**:197-213.
- Brownlee, C.** (2000) Cellular calcium imaging: so, what's new? *Trends In Cell Biology* **10**: 451-457.
- Brunger, A.T.** (2001) Structural insights into the molecular mechanism of calcium-dependent vesicle-membrane fusion. *Current Opinion in Structural Biology* **11**:163-173.

**Bucci, C., Parton, R.G., Mather, I.H., Stunnenberg, H., Simons, K., Hoflack, B., and Zerial, M.** (1992) The small GTPase Rab5 functions as a regulatory factor in the early endocytic pathway. *Cell* **70**:715-728.

**Butt, E., Eigenthaler, M., and Genieser, H.G.** (1994) (Rp)-8-pCPT-cGMPS, a novel cGMP-dependent protein kinase inhibitor. *Eur.J.Pharmacol.* **269**:265-268.

**Calakos, N., Bennett, M.K., Peterson, K.E., and Scheller, R.H.** (1994) Protein-protein interactions contributing to the specificity of intracellular vesicular trafficking. *Science* **263**:1146-1149.

**Campos, K.L., Giovanelli, J., and Kaufman, S.** (1995) Characteristics of the Nitric-Oxide Synthase-Catalyzed Conversion of Arginine to N-Hydroxyarginine, the First Oxygenation Step in the Enzymatic-Synthesis of Nitric-Oxide. *J.Biol.Chem.* **270**:1721-1728.

**Cao, X.C., Ballew, N., and Barlowe, C.** (1998) Initial docking of ER-derived vesicles requires Usa1p and Ypt1p but is independent of SNARE proteins. *EMBO J.* **17**:2156-2165.

**Carafoli, E.** (2003) Calcium signaling: a tale for all seasons. *Proc.Nat.Acad.Sci.USA* **99**: 1115-1122.

**Carafoli, E., Santella, L., Branca, D., and Brini, M.** (2001) Generation, control, and processing of cellular calcium signals. *Critical Reviews in Biochemistry and Molecular Biology* **36**:107-260.

**Carr, C.M., Grote, E., Munson, M., Hughson, F.M., and Novick, P.J.** (1999) Sec1p binds to SNARE complexes and concentrates at sites of secretion. *J.Cell Biol.* **146**:333-344.

**Carvajal, J.A., Germain, A.M., Huidobro-Toro, J.P., and Weiner, C.P.** (2000) Molecular mechanism of cGMP-mediated smooth muscle relaxation. *Journal of Cellular Physiology* **184**:409-420.

**Catterall, W.A.** (1998) Structure and function of neuronal  $\text{Ca}^{2+}$  channels and their role in neurotransmitter release. *Cell Calcium* **24**:307-323.

**Chandok, M.R., Ytterberg, A.J., van Wijk, K.J., and Klessig, D.F.** (2003) The pathogen-inducible nitric oxide synthase (iNOS) in plants is a variant of the P protein of the glycine decarboxylase complex. *Cell* **113**:469-482.

**Chapman, E.R., An, S., Barton, N., and Jahn, R.** (1994) SNAP-25, a t-SNARE which binds to both syntaxin and synaptobrevin via domains that may form coiled coils. *J.Biol.Chem.* **269**:27427-27432.

- Chapman, E.R., Hanson, P.I., An, S., and Jahn, R.** (1995)  $\text{Ca}^{2+}$  regulates the interaction between synaptotagmin and syntaxin-1. *J.Biol.Chem.* **270**:23667-23671.
- Chen, Y.A. and Scheller, R.H.** (2001) SNARE-mediated membrane fusion. *Nature Reviews Molecular Cell Biology* **2**:98-106.
- Cheng, H., Lederer, W.J., and Cannell, M.B.** (1993) Calcium sparks - elementary events underlying excitation-contraction coupling in heart-muscle. *Science* **262**:740-744.
- Cheng, H.P., Fill, M., Valdivia, H., and Lederer, W.J.** (1995) Models of  $\text{Ca}^{2+}$  Release Channel Adaptation. *Science* **267**:2009-2010.
- Churchill, G.C., Okada, Y., Thomas, J.M., Genazzani, A.A., Patel, S., and Galione, A.** (2002) NAADP mobilizes  $\text{Ca}^{2+}$  from reserve granules, lysosome-related organelles, in sea urchin eggs. *Cell* **111**:703-708.
- Clapham, D.E.** (1995) Calcium signaling. *Cell* **80**:259-268.
- Clarke, A., Desikan, R., Hurst, R.D., Hancock, J.T., and Neill, S.J.** (2000) NO way back : nitric oxide and programmed cell death in *Arabidopsis thaliana* suspension cultures. *Plant J.* **24**:667-677.
- Clary, D.O., Griff, I.C., and Rothman, J.E.** (1990) SNAPs, a family of NSF attachment proteins involved in intracellular membrane fusion in animals and yeast. *Cell* **61**:709-721.
- Clayton, H., Knight, M.R., Knight, H., McAinsh, M.R., and Hetherington, A.M.** (1999) Dissection of the ozone-induced calcium signature. *Plant J.* **17**:575-579.
- Clementi, E. and Meldolesi, J.** (1997) The cross-talk between nitric oxide and  $\text{Ca}^{2+}$ : A story with a complex past and a promising future. *Trends Pharm.Sci.* **18**:266-269.
- Cooney, R.V., Harwood, P.J., Custer, L.J., and Franke, A.A.** (1994) Light-Mediated Conversion of Nitrogen-Dioxide to Nitric-Oxide by Carotenoids. *Environmental Health Perspectives* **102**:460-462.
- Cutler, S., Ghassemian, M., Bonetta, D., Cooney, S., and McCourt, P.** (1996) A protein farnesyl transferase involved in abscisic acid signal transduction in *Arabidopsis*. *Science* **273**:1239-1241.
- Darley, C.P., Skiera, L.A., Northrop, F., Sanders, D., and Davies, J.M.** (1998) Tonoplast inorganic pyrophosphatase in *Vicia faba* guard cells. *Planta* **206**:272-277.
- Davies, J.M., Poole, R.J., Rea, P.A., and Sanders, D.** (1992) Potassium-Transport Into Plant Vacuoles Energized Directly by A Proton-Pumping Inorganic Pyrophosphatase. *Proc.Nat.Acad.Sci.USA* **89**:11701-11705.
- Degtjar, V.E., Scheller, R.H., and Tsien, R.W.** (2000) Syntaxin modulation of slow inactivation of N-type calcium channels. *J.Neurosci.* **20**:4355-4367.



**DeKoninck, P. and Schulman, H.** (1998) Sensitivity of CaM kinase II to the frequency of  $\text{Ca}^{2+}$  oscillations. *Science* **279**:227-230.

**Delledonne, M., Xia, Y.J., Dixon, R.A., and Lamb, C.** (1998) Nitric oxide functions as a signal in plant disease resistance. *Nature* **394**:585-588.

**Desai, R.C., Vyas, B., Earles, C.A., Littleton, J.T., Kowalchuck, J.A., Martin, T.F.J., and Chapman, E.R.** (2000) The C2B domain of synaptotagmin is a  $\text{Ca}^{2+}$ -sensing module essential for exocytosis. *J. Cell Biol.* **150**:1125-1135.

**Desikan, R., Griffiths, R., Hancock, J., and Neill, S.** (2002) A new role for an old enzyme: Nitrate reductase-mediated nitric oxide generation is required for abscisic acid-induced stomatal closure in *Arabidopsis thaliana*. *Proc. Nat. Acad. Sci. USA* **99**:16314-16318.

**deSouza, N., Reiken, S., Ondrias, K., Yang, Y.M., Matkovich, S., and Marks, A.R.** (2002) Protein kinase A and two phosphatases are components of the inositol 1,4,5-trisphosphate receptor macromolecular signaling complex. *J. Biol. Chem.* **277**:39397-39400.

**Dierks, E.A. and Burstyn, J.N.** (1996) Nitric oxide ( $\text{NO}^{\cdot}$ ), the only nitrogen monoxide redox form capable of activating soluble guanylyl cyclase. *Biochem. Pharmacol.* **51**:1593-1600.

**Dietrich, P. and Hedrich, R.** (1998) Anions permeate and gate GCAC1, a voltage-dependent guard cell anion channel. *Plant J.* **15**:479-487.

**Dolmetsch, R.E., Xu, K.L., and Lewis, R.S.** (1998) Calcium oscillations increase the efficiency and specificity of gene expression. *Nature* **392**:933-936.

**Dulubova, I., Sugita, S., Hill, S., Hosaka, M., Fernandez, I., Sudhof, T.C., and Rizo, J.** (1999) A conformational switch in syntaxin during exocytosis: role of munc18. *EMBO J.* **18**:4372-4382.

**Durner, J., Wendehenne, D., and Klessig, D.F.** (1998) Defense gene induction in tobacco by nitric oxide, cyclic GMP, and cyclic ADP-ribose. *Proc. Nat. Acad. Sci. USA* **95**:10328-10333.

**Eun, S.O., Bae, S.H., and Lee, Y.** (2001) Cortical actin filaments in guard cells respond differently to abscisic acid in wild-type and *abi1-1* mutant *Arabidopsis*. *Planta* **212**:466-469.

**Eun, S.O. and Lee, Y.S.** (1997) Actin filaments of guard cells are reorganized in response to light and abscisic acid. *Plant Physiol.* **115**:1491-1498.

**Evans, N.H.** (2003) Modulation of guard cell plasma membrane potassium currents by methyl jasmonate. *Plant Physiol.* **131**:8-11.

**Evans, N.H., McAinsh, M.R., and Hetherington, A.M.** (2001) Calcium oscillations in higher plants. *Current Opinion In Plant Biology* **4**:415-420.

**Fairley, G.K. and Assmann, S.M.** (1991) Evidence for G-protein regulation of inward potassium ion channel current in guard cells of fava bean. *Plant Cell* **3**:1037-1044.

**Fernandez, I., Ubach, J., Dulubova, I., Zhang, X.Y., Sudhof, T.C., and Rizo, J.** (1998) Three-dimensional structure of an evolutionarily conserved N-terminal domain of syntaxin 1A. *Cell* **94**:841-849.

**Finger, F.P., Hughes, T.E., and Novick, P.** (1998) Sec3p is a spatial landmark for polarized secretion in budding yeast. *Cell* **92**:559-571.

**Fleming, K.G., Hohl, T.M., Yu, R.C., Muller, S.A., Wolpensinger, B., Engel, A., Engelhardt, H., Brunger, A.T., Sollner, T.H., and Hanson, P.I.** (1998) A revised model for the oligomeric state of the N-ethylmaleimide-sensitive fusion protein, NSF. *J.Biol.Chem.* **273**:15675-15681.

**Forestier, C., Bouteau, F., Leonhardt, N., and Vavasseur, A.** (1998) Pharmacological properties of slow anion currents in intact guard cells of *Arabidopsis*. Application of the discontinuous single-electrode voltage-clamp to different species. *Pflügers Archiv-European Journal Of Physiology* **436**:920-927.

**Fricker, M.D., Gilroy, S., Read, N.D., and Trewavas, A.J.** (1991) Visualisation and measurement of the calcium message in guard cells. In *Molecular Biology of Plant Development*, W.Schuch and G.Jenkins, eds (Cambridge: Cambridge Univ. Press), pp. 177-190.

**Friebe, A. and Koesling, D.** (2003) Regulation of nitric oxide-sensitive guanylyl cyclase. *Circ.Res.* **93**:96-105.

**Furchgott, R.F.** (1995) Special topic : nitric oxide. *Ann.Rev.Physiol.* **57**:659-682.

**Galione, A., White, A., Willmott, N., Turner, M., and Potter, B.V.** (1993) cGMP mobilizes intracellular  $Ca^{2+}$  in sea urchin eggs by stimulating cyclic ADP-ribose synthesis. *Nature* **365**:456-459.

**Garcia-Mata, C. and Lamattina, L.** (2001) Nitric oxide induces stomatal closure and enhances the adaptive plant responses against drought stress. *Plant Physiol.* **126**:1196-1204.

**Garcia-Mata, C. and Lamattina, L.** (2002) Nitric oxide and abscisic acid cross talk in guard cells. *Plant Physiol.* **128**:790-792.

**Garcia-Mata, C. and Lamattina, L.** (2003) Abscisic acid, nitric oxide and stomatal closure - is nitrate reductase one of the missing links? *Trends Plant Sci.* **8**:20-26.

**Geelen, D., Leyman, B., Batoko, H., DiSansebastiano, G.P., Moore, I., and Blatt, M.R.** (2002) The Absciscic Acid-Related SNARE Homolog NtSyr1 Contributes to Secretion and Growth: Evidence from Competition with Its Cytosolic Domain. *Plant Cell* **14**:387-406.

**Gehring, C.A., Irving, H.R., and Parish, R.W.** (1990) Effects of auxin and abscisic acid on cytosolic calcium and pH in plant cells. *Proc.Nat.Acad.Sci.USA* **87**:9645-9649.

**Geppert, M., Goda, Y., Hammer, R.E., Li, C., Rosahl, T.W., Stevens, C.F., and Sudhof, T.C.** (1994) Synaptotagmin-I - A Major  $\text{Ca}^{2+}$  Sensor for Transmitter Release at A Central Synapse. *Cell* **79**:717-727.

**Geppert, M., Goda, Y., Stevens, C.F., and Sudhof, T.C.** (1997) The small GTP-binding protein Rab3A regulates a late step in synaptic vesicle fusion. *Nature* **387**:810-814.

**Gibbon, B. C., Kovar, D.R., and Staiger, C.J.** (1999) Latrunculin B has different effects on pollen germination and tube growth. *Plant Cell* **11**:2349-2363.

**Gibson, A.D. and Garbers, D.L.** (2000) Guanylyl cyclases as a family of putative odorant receptors. *Annual Review Of Neuroscience* **23**:417-439.

**Gilroy, S., Read, N.D., and Trewavas, A.J.** (1990) Elevation of cytoplasmic calcium by caged calcium or caged inositol trisphosphate initiates stomatal closure. *Nature* **346**:769-771.

**Gou, F.-Q., Okamoto, M., and Crawford, N.M.** (2003) Identification of a Plant Nitric Oxide Synthase Gene Involved in Hormonal Signaling. *Science* **302**:100-103.

**Grabov, A. and Blatt, M.R.** (1997) Parallel control of the inward-rectifier  $\text{K}^{+}$  channel by cytosolic-free  $\text{Ca}^{2+}$  and pH in *Vicia* guard cells. *Planta* **201**:84-95.

**Grabov, A. and Blatt, M.R.** (1998a) Membrane voltage initiates  $\text{Ca}^{2+}$  waves and potentiates  $\text{Ca}^{2+}$  increases with abscisic acid in stomatal guard cells. *Proc.Nat.Acad.Sci.USA* **95**:4778-4783.

**Grabov, A. and Blatt, M.R.** (1999) A steep dependence of inward-rectifying potassium channels on cytosolic free calcium concentration increase evoked by hyperpolarization in guard cells. *Plant Physiol.* **119**:277-287.

**Grabov, A., Leung, J., Giraudat, J., and Blatt, M.R.** (1997) Alteration of anion channel kinetics in wild-type and *abi1-1* transgenic *Nicotiana benthamiana* guard cells by abscisic acid. *Plant J.* **12**:203-213.

**Gradmann, D., Hansen, U.-P., Long, W., Slayman, C.L., and Warnke, J.** (1978) Current-voltage relationships for the plasma membrane and its principle electrogenic pump in *Neurospora crassa*. I. Steady- state conditions. *J.Membr.Biol.* **29**:333-367.

- Graeff, R.M., Franco, L., Deflora, A., and Lee, H.C.** (1998) Cyclic GMP-dependent and -independent effects on the synthesis of the calcium messengers cyclic ADP-ribose and nicotinic acid adenine dinucleotide phosphate. *J.Biol.Chem.* **273**:118-125.
- Groves, J.T. and Wang, C.C.Y.** (2000) Nitric oxide synthase: models and mechanisms. *Current Opinion in Chemical Biology* **4**:687-695.
- Grynkiewicz, G., Poenie, M., and Tsien, R.Y.** (1985) A new generation of  $\text{Ca}^{2+}$  indicators with greatly improved fluorescence properties. *J.Biol.Chem.* **260**:3440-3450.
- Hain, J., Onoue, H., Mayrleitner, M., Fleischer, S., and Schindler, H.** (1995) Phosphorylation Modulates the Function of the Calcium-Release Channel of Sarcoplasmic-Reticulum from Cardiac-Muscle. *J.Biol.Chem.* **270**:2074-2081.
- Hamilton, D.W.A., Hills, A., and Blatt, M.R.** (2001) Extracellular  $\text{Ba}^{2+}$  and voltage interact to gate  $\text{Ca}^{2+}$  channels at the plasma membrane of stomatal guard cells. *FEBS Lett.* **491**:99-103.
- Hamilton, D.W.A., Hills, A., Kohler, B., and Blatt, M.R.** (2000)  $\text{Ca}^{2+}$  channels at the plasma membrane of stomatal guard cells are activated by hyperpolarization and abscisic acid. *Proc.Nat.Acad.Sci.USA* **97**:4967-4972.
- Han, S., Tang, R., Anderson, L. K., Woerner, T. E., and Pei, Z. M.** (2003) A cell surface receptor mediates extracellular  $\text{Ca}^{2+}$  sensing in guard cells. *Nature* **425**: 196-200.
- Hedrich, R., Barbier-Brygoo, H., Felle, H., Fluegge, U.I., Luetge, U., Maathuis, F.J.M., Marx, S., Prins, H.B.A., Raschke, K., Schnabl, H., Schroeder, J.I., Struve, I., Taiz, L., and Zeigler, P.** (1988) General mechanisms for solute transport across the tonoplast of plant vacuoles: a patch-clamp survey of ion channels and proton pumps. *Bot.Acta* **101**:7-13.
- Hedrich, R., Busch, H., and Raschke, K.** (1990)  $\text{Ca}^{2+}$  and nucleotide dependent regulation of voltage dependent anion channels in the plasma membrane of guard cells. *EMBO J.* **9**:3889-3892.
- Henriksen, G.H., Taylor, A.R., Brownlee, C., and Assmann, S.M.** (1996) Laser microsurgery of higher-plant cell walls permits patch clamp access. *Plant Physiol.* **110**:1063-1068.
- Hess, D.T., Matsumoto, K., Nudelman, R., and Stamler, J.S.** (2001) S-nitrosylation: spectrum and specificity. *Nature Cell Biology* **3**:46-49.
- Hill, E., Clarke, N., and Barr, F.A.** (2000) The Rab6-binding kinesin, Rab6-KIFL, is required for cytokinesis. *EMBO J.* **19**:5711-5719.
- Hofer, A. M. and Brown, E. M.** (2003) Extracellular calcium sensing and signalling. *Nature Reviews Molecular Cell Biology* **4**: 530-538.

**Homann, U.** (1998) Fusion and fission of plasma membrane material accommodates for osmotically induced changes in the surface area of guard cell protoplasts. *Planta* **206**:329-333.

**Homann, U. and Tester, M.** (1998) Patch-clamp measurements of capacitance to study exocytosis and endocytosis. *Trends Plant Sci.* **3**:110-114.

**Homann, U. and Thiel, G.** (1999) Unitary exocytotic and endocytotic events in guard cell protoplasts during osmotically driven volume changes. *FEBS Lett.* **460**:495-499.

**Homann, U. and Thiel, G.** (2002) The number of K<sup>+</sup> channels in the plasma membrane of guard cell protoplasts changes in parallel with the surface area. *Proc.Nat.Acad.Sci.USA* **99**:10215-10220.

**Hosoi, S., Iino, M., and Shimazaki, K.** (1988) Outward-rectifying K<sup>+</sup> channels in stomatal guard cell protoplasts. *Plant Cell Physiol.* **29**:907-911.

**Hoth, S., Dreyer, I., Dietrich, P., Becker, D., Muller-Rober, B., and Hedrich, R.** (1997) Molecular basis of plant-specific acid activation of K<sup>+</sup> uptake channels. *Proc.Nat.Acad.Sci.USA* **94**:4806-4810.

**Hoth, S., Geiger, D., Becker, D., and Hedrich, R.** (2001) The pore of plant K<sup>+</sup> channels is involved in voltage and pH sensing: Domain-swapping between different K<sup>+</sup> channel alpha- subunits. *Plant Cell* **13**:943-952.

**Hrabak, E.M., Chan, C.W.M., Gribskov, M., Harper, J. F., Choi, J. H., Halford, N., Kudla, J., Luan, S., Nimmo, H.G., Sussman, M.R., Thomas, M., Walker-Simmons, K., Zhu, J.K., and Harmon, A.C.** (2003) The *Arabidopsis* CDPK-SnRK superfamily of protein kinases. *Plant Physiol.* **132**:666-680.

**Hunt, L., Mills, L.N., Pical, C., Leckie, C.P., Aitken, F.L., Kopka, J., Mueller-Roeber, B., McAinsh, M.R., Hetherington, A.M., and Gray, J.E.** (2003) Phospholipase C is required for the control of stomatal aperture by ABA. *Plant J.* **34**:47-55.

**Hurst, A.C., Meckel, T., Tayefeh, S., Thiel, G., and Homann, U.** (2004) Trafficking of the plant potassium inward rectifier KAT1 in guard cell protoplasts of *Vicia faba*. *The Plant Journal* **37**:391-397.

**Hwang, J.U. and Lee, Y.** (2001) Abscise acid-induced actin reorganization in guard cells of dayflower is mediated by cytosolic calcium levels and by protein kinase and protein phosphatase activities. *Plant Physiol.* **125**:2120-2128.

**Hwang, J.U., Suh, S., Yi, H.J., Kim, J., and Lee, Y.** (1997) Actin filaments modulate both stomatal opening and inward K<sup>+</sup>-channel activities in guard cells of *Vicia faba* L. *Plant Physiol.* **115**:335-342.

**Igami, K., Yamaguchi, N., and Kasai, M.** (1999) Regulation of depolarization-induced calcium release from skeletal muscle triads by cyclic AMP-dependent protein kinase. *Japanese Journal of Physiology* **49**:81-87.

**Ignarro, L.J., Byrns, R.E., Buga, G.M., and Wood, K.S.** (1987) Endothelium-Derived Relaxing Factor from Pulmonary-Artery and Vein Possesses Pharmacological and Chemical-Properties Identical to Those of Nitric-Oxide Radical. *Circ.Res.* **61**:866-879.

**Ilan, N., Schwartz, A., and Moran, N.** (1996) External protons enhance the activity of the hyperpolarization- activated  $K^+$  channel in guard cell protoplasts of *Vicia faba*. *J.Membr.Biol.* **154**:169-181.

**Irving, H.R., Gehring, C.A., and Parish, R.W.** (1992) Changes in cytosolic pH and calcium of guard cells precede stomatal movements. *Proc.Nat.Acad.Sci.USA* **89**:1790-1794.

**Irvine, R.F.** (2003) 20 years of  $Ins(1,4,5)P_3$  and 40 years before. *Nature Reviews Molecular Cell Biology* **4**:586-590.

**Jackson, C.L. and Casanova, J.E.** (2000) Turning on ARF: the Sec7 family of guanine-nucleotide-exchange factors. *Trends Cell Biol.* **10**:60-67.

**Jacob, T., Ritchie, S., Assmann, S.M., and Gilroy, S.** (1999) Abscissic acid signal transduction in guard cells is mediated by phospholipase D activity. *Proc.Nat.Acad.Sci.USA* **96**:12192-12197.

**Jaffrey, S.R. and Snyder, S.H.** (1995) Nitric oxide: A neural messenger. *Ann.Rev.Cell Dev.Biol.* **11**:417-440.

**Jahn, R. and Sudhof, T.C.** (1999) Membrane fusion and exocytosis. *Annual Review Of Biochemistry* **68**:863-911.

**Jiang, L.H., Gawler, D.J., Hodson, N., Milligan, C.J., Pearson, H.A., Porter, V., and Wray, D.** (2000) Regulation of cloned cardiac L-type calcium channels by cGMP-dependent protein kinase. *J.Biol.Chem.* **275**:6135-6143.

**Kamasani, U.R., Zhang, X., Lawton, M., and Berkowitz, G.A.** (1997) Ca-dependent protein kinase modulates activity of the  $K^+$  channel KAT1. *Plant Physiol.* **114**:980.

**Kase, H., Iwahashi, K., Nakanishi, S., Matsui, Y., Yamada, K., Takahashi, M., Murakata, C., Sato, A., and Kaneko, M.** (1987) K-252 compounds, novel and potent inhibitors of protein kinase C and cyclic nucleotide dependent protein kinases. *Biochem.Biophys.Res.Com.* **142**:436-440.

**Kelly, W.B., Esser, J.E., and Schroeder, J.I.** (1995) Effects of cytosolic calcium and limited, possible dual, effects of G-protein modulators on guard cell inward potassium channels. *Plant J.* **8**:479-489.

**Ketelaar, T., de Ruijter, N.C.A., and Emons, A.M.C.** (2003) Unstable F-actin specifies the area and microtubule direction of cell expansion in *Arabidopsis* root hairs. *Plant Cell* **15**:285-292.

**Kim, D., Jun, K.S., Lee, S.B., Kang, N.G., Min, D.S., Kim, Y.H., Ryu, S.H., Suh, P.G., and Shin, H.S.** (1997) Phospholipase C isozymes selectively couple to specific neurotransmitter receptors. *Nature* **389**:290-293.

**Kim, M., Hepler, P.K., Fan, S.O., Ha, K.S., and Lee, Y.** (1995) Actin filaments in mature guard cells are radially distributed and involved in stomatal movement. *Plant Physiol.* **109**:1077-1084.

**Klepper, L.A.** (1979) Nitric oxide (NO) and nitrogen dioxide (NO<sub>2</sub>) emissions from herbicide-treated soybean plants. *Atmos.Env.* **13**:537.

**Kohler, B. and Blatt, M.R.** (2002) Protein phosphorylation activates the guard cell Ca<sup>2+</sup> channel and is a prerequisite for gating by abscisic acid. *Plant J.* **32**:185-194.

**Kojima, H., Nakatsubo, N., Kikuchi, K., Kawahara, S., Kirino, Y., Nagoshi, H., Hirata, Y., and Nagano, T.** (1998) Detection and imaging of nitric oxide with novel fluorescent indicators: Diaminofluoresceins. *Analytical Chemistry* **70**:2446-2453.

**Komalavilas, P. and Lincoln, T.M.** (1994) Phosphorylation of the Inositol 1,4,5-Trisphosphate Receptor by Cyclic Gmp-Dependent Protein-Kinase. *J.Biol.Chem.* **269**:8701-8707.

**Komalavilas, P. and Lincoln, T.M.** (1996) Phosphorylation of the inositol 1,4,5-trisphosphate receptor - Cyclic GMP-dependent protein kinase mediates cAMP and cGMP dependent phosphorylation in the intact rat aorta. *J.Biol.Chem.* **271**:21933-21938.

**Koornneef, M., Reuling, G., and Karssen, C.M.** (1984) The isolation and characterization of abscisic acid-insensitive mutants of *Arabidopsis thaliana*. *Physiol.Plant.* **61**:377-383.

**Korchev, Y.E., Negulyaev, Y.A., Edwards, C.R.W., Vodyanoy, I., and Lab, M.J.** (2000) Functional localization of single active ion channels on the surface of a living cell. *Nature Cell Biology* **2**:616-619.

**Korth, H.G., Sustmann, R., Thater, C., Butler, A.R., and Ingold, K.U.** (1994) On the Mechanism of the Nitric-Oxide Synthase-Catalyzed Conversion of N-Omega-Hydroxy-L-Arginine to Citrulline and Nitric-Oxide. *J.Biol.Chem.* **269**:17776-17779.

**Kruse, T., Tallman, G., and Zeiger, E.** (1989) Isolation of guard cell protoplasts from mechanically prepared epidermis of *Vicia faba* leaves. *Plant Physiol.* **90**:1382-1386.

**Kubitscheck, U., Homann, U., and Thiel, G.** (2000) Osmotically evoked shrinking of guard-cell protoplasts causes vesicular retrieval of plasma membrane into the cytoplasm. *Planta* **210**:423-431.

**Kuchitsu, K., Ward, J.M., Allen, G.J., Schelle, I., and Schroeder, J.I.** (2002) Loading acetoxymethyl ester fluorescent dyes into the cytoplasm of *Arabidopsis* and *Commelina* guard cells. *New Phytol.* **153**:527-533.

**Kwak, J.M., Mori, I.C., Pei, Z.M., Leonhardt, N., Torres, M.A., Dangi, J.L., Bloom, R.E., Bodde, S., Jones, J.D.G., and Schroeder, J.I.** (2003) NADPH oxidase AtrbohD and AtrbohF genes function in ROS- dependent ABA signaling in *Arabidopsis*. *EMBO J.* **22**:2623-2633.

**Lamattina, L., Garcia-Mata, C., Graziano, M., and Pagnussat, G.** (2003) Nitric oxide: The versatility of an extensive signal molecule. *Annual Review of Plant Biology* **54**:109-136.

**Lang, R.J. and Watson, M.J.** (1998) Effects of nitric oxide donors, S-nitroso-L-cysteine and sodium nitroprusside, on the whole-cell and single channel currents in single myocytes of the guinea-pig proximal colon. *Brit.J.Pharmacol.* **123**:505-517.

**Lang, T., Bruns, D., Wenzel, D., Riedel, D., Holroyd, P., Thiele, C., and Jahn, R.** (2001) SNAREs are concentrated in cholesterol-dependent clusters that define docking and fusion sites for exocytosis. *EMBO J.* **20**:2202-2213.

**Lauber, M.H., Waizenegger, I., Steinmann, T., Schwarz, H., Mayer, U., Hwang, I., Lukowitz, W., and Jurgens, G.** (1997) The *Arabidopsis* KNOLLE protein is a cytokinesis-specific syntaxin. *J.Cell Biol.* **139**:1485-1493.

**Leckie, C.P., McAinsh, M.R., Allen, G.J., Sanders, D., and Hetherington, A.M.** (1998) Absciscic acid-induced stomatal closure mediated by cyclic ADP-ribose. *Proc.Nat.Acad.Sci.USA* **95**:15837-15842.

**Lee, H.C.** (1997) Mechanisms of calcium signaling by cyclic ADP-ribose and NAADP. *Physiological Reviews* **77**:1133-1164.

**Lee, H.C.** (2001) Physiological functions of cyclic ADP-ribose and NAADP as calcium messengers. *Annual Review Of Pharmacology And Toxicology* **41**:317-345.

**Lee, M.H., Min, M.K., Lee, Y.J., Jin, J.B., Shin, D.H., Kim, D.H., Lee, K.H., and Hwang, I.** (2002) ADP-ribosylation factor 1 of *Arabidopsis* plays a critical role in intracellular trafficking and maintenance of endoplasmic reticulum morphology in *Arabidopsis*. *Plant Physiol.* **129**:1507-1520.

**Lee, Y.S., Choi, Y.B., Suh, S., Lee, J., Assmann, S.M., Joe, C.O., Kelleher, J.F., and Crain, R.C.** (1996) Absciscic acid-induced phosphoinositide turnover in guard-cell protoplasts of *Vicia faba*. *Plant Physiol.* **110**:987-996.

**Lemtiri-Chlieh, F., MacRobbie, E.A.C., and Brearley, C.A.** (2000) Inositol hexakisphosphate is a physiological signal regulating the K<sup>+</sup>-inward rectifying conductance in guard cells. *Proc.Nat.Acad.Sci.USA* **97**:8687-8692.



**Lemtiri-Chlieh, F., MacRobbie, E.A.C., Webb, A.A.R., Manison, N.F., Brownlee, C., Skepper, J.N., Chen, J., Prestwich, G.D., and Brearley, C.A. (2003)** Inositol hexakisphosphate mobilizes an endomembrane store of calcium in guard cells. *Proc.Nat.Acad.Sci.USA* **100**:10091-10095.

**Leonhardt, N., Vavasseur, A., and Forestier, C. (1999)** ATP binding cassette modulators control abscisic acid-regulated slow anion channels in guard cells. *Plant Cell* **11**:1141-1151.

**Leung, J., Bouvier-Durand, M., Morris, P.-C., Guerrier, D., Chefdor, F., and Giraudat, J. (1994)** *Arabidopsis* ABA response gene *ABI1*: features of a calcium-modulated protein phosphatase. *Science* **264**:1448-1452.

**Leung, J., Merlot, S., and Giraudat, J. (1997)** The *Arabidopsis* abscisic acid-insensitive2 (*abi2*) and *abi1* genes encode homologous protein phosphatases 2C involved in abscisic acid signal transduction. *Plant Cell* **9**:759-771.

**Leveque, C., Elfar, O., Martinmoutot, N., Sato, K., Kato, R., Takahashi, M., and Seagar, M.J. (1994)** Purification of the N-type calcium-channel associated with syntaxin and synaptotagmin - a complex implicated in synaptic vesicle exocytosis. *J.Biol.Chem.* **269**:6306-6312.

**Leyman, B., Geelen, D., and Blatt, M.R. (2000)** Localization and control of expression of Nt-Syrl, a tobacco SNARE protein. *Plant J.* **24**:369-381.

**Leyman, B., Geelen, D., Quintero, F.J., and Blatt, M.R. (1999)** A tobacco syntaxin with a role in hormonal control of guard cell ion channels. *Science* **283**:537-540.

**Li, J.X., Lee, Y.R.J., and Assmann, S.M. (1998)** Guard cells possess a calcium-dependent protein kinase that phosphorylates the KAT1 potassium channel. *Plant Physiol.* **116**:785-795.

**Li, J.X., Wang, X.Q., Watson, M.B., and Assmann, S.M. (2000)** Regulation of abscisic acid-induced stomatal closure and anion channels by guard cell AAPK kinase. *Science* **287**:300-303.

**Li, W.W., Luan, S., Schreiber, S.L., and Assmann, S.M. (1994)** Evidence for protein phosphatase 1 and phosphatase 2A regulation of K<sup>+</sup> channels in 2 types of leaf cells. *Plant Physiol.* **106**:963-970.

**Lin, R.C. and Scheller, R.H. (2000)** Mechanisms of synaptic vesicle exocytosis. *Ann.Rev.Cell Dev.Biol.* **16**:19-49.

**Lindau, M. and Almers, W. (1995)** Structure and Function of Fusion Pores in Exocytosis and Ectoplasmic Membrane-Fusion. *Current Opinion In Cell Biology* **7**:509-517.

**Lipp, P. and Niggli, E.** (1998) Fundamental calcium release events revealed by two-photon excitation photolysis of caged calcium in guinea-pig cardiac myocytes. *J.Physiol.* **508**:801-809.

**Liu, K. and Luan, S.** (1998) Voltage-dependent  $K^+$  channels as targets of osmosensing in guard cells. *Plant Cell* **10**:1957-1970.

**Llinas, R., Sugimori, M., and Silver, R.B.** (1992) Microdomains of High Calcium-Concentration in A Presynaptic Terminal. *Science* **256**:677-679.

**Luan, S., Li, W., Rusnak, F., Assmann, S.M., and Schreiber, S.L.** (1993) Immunosuppressants implicate protein phosphatase regulation of  $K^+$  channels in guard cells. *Proc.Nat.Acad.Sci.USA* **90**:2202-2206.

**Lukowitz, W., Mayer, U., and Jurgens, G.** (1996) Cytokinesis in the *Arabidopsis* embryo involves the syntaxin related *knolle* gene product. *Cell* **84**:61-71.

**Maathuis, F.J.M., May, S.T., Graham, N.S., Bowen, H.C., Jelitto, T.C., Trimmer, P., Bennett, M.J., Sanders, D., and White, P.J.** (1998) Cell marking in *Arabidopsis thaliana* and its application to patch-clamp studies. *Plant J.* **15**:843-851.

**MacRobbie, E.A.C.** (1981) Ion fluxes in 'isolated' guard cells of *Commelina communis* L. *J.Exp.Bot.* **32**:545-562.

**MacRobbie, E.A.C.** (1995) Effects of ABA on  $^{86}Rb^+$  fluxes at plasmalemma and tonoplast of stomatal guard cells. *Plant J.* **7**:835-843.

**MacRobbie, E.A.C.** (1999) Vesicle trafficking: a role in trans-tonoplast ion movements? *J.Exp.Bot.* **50**:925-934.

**MacRobbie, E.A.C.** (2000) ABA activates multiple  $Ca^{2+}$  fluxes in stomatal guard cells, triggering vacuolar  $K^+(Rb^+)$  release. *Proc.Nat.Acad.Sci.USA* **97**:12361-12368.

**MacRobbie, E.A.C.** (2002) Evidence for a role for protein tyrosine phosphatase in the control of ion release from the guard cell vacuole in stomatal closure. *Proc.Nat.Acad.Sci.USA* **99**:11963-11968.

**Martin, T.F.J.** (1997) Phosphoinositides as spatial regulators of membrane traffic. *Current Opinion In Neurobiology* **7**:331-338.

**McAinsh, M.R., Brownlee, C., and Hetherington, A.M.** (1990) Absciscic acid-induced elevation of guard cell cytosolic  $Ca^{2+}$  precedes stomatal closure. *Nature* **343**:186-188.

**McAinsh, M.R., Brownlee, C., and Hetherington, A.M.** (1991) Partial inhibition of ABA-induced stomatal closure by calcium- channel blockers. *Proc.R.Soc.Lond.Ser.B.Biol.Sci.* **243**:195-202.

**McAinsh, M.R., Brownlee, C., and Hetherington, A.M.** (1992) Visualizing changes in cytosolic-free  $\text{Ca}^{2+}$  during the response of stomatal guard cells to abscisic acid. *Plant Cell* **4**:1113-1122.

**McAinsh, M.R., Clayton, H., Mansfield, T.A., and Hetherington, A.M.** (1996) Changes in stomatal behavior and guard cell cytosolic free calcium in response to oxidative stress. *Plant Physiol.* **111**:1031-1042.

**McAinsh, M.R., Webb, A.A.R., Taylor, J.E., and Hetherington, A.M.** (1995) Stimulus-induced oscillations in guard cell cytosolic-free calcium. *Plant Cell* **7**:1207-1219.

**McCormack, J. G. and Cobbold, P. H.** *Cellular Calcium*. (1991) 1, 1-418. Oxford, Oxford University Press.

**Meffert, M.K., Calakos, N.C., Scheller, R.H., and Schulman, H.** (1996) Nitric oxide modulates synaptic vesicle docking/fusion reactions. *Neuron* **16**:1229-1236.

**Menasche, G., Pastural, E., Feldmann, J., Certain, S., Ersoy, F., Dupuis, S., Wulffraat, N., Bianchi, D., Fischer, A., Le Deist, F., and Saint Basile, G.** (2000) Mutations in RAB27A cause Griscelli syndrome associated with haemophagocytic syndrome. *Nature Genetics* **25**:173-176.

**Meyer, K., Leube, M.P., and Grill, E.** (1994) A protein phosphatase 2C involved in ABA signal transduction in *Arabidopsis thaliana*. *Science* **264**:1452-1455.

**Miedema, H. and Assmann, S.M.** (1996) A membrane-delimited effect of internal pH on the  $\text{K}^{+}$  outward rectifier of *Vicia faba* guard cells. *J.Membr.Biol.* **154**:227-237.

**Misura, K.M.S., Scheller, R.H., and Weis, W.I.** (2000) Three-dimensional structure of the neuronal-Sec1-syntaxin 1a complex. *Nature* **404**:355-362.

**Miyawaki, A., Griesbeck, O., Heim, R., and Tsien, R.Y.** (1999) Dynamic and quantitative  $\text{Ca}^{2+}$  measurements using improved cameleons. *Proc.Nat.Acad.Sci.USA* **96**:2135-2140.

**Miyawaki, A., Llopis, J., Heim, R., McCaffery, J.M., Adams, J.A., Ikura, M., and Tsien, R.Y.** (1997) Fluorescent indicators for  $\text{Ca}^{2+}$  based on green fluorescent proteins and calmodulin. *Nature* **388**:882-887.

**Moncada, S., Palmer, R.M.J., and Higgs, E.A.** (1991) Nitric-Oxide - Physiology, Pathophysiology, and Pharmacology. *Pharmacological Reviews* **43**:109-142.

**Monck, J.R., Oberhauser, A.F., and Fernandez, J.M.** (1995) The Exocytotic Fusion Pore Interface - A Model of the Site of Neurotransmitter Release. *Molecular Membrane Biology* **12**:151-156.

- Montell, C., Birnbaumer, L., and Flockerzi, V.** (2002) The TRP channels, a remarkable functional family. *Cell* **108**: 595-598.
- Mori, I.C. and Muto, S.** (1997) Abscissic acid activates a 48-kilodalton protein kinase in guard cell protoplasts. *Plant Physiol.* **113**:833-839.
- Muir, S.R. and Sanders, D.** (1996) Pharmacology of  $\text{Ca}^{2+}$  release from red beet microsomes suggests the presence of ryanodine receptor homologs in higher-plants. *FEBS Lett.* **395**:39-42.
- Murata, Y., Pei, Z.M., Mori, I.C., and Schroeder, J.** (2001) Abscissic acid activation of plasma membrane  $\text{Ca}^{2+}$  channels in guard cells requires cytosolic NAD(P)H and is differentially disrupted upstream and downstream of reactive oxygen species production in *abi1-1* and *abi2-1* protein phosphatase 2C mutants. *Plant Cell* **13**:2513-2523.
- Naren, A.P., Nelson, D.J., Xie, W.W., Jovov, B., Pevsner, J., Bennett, M.K., Benos, D.J., Quick, M.W., and Kirk, K.L.** (1997) Regulation of CFTR chloride channels by syntaxin and Munc18 isoforms. *Nature* **390**:302-305.
- Naren, A.P., Quick, M.W., Collawn, J.F., Nelson, D.J., and Kirk, K.L.** (1998) Syntaxin 1A inhibits CFTR chloride channels by means of domain-specific protein-protein interactions. *Proc.Nat.Acad.Sci.USA* **95**:10972-10977.
- Nebenfuhr, A., Gallagher, L.A., Dunahay, T.G., Frohlick, J.A., Mazurkiewicz, A.M., Meehl, J.B., and Staehelin, L.A.** (1999) Stop-and-go movements of plant Golgi stacks are mediated by the acto- myosin system. *Plant Physiol.* **121**:1127-1141.
- Nebenfuhr, A., Ritzenthaler, C., and Robinson, D.G.** (2002) Brefeldin A: Deciphering an enigmatic inhibitor of secretion. *Plant Physiol.* **130**:1102-1108.
- Neill, S.J., Desikan, R., Clarke, A., and Hancock, J.T.** (2002) Nitric oxide is a novel component of abscissic acid signaling in stomatal guard cells. *Plant Physiol.* **128**:13-16.
- Neill, S.J., Desikan, R., and Hancock, J.T.** (2003) Nitric oxide signalling in plants. *New Phytol.* **159**:11-35.
- Neumann, U., Brandizzi, F., and Hawes, C.** (2003) Protein transport in plant cells: In and out of the Golgi. *Ann Bot* **92**:167-180.
- Newton, R.P., Roef, L., Witters, E., and Van Onckelen, H.** (1999) Cyclic nucleotides in higher plants: the enduring paradox. *New Phytol.* **143**:427-455.
- Ng, C.K.Y., McAinsh, M.R., Gray, J.E., Hunt, I., Leckie, C.P., Mills, L., and Hetherington, A.M.** (2001) Calcium-based signalling systems in guard cells. *New Phytol.* **151**:109-120.

**Noguchi, N., Takasawa, S., Nata, K., Tohgo, A., Kato, I., Ikehata, F., Yonekura, H., and Okamoto, H.** (1997) Cyclic ADP-ribose binds to FK506-binding protein 12.6 to release  $\text{Ca}^{2+}$  from islet microsomes. *J.Biol.Chem.* **272**:3133-3136.

**Nonet, M.L., Staunton, J.E., Kilgard, M.P., Fergestad, T., Hartwig, E., Horvitz, H.R., Jorgensen, E.M., and Meyer, B.J.** (1997) *Caenorhabditis elegans* *rab-3* mutant synapses exhibit impaired function and are partially depleted of vesicles. *J.Neurosci.* **17**:8061-8073.

**Nuoffer, C. and Balch, W.E.** (1994) GTPases - multifunctional molecular switches regulating vesicular traffic. *Annual Review Of Biochemistry* **63**:949-990.

**Ostermeier, C. and Brunger, A.T.** (1999) Structural basis of Rab effector specificity: Crystal structure of the small G protein Rab3A complexed with the effector domain of Rabphilin-3A. *Cell* **96**:363-374.

**Oyler, G.A., Higgins, G.A., Hart, R.A., Battenberg, E., Billingsley, M., Bloom, F.E., and Wilson, M.C.** (1989) The Identification of A Novel Synaptosomal-Associated Protein, SNAP-25, Differentially Expressed by Neuronal Subpopulations. *J.Cell Biol.* **109**:3039-3052.

**Pandey, S., Wang, X.Q., Coursol, S.A., and Assmann, S.M.** (2002) Preparation and applications of *Arabidopsis thaliana* guard cell protoplasts. *New Phytol.* **153**:517-526.

**Parmar, P.N. and Brearley, C.A.** (1993) Identification of 3-phosphorylated and 4-phosphorylated phosphoinositides and inositol phosphates in stomatal guard cells. *Plant J.* **4**:255-263.

**Parmar, P.N. and Brearley, C.A.** (1995) Metabolism of 3-phosphorylated and 4-phosphorylated phosphatidylinositols in stomatal guard cells of *Commelina communis* L. *Plant J.* **8**:425-433.

**Patel, S., Churchill, G.C., and Galione, A.** (2001) Coordination of  $\text{Ca}^{2+}$  signalling by NAADP. *Trends in Biochemical Sciences* **26**:482-489.

**Pei, Z.M., Ghassemian, M., Kwak, C.M., McCourt, P., and Schroeder, J.I.** (1998) Role of farnesyltransferase in ABA regulation of guard cell anion channels and plant water loss. *Science* **282**:287-290.

**Pei, Z.M., Kuchitsu, K., Ward, J.M., Schwarz, M., and Schroeder, J.I.** (1997) Differential abscisic acid regulation of guard cell slow anion channels in *Arabidopsis* wild-type and *abi1* and *abi2* mutants. *Plant Cell* **9**:409-423.

**Pei, Z.M., Murata, Y., Benning, G., Thomine, S., Klusener, B., Allen, G.J., Grill, E., and Schroeder, J.I.** (2000) Calcium channels activated by hydrogen peroxide mediate abscisic acid signalling in guard cells. *Nature* **406**:731-734.

**Pei, Z.M., Ward, J.M., Harper, J.F., and Schroeder, J.I.** (1996) A novel chloride channel in *Vicia faba* guard cell vacuoles activated by the serine/threonine kinase, CDPK. *EMBO J.* **15**:6564-6574.

**Perin, M.S., Fried, V.A., Mignery, G.A., Jahn, R., and Sudhof, T.C.** (1990) Phospholipid Binding by A Synaptic Vesicle Protein Homologous to the Regulatory Region of Protein Kinase-C. *Nature* **345**:260-263.

**Piltz, R.B. and Casteel, D.E.** (2003) Regulation of gene expression by cyclic GMP. *Circ.Res.* **93**:1034-1046.

**Raschke, K.** (1979) Movements of stomata. In *Encyclopedia of Plant Physiology*, N.S. Vol. 7, W.Haupt and M.E.Feinleib, eds (Berlin: Springer), pp. 373-441.

**Raschke, K.** (2003) Alternation of the slow with the quick anion conductance in whole guard cells effected by external malate. *Planta* **217**:651-657.

**Raschke, K., Shabahang, M., and Wolf, R.** (2003) The slow and the quick anion conductance in whole guard cells: their voltage-dependent alternation, and the modulation of their activities by abscisic acid and CO<sub>2</sub>. *Planta* **217**:639-650.

**Renganathan, M., Cummins, T.R., and Waxman, S.G.** (2001) Contribution of Na(v)1.8 sodium channels to action potential electrogenesis in DRG neurons. *Journal of Neurophysiology* **86**:629-640.

**Rettig, J., Heinemann, C., Ashery, U., Sheng, Z.H., Yokoyama, C.T., Catterall, W.A., and Neher, E.** (1997) Alteration of Ca<sup>2+</sup> dependence of neurotransmitter release by disruption of Ca<sup>2+</sup> channel/syntaxin interaction. *J.Neurosci.* **17**:6647-6656.

**Ribeiro, E.A., Cunha, F.Q., Tamashiro, W.M.S.C., and Martins, I.S.** (1999) Growth phase-dependent subcellular localization of nitric oxide synthase in maize cells. *FEBS Lett.* **445**:283-286.

**Ritzenthaler, C., Nebenfuhr, A., Movafeghi, A., Stussi-Garaud, C., Behnia, L., Pimpl, P., Staehelin, L.A., and Robinson, D.G.** (2002) Reevaluation of the effects of brefeldin A on plant cells using tobacco bright yellow 2 cells expressing Golgi-targeted green fluorescent protein and COPI antisera. *Plant Cell* **14**:237-261.

**Rockel, P., Strube, F., Rockel, A., Wildt, J., and Kaiser, W.M.** (2002) Regulation of nitric oxide (NO) production by plant nitrate reductase *in vivo* and *in vitro*. *J.Exp.Bot.* **53**:103-110.

**Roelfsema, M.R.G. and Hedrich, R.** (2002) Studying guard cells in the intact plant: modulation of stomatal movement by apoplastic factors. *New Phytol.* **153**:425-431.

**Ros, R., Romieu, C., Gibrat, R., and Grignon, C.** (1995) The plant inorganic pyrophosphatase does not transport K<sup>+</sup> in vacuole membrane vesicles multilabeled with fluorescent-probes for H<sup>+</sup>, K<sup>+</sup>, and membrane potential. *J.Biol.Chem.* **270**:4368-4374.

**Rutherford, S. and Moore, I.** (2002) The *Arabidopsis* Rab GTPase family: another enigma variation. *Current Opinion In Plant Biology* **5**:518-528.

**Saint-Jore, C.M., Evins, J., Batoko, H., Brandizzi, F., Moore, I., and Hawes, C.** (2002) Redistribution of membrane proteins between the Golgi apparatus and endoplasmic reticulum in plants is reversible and not dependent on cytoskeletal networks. *Plant J.* **29**:661-678.

**Sanderfoot, A.A., Assaad, F.F., and Raikhel, N.V.** (2000) The *Arabidopsis* genome. An abundance of soluble N-ethylmaleimide-sensitive factor adaptor protein receptors. *Plant Physiol.* **124**:1558-1569.

**Sanderfoot, A.A., Kovaleva, V., Bassham, D.C., and Raikhel, N.V.** (2001a) Interactions between syntaxins identify at least five SNARE complexes within the golgi/prevacuolar system of the *Arabidopsis* cell. *Mol.Biol.Cell* **12**:3733-3743.

**Sanderfoot, A.A., Pilgrim, M., Adam, L., and Raikhel, N.V.** (2001b) Disruption of individual members of *Arabidopsis* syntaxin gene families indicates each has essential functions. *Plant Cell* **13**:659-666.

**Sanders, D.** (1988) Fungi. In *Solute Transport in Plant Cells and Tissues*, D.A.Baker and J.L.Hall, eds (Harlow: Longman Press), pp. 106-165.

**Satiat-Jeunemaitre, B., Cole, L., Bourett, T., Howard, R., and Hawes, C.** (1996a) Brefeldin A effects in plant and fungal cells: Something new about vesicle trafficking? *Journal Of Microscopy* **181**:162-177.

**Satiat-Jeunemaitre, B., Steele, C., and Hawes, C.** (1996b) Golgi-membrane dynamics are cytoskeleton dependent: A study on Golgi stack movement induced by brefeldin A. *Protoplasma* **191**:21-33.

**Sato, M.H., Kasahara, M., Ishii, N., Homareda, H., Matsui, H., and Yoshida, M.** (1994) Purified vacuolar inorganic pyrophosphatase consisting of a 75kDa polypeptide can pump  $H^+$  into reconstituted proteoliposomes. *J.Biol.Chem.* **269**:6725-6728.

**Scales, S.J., Gomez, M., and Kreis, T.E.** (2000) Coat proteins regulating membrane traffic. *International Review of Cytology* **195**:67-144.

**Schiavo, G., Stenbeck, G., Rothman, J.E., and Sollner, T.H.** (1997) Binding of the synaptic vesicle v-SNARE, synaptotagmin, to the plasma membrane t-SNARE, SNAP-25, can explain docked vesicles at neurotoxin- treated synapses. *Proc.Nat.Acad.Sci.USA* **94**:997-1001.

**Schmidt, C., Schelle, I., Liao, Y.J., and Schroeder, J.I.** (1995) Strong regulation of slow anion channels and abscisic acid signaling in guard cells by phosphorylation and dephosphorylation events. *Proc.Nat.Acad.Sci.USA* **92**:9535-9539.

**Schott, D., Ho, J., Pruyn, D., and Bretscher, A.** (1999) The COOH-terminal domain of Myo2p, a yeast myosin V, has a direct role in secretory vesicle targeting. *J. Cell Biol.* **147**:791-807.

**Schroeder, J.I., Allen, G.J., Hugouvieux, V., Kwak, J.M., and Waner, D.** (2001) Guard cell signal transduction. *Ann. Rev. Plant Physiol. Mol. Biol.* **52**:627-658.

**Schroeder, J.I. and Hagiwara, S.** (1989) Cytosolic calcium regulates ion channels in the plasma membrane of *Vicia faba* guard cells. *Nature* **338**:427-430.

**Schroeder, J.I. and Hagiwara, S.** (1990) Voltage-dependent activation of  $\text{Ca}^{2+}$ -regulated anion channels and  $\text{K}^{+}$  uptake channels in *Vicia faba* guard cells. In *Calcium and Plant Growth and Development*, R.T. Leonard and P.K. Hepler, eds (Beltsville, MD: American Soc. Plant Physiol.), pp. 144-150.

**Schroeder, J.I., Raschke, K., and Neher, E.** (1987) Voltage dependence of  $\text{K}^{+}$  channels in guard-cell protoplasts. *Proc. Nat. Acad. Sci. USA* **84**:4108-4112.

**Schwarz, M. and Schroeder, J.I.** (1998) Abscissic acid maintains S-type anion channel activity in ATP-depleted *Vicia faba* guard cells. *FEBS Lett.* **428**:177-182.

**Sciaky, N., Presley, J., Smith, C., Zaal, K.J.M., Cole, N., Moreira, J.E., Terasaki, M., Siggia, E., and Lippincott-Schwartz, J.** (1997) Golgi tubule traffic and the effects of Brefeldin A visualized in living cells. *J. Cell Biol.* **139**:1137-1155.

**Sheng, Z.H., Rettig, J., Takahashi, M., and Catterall, W.A.** (1994) Identification of a syntaxin-binding site on N-type calcium channels. *Neuron* **13**:1303-1313.

**Sheng, Z.H., Rettig, L., Cook, T., and Catterall, W.A.** (1996) Calcium-dependent interaction of N-type calcium channels with the synaptic core complex. *Nature* **379**:451-454.

**Sheng, Z.H., Yokoyama, C.T., and Catterall, W.A.** (1997) Interaction of the synprint site of N-type  $\text{Ca}^{2+}$  channels with the C2B domain of synaptotagmin I. *Proc. Nat. Acad. Sci. USA* **94**:5405-5410.

**Siddhanta, A. and Shields, D.** (1998) Secretory vesicle budding from the trans-Golgi network is mediated by phosphatidic acid levels. *J. Biol. Chem.* **273**:17995-17998.

**Sogaard, M., Tani, K., Ye, R.R., Geromanos, S., Tempst, P., Kirchhausen, T., Rothman, J.E., and Sollner, T.** (1994) A rab protein is required for the assembly of SNARE complexes in the docking of transport vesicles. *Cell* **78**:937-948.

**Sollner, T., Whitehart, S.W., Brunner, M., Erdjument-Bromage, H., Geromanos, S., Tempst, P., and Rothman, J.E.** (1993) SNAP receptors implicated in vesicle targeting and fusion. *Nature* **362**:318-324.



**Sonnleitner, A., Fleischer, S., and Schindler, H.** (1997) Gating of the skeletal calcium release channel by ATP is inhibited by protein phosphatase 1 but not by  $Mg^{2+}$ . *Cell Calcium* **21**:283-290.

**Spring, J., Kato, M., and Bernfield, M.** (1993) Epimorphin is related to a new class of neuronal and yeast vesicle targeting proteins. *Trends in Biochemical Sciences* **18**:124-125.

**Stahl, B., Chou, J.H., Li, C., Sudhof, T.C., and Jahn, R.** (1996) Rab3 reversibly recruits rabphilin to synaptic vesicles by a mechanism analogous to raf recruitment by ras. *EMBO J.* **15**:1799-1809.

**Stamler, J.S.** (1994) Redox signaling: nitrosylation and related target interactions of nitric oxide. *Cell* **78**:931-936.

**Stamler, J.S., Singel, D.J., and Loscalzo, J.** (1992) Biochemistry of Nitric-Oxide and Its Redox-Activated Forms. *Science* **258**:1898-1902.

**Stamler, J.S., Tooner, E.J., Lipton, S.A., and Sucher, N.J.** (1997) (S)NO signals: translocation, regulation, and a consensus motif. *Neuron* **18**:691-696.

**Staxen, I., Pical, C., Montgomery, L.T., Gray, J.E., Hetherington, A.M., and McAinsh, M.R.** (1999) Abscissic acid induces oscillations in guard-cell cytosolic free calcium that involve phosphoinositide-specific phospholipase C. *Proc.Nat.Acad.Sci.USA* **96**:1779-1784.

**Steinmann, T., Geldner, N., Grebe, M., Mangold, S., Jackson, C.L., Paris, S., Galweiler, L., Palme, K., and Jurgens, G.** (1999) Coordinated polar localization of auxin efflux carrier PIN1 by GNOM ARF GEF. *Science* **286**:316-318.

**Sudhof, T.C.** (1997) Function of Rab3 GDP-GTP exchange. *Neuron* **18**:519-522.

**Sun, J.H., Xin, C.L., Eu, J.P., Stamler, J.S., and Meissner, G.** (2001) Cysteine-3635 is responsible for skeletal muscle ryanodine receptor modulation by NO. *Proc.Nat.Acad.Sci.USA* **98**:11158-11162.

**Sutton, R.B., Fasshauer, D., Jahn, R., and Brunger, A.T.** (1998) Crystal structure of a SNARE complex involved in synaptic exocytosis at 2.4 angstrom resolution. *Nature* **395**:347-353.

**Takeshima, H., Nishimura, S., Matsumoto, T., Ishida, H., Kangawa, K., Minamino, N., Matsuo, H., Ueda, M., Hanaoka, M., Hirose, T., and Numa, S.** (1989) Primary structure and expression from complementary DNA of skeletal muscle ryanodine receptor. *Nature* **339**:439-445.

**Tang, T.S., Tu, H.P., Wang, Z.N., and Bezprozvanny, I.** (2003) Modulation of type 1 inositol (1,4,5)-trisphosphate receptor function by protein kinase A and protein phosphatase 1 alpha. *J.Neurosci.* **23**:403-415.

- Tang, X.D., Daggett, H., Hanner, M., Garcia, M.L., Mcmanus, O.B., Brot, N., Weissbach, H., Heinemann, S.H., and Hoshi, T.** (2001) Oxidative regulation of large conductance calcium-activated potassium channels. *J.Gen.Physiol.* **117**:253-273.
- Tester, M.** (1988) Pharmacology of K<sup>+</sup> channels in the plasmalemma of the green alga *Chara corallina*. *Journal Of Membrane Biology* **103**, 159-169.
- Tester, M.** (1990) Plant ion channels: whole-cell and single-channel studies. *New Phytol.* **114**:305-340.
- Thiel, G. and Blatt, M.R.** (1994) Phosphate antagonist okadaic acid inhibits steady-state K<sup>+</sup> currents in guard cells of *Vicia faba*. *Plant J.* **5**:727-733.
- Thiel, G., Blatt, M.R., Fricker, M.D., White, I.R., and Millner, P.A.** (1993) Modulation of K<sup>+</sup> channels in *Vicia* stomatal guard cells by peptide homologs to the auxin-binding protein C-terminus. *Proc.Nat.Acad.Sci.USA* **90**:11493-11497.
- Trimble, W.S., Cowan, D.M., and Scheller, R.H.** (1988) Vamp-1 - A Synaptic Vesicle-Associated Integral Membrane Protein. *Proc.Nat.Acad.Sci.USA* **85**:4538-4542.
- Tsien, R.Y. and Poenie, M.** (1986) Fluorescence ration imaging: a new window into intracellular ionic signaling. *TIBS* **11**:450-455.
- Valdivia ,H.H., Kaplan, J.H., Ellisdavies, G.C.R., and Lederer, W.J.** (1995) Rapid Adaptation of Cardiac Ryanodine Receptors - Modulation by Mg<sup>2+</sup> and Phosphorylation. *Science* **267**:1997-2000.
- van der Wal, J., Habets, R., Varnai, P., Balla, T., and Jalink, K.** (2001) Monitoring agonist-induced phospholipase C activation in live cells by fluorescence resonance energy transfer. *J.Biol.Chem.* **276**:15337-15344.
- Vidali, L., McKenna, S.T., and Hepler, P.K.** (2001) Actin polymerization is essential for pollen tube growth. *Mol.Biol.Cell* **12**:2534-2545.
- Wang, X.Q., Ullah, H., Jones, A.M., and Assmann, S.M.** (2001) G protein regulation of ion channels and abscisic acid signaling in Arabidopsis guard cells. *Science* **292**:2070-2072.
- Wang, Y., Okamoto, M., Schmitz, F., Hofmann, K., and Sudhof, T.C.** (1997) Rim is a putative Rab3 effector in regulating synaptic-vesicle fusion. *Nature* **388**:593-598.
- Ward, J.M.** (1997) Patch-clamping and other molecular approaches for the study of plasma membrane transporters demystified. *Plant Physiol.* **114**:1151-1159.
- Ward, J.M. and Schroeder, J.I.** (1994) Calcium-activated K<sup>+</sup> channels and calcium-induced calcium release by slow vacuolar ion channels in guard-cell vacuoles implicated in the control of stomatal closure. *Plant Cell* **6**:669-683.

- Webb, A.A.R., McAinsh, M.R., Mansfield, T.A., and Hetherington, A.M.** (1996) Carbon dioxide induces increases in guard cell cytosolic free calcium. *Plant J.* **9**:297-304.
- Weber, T., Zemelman, B.V., Mcnew, J.A., Westermann, B., Gmachl, M., Parlati, F., Sollner, T.H., and Rothman, J.E.** (1998) SNAREpins: Minimal machinery for membrane fusion. *Cell* **92**:759-772.
- Weller, U., Bernhardt, U., Siemen, D., Dreyer, F., Vogel, W., and Habermann, E.** (1985) Electrophysiological and neurobiochemical evidence for the blockade of a potassium channel by dendrotoxin. *Naunyn-Schmied. Arch. Pharmacol.* **330**:77-83.
- Wendehenne, D., Pugin, A., Klessig, D.F., and Durner, J.** (2001) Nitric oxide: comparative synthesis and signaling in animal and plant cells. *Trends Plant Sci.* **6**:177-183.
- White, P.J. and Tester, M.** (1994) Using planar lipid-bilayers to study plant ion channels. *Physiol. Plant.* **91**:770-774.
- Whiteheart, S.W., Rossnagel, K., Buhrow, S.A., Brunner, M., Jaenicke, R., and Rothman, J.E.** (1994) N-ethylmaleimide-sensitive fusion protein - a trimeric ATPase whose hydrolysis of ATP is required for membrane fusion. *J. Cell Biol.* **126**:945-954.
- Wickman, K.D. and Clapham, D.E.** (1995) G-protein regulation of ion channels. *Current Opinion In Neurobiology* **5**:278-285.
- Willmer, C. and Fricker, M. D.** (1996) Stomata. pp1-375. Chapman and Hall. (London).
- Willmott, N., Sethi, J.K., Walseth, T.F., Lee, H.C., White, A.M., and Galione, A.** (1996) Nitric oxide-induced mobilization of intracellular calcium via the cyclic ADP-ribose signaling pathway. *J. Biol. Chem.* **271**:3699-3705.
- Wiser, O., Bennett, M.K., and Atlas, D.** (1996) Functional interaction of syntaxin and SNAP-25 with voltage-sensitive L-type and N-type  $\text{Ca}^{2+}$  channels. *EMBO J.* **15**:4100-4110.
- Wiser, O., Trus, M., Hernandez, A., Renstrom, E., Barg, S., Rorsman, P., and Atlas, D.** (1999) The voltage-sensitive Lc-type  $\text{Ca}^{2+}$  channel is functionally coupled to the exocytotic machinery. *Proc. Nat. Acad. Sci. USA* **96**:248-253.
- Wojtaszek, P.** (2000) Nitric oxide in plants - To NO or not to NO. *Phytochemistry* **54**:1-4.
- Wolfe, J. and Steponkus, P.L.** (1981) The stress-strain relation of the plasma-membrane of isolated plant- protoplasts. *Biochimica Et Biophysica Acta* **643**:663-668.

**Wolfe, J. and Steponkus, P.L.** (1983) Mechanical-properties of the plasma-membrane of isolated plant- protoplasts - mechanism of hyperosmotic and extracellular freezing-injury. *Plant Physiol.* **71**:276-285.

**Wu, W.H. and Assmann, S.M.** (1994) A membrane-delimited pathway of G protein regulation of the guard cell inward  $K^+$  channel. *Proc.Nat.Acad.Sci.USA* **91**:6310-6314.

**Xu, L., Eu, J.P., Meissner, G., and Stamler, J.S.** (1998) Activation of the cardiac calcium release channel (ryanodine receptor) by poly-S-nitrosylation. *Science* **279**:234-237.

**Yamasaki, H. and Sakihama, Y.** (2000) Simultaneous production of nitric oxide and peroxynitrite by plant nitrate reductase: in vitro evidence for the NR-dependent formation of active nitrogen species. *FEBS Lett.* **468**:89-92.

**Yao, Y., Choi, J., and Parker, I.** (1995) Quantal puffs of intracellular  $Ca^{2+}$  evoked by inositol trisphosphate in *Xenopus* oocytes. *J.Physiol.* **482**:533-553.

**Yokoshiki, H., Katsube, Y., Sunagawa, M., Seki, T., and Sperelakis, N.** (1997) Disruption of actin cytoskeleton attenuates sulfonylurea inhibition of cardiac ATP-sensitive  $K^+$  channels. *Pflugers Archiv-European Journal Of Physiology* **434**:203-205.

**Zerial, M. and McBride, H.** (2001) Rab proteins as membrane organizers. *Nature Reviews Molecular Cell Biology* **2**:216.

**Zhong, H.J., Yokoyama, C.T., Scheuer, T., and Catterall, W.A.** (1999) Reciprocal regulation of P/Q-type  $Ca^{2+}$  channels by SNAP-25, syntaxin and synaptotagmin. *Nature Neuroscience* **2**:939-941.